This is to certify that the

dissertation entitled
PHASE TRANSITIONS IN TWO DIMENSIONAL
DIATOMIC MOLECULAR SYSTEMS

presented by

SAN-YI TANG

has been accepted towards fulfillment
of the requirements for

Ph. D degree in PHYSICS

S. D. Mahanti
Major professor

Date 10.24.1985

PHASE TRANSITIONS IN TWO DIMENSIONAL DIATOMIC MOLECULAR SYSTEMS

by

San-yi Tang

A DISSERTATION

Submitted to

Michigan State University

in partial fulfilment of the requirements

for the degree of

DOCTOR OF PHILOSOPHY

Department of Physics and Astronomy

1985

ABSTRACT

PHASE TRANSITIONS IN TWO DIMENSIONAL

DIATOMIC MOLECULAR SYSTEMS

by

San-yi Tang

Phase transitions in two dimensional diatomic molecular systems are studied in this thesis by using various theoretical methods and computer simulations.

It is shown that realistic molecular interaction can be represented reasonably well by a spin Hamiltonian for a rigid lattice which corresponds to fix the mass centers of the molecules. A practical method to derive such a spin Hamiltonian is given. Under very general conditions, this mapping leads to an aniostropic XY model.

The effect of this anisotropy on the isotropic XY model is investigated. If the anisotropy is present, no matter how small it is, the long-range order can exist, and as temperature rises, the system undergoes an Ising-like order-disorder transition instead of the Kosterlitz-Thouless transition seen in the isotropic XY model. The physical reason is that the dominant term in the excitation energy of vortex-antivortex pair is now proportional linearly to the separation between the opposite vortices instead of logarithmically in the isotropic phase.

Naturally, the next step is to release the mass centers of the molecules.

After solving the problem of incorparating the orientational contribution to the deformation of lattice within a constant-pressure molecular dynamics scheme, the phase transitions in a two-dimensional diatomic Lennard-Jones molecular system consisting of 400 molecules are studied. The computer simulations show that the coupling between the orientational and translational degrees of freedom drives the orientational order-disoder transition first order. Topological defects play an important role in the driving mechanism for this transition. Through this transition the system transforms from a ferroelastic phase to a paraelastic phase. Simulations also suggest that the melting transition of this system is first-order as has been seen in 2D monoatomic systems.

DEDICATION

To my contemporaries in China:

Who suffer,

Who struggle,

Who conquer.

ACKNOWLEDGEMENTS

I would like to thank professor S.D. Mahanti for his invaluable help and guidance as my thesis advisor. His encouragements made this work possible and his theoretical insight made it a pleasant expedition. The enthusiasm he devotes to the research will be a life-long inspiration for me. Despite the sincerity of all these gratitudes, yet only the time coming in future could tell the true extent of his influence.

I would also like to thank Professor G. Kemeny and Professor T.A. Kaplan for many instructive discussions and their constant interest in my work.

I am grateful to Professor D. Bruce, Professor J. Kovacs and Professor D. Stump for their service on my guidance committee and the very helpful comments on this thesis.

I wish to thank Dr. R.K. Kalia, Argonne National Laboratory, for stimulating discussions when I was visiting Argonne.

The faculty of the Department of Applied Physics, the Shanghai University of Technology and Science, are greatly appreciated for their hospitality when I was in China in 1984.

Finally, I would like to emphasise that without the commitments and supports of the all members of my family, this work would never be produced. Especially, I feel very indebted to my wife, Renqiu, and my daughter, Yan, for those years I have had to leave them in order to complete my education.

TABLE OF CONTENTS

LIST OF TABLES

LIST OF FIGURES

CHAPTER 1

Two-dimensional Molecular System:

a General Introduction

In condensed matter physics, the rapid growth of research on two-dimensional systems is a notable phenomenon in the past ten years.[1.1] Indulging in the fascinating new dimensions opened by modern technology and science, we are reluctant to recall the historical fact that for millions years the human being had been a poor creation confined to a two-dimensional manifold—the surface of the earth. So it is no wonder that an essentially two-dimensional theoretical system--celestial mechanics, reached its maturity first in history among all branches of the physics, and 2000 years ago the ancient Chinese astronomers already thought that the planets were traveling in a 2D circular orbit.[1.2] However, at the microscopic level, the realization of true 2D systems has been achieved only in the recent decade, though physicists long before have known that some kinds of layered compounds can be described quite well by 2D theories. A prominent member of the class of 2D systems is the molecular monolayers physisorbed on graphite substrate. The commercially available graphite materials with high-quality surfaces have helped the advance of experiments in the 70's; these experiments have found close correspondence between the measurements and expected 2D behavior in many cases. Extensive research has been carried out on relatively simple systems like noble gas molecules Ar, Kr, Xe on graphite,[1.3] and N_2 molecular monolayer which

is commensurate with the graphite substrate.[1.4] The mutual stimulation between experiment and theory with computer simulation as a powerful weapon, naturaly extends the frontier further forward to more complicated molecules such as O_2 whose monolayers are incommensurate with the graphite substrate. Methane, ethane,[1.5] and ethylene[1.6] on graphite substrate are of great current interest. For these systems, richer phase diagrams have been unveiled.

In this thesis, I have used a realistic interaction model—Lennard-Jones potential to investigate the properties of a diatomic molecular system, which resembles closely the δ-phase of the oxygen monolayer on graphite below 40K. In this phase, the oxygen molecules lie flat on the substrate forming an almost centered rectangular structure which is incommensurate with the underlying carbon triangular lattice.

In the middle seventies, McTague and Nielson[1.7] conducted neutron scattering experiments to explore the phase diagram of an oxygen monolayer on graphite in the temperature region $4.2K<T<50K$, and coverage region $0.7<\rho<2.6$. (The coverage 1 corresponds to a $\sqrt{3}x\sqrt{3}$ monolayer which is the structure of Kr molecular monolayer on graphite. Although we know the oxygen monolayer never shows this structure, people still use this unit for reasons of convenience or tradition.) At high coverage, $\rho>1.6$, they observed two phases: above 11.9K they saw a single diffraction peak at reciprocal lattice position $Q=2.204\mathring{A}^{-1}$, below 11.9K this peak split into a doublet at 2.17 and $2.30\mathring{A}^{-1}$. A peak at $1.14\mathring{A}^{-1}$ which was ascribed to magnetic ordering, was also observed. They labelled the low-T phase as α, thought it had the same positional

and magnetic structure as the densest packed planes of bulk α-O_2. The other phase, labelled β, was deduced to have the same triangular structure as the basal planes of bulk β-O_2. These two phases are relabelled by Stephens et al.[1.9] as ϵ and ζ, who argued that there was no clear connection between the phases of bulk and adsorbed oxygen. The transition between these two phases has an interesting and yet unfinished story by itself, my interest in this thesis, however, is on the low-coverage δ-phase. When $\rho<1.6$, McTague and Nielson found a single peak at $2.15\mathring{A}^{-1}$, they thought that the δ-phase had a triangular structure. However, it turned out that a peak at $1.57\mathring{A}^{-1}$ was missing, and was discovered in the X-ray experiment performed by Stephens et al..[1.9] They also found that the peak at $2.15\mathring{A}^{-1}$ was in fact a doublet with two closely separated, resolution-limited peaks. It was inferred that the δ-phase had a centered parallelogram structure with side lengths $a=3.17\text{-}3.25\mathring{A}$, $b=7.97\text{-}8.85\mathring{A}$. The axes of O_2 molecules are parallel to the substrate plane. Independently, by using a pattern search program to calculate the minimum of potential energy, Etters et al.[1.10] predicted the existence of this phase with a=3.32A and b=8.34A, in very good agreement with the experiment. Later the low-energy electron diffraction (LEED) experiment carried out by Toney et al.[1.11] confirmed this discovery. Now there is a true 2D diatomic molecular system whose phase diagram is very attractive for its potential richness.

The two-dimensional solids are rather different objects than ordinary three-dimensional crystals and the simple idea of long-range density-density order is not satisfactory to characterize them. In the

thermodynamic limit, the Debye-Waller factor describing the thermal vibrations diverges in 2D at any finite temperature. Kosterlitz and Thouless[1.12] proposed a different definition of long-range order for 2D solids depending on the overall properties of the system rather than the pair correlation function. They called it "topological long-range order". This new criterion for solids is based on the supposition that the 2D system has enough short-range order so that the local crystal structure can be defined, then if there are no free dislocations present, the system is rigid, while if the free dislocations are present, an arbitrary small shear stress will cause the dislocations to move and the system will have a response characteristic of a viscous liquid. Thus the presence or absence of free dislocations determines which phase the system has. The great advantage of this theory is that the topological defects are much easier to deal with in 2D than in 3D because now they are point defects. Nelson and Halperin[1.13] developed this idea, by defining an order parameter for bond orientation. They argued, for spherical molecules on a smooth substrate, the melting from solid to liquid might take place in two steps; there was an intermediate liquid-crystal (hexatic) phase with exponential decay of translational order but algebraic decay of six-fold orientational order. Similiar conclusion has been reached by Young independently.[1.14] This proposition invokes a long controversial problem about the nature of 2D melting. Contrary to the experimetal evidence and the results of computer simulations[1.15] for first order melting, this theory predicts two continuous transitions for 2D melting. Later, Ostlund and Halperin[1.16] applied this dislocation-mediated 2D melting theory to

anisotropic layers possibly consisting of rodlike molecules, and concluded that the melting transition might also go through two stages, but the properties of the intermediate liquid-crystal phase was more complicated because now the system has two types of dislocations. However, there are attempts to unify these two sides. Saito proposed that the order of the 2D melting transition might depend on the core energy needed to produce a topological defect pair, for large core-energy the transition is continuous, and first-order melting is found in small core-energy case.[1.17] For 2D diatomic molecular systems, the presence of the additional orientational degrees of freedom which is absent for spherical molecules, can introduce other types of possible new phases. Although the true translational long-range order is absent, the long-range orientational order can exist due to the anisotropic nature of the intermolecular interaction. Thus, between the solid and isotropic liquid phases, a plastic phase with exponential decay of orientational order but algebraic decay of translational order can emerge. The properties of the 2D plastic phase and the ferro-paraelastic phase transition are almost untouched in the literature. In addition, a liquid-crystal phase is also possible for 2D diatomic molecular systems under certain conditions.

To describe such a molecular system, we ought to know the intermolecular interaction potential. The most direct way to determine it is to solve the electronic Schrödinger equations for all relevent values of the molecular coordinates. However, to attain the accuracy required for meaningful thermodynamic calculations it is necessary to take into account the electron correlation effects, a task which has not

been performed by completely *ab initio* quantum-mechanical methods. The cohesive force which binds nonpolar molecular crystals and fluids are largely intermolecular electron correlation effects,[1.18] and are not included, for example, in a Hartree-Fock calculation. Various attempts have been made to construct an intermolecular interaction from additive atom-atom potentials which are assumed to be transferrable from one molecule to another with some success.[1.19] As mentioned above, by using an additive atom-atom potential consisting of a Lennard-Jones part and a quadrupole-quadrupole part, Etters et al.[1.10] successfully predicted the δ-phase even when the earlier neutron scattering experiment seemed to contradict their results. Because oxygen has a relatively small quadrupole moment and the magnetic coupling constant is also small compared to the intermolecular dispersion potential,[1.20] (though it is expected to play an important role at the ϵ-ζ phase transition in the high-coverage region), we did not include them in our calculations. The absence of a commensurate phase shows that the interaction between the adsorbed O_2 molecules and the graphite substrate is weak, we believe that its main role is to make the molecule lie flat on the substrate in the δ-phase. The substrate corrugation potential can be integrated over the surface resulting in a constant term which can be added to the internal energy of the system. The molecules are treated as rigid rotors. It is a good approximation to regard the lattice vibrations as consisting of translations and rotations of those rotors, since the intramolecular vibrations are generally not excited at low temperatures considered here. The system studied in this thesis consists of diatomic molecules interacting via an

intermolecular potential which is the sum of the atom-atom Lennard-Jones potentials between the constituent atoms of different molecules.

A basic concept of the modern theory of critical phenomena is "universality"; it claims that the nature of the phase transition in a particular system is determined by the symmetry of the Hamiltonian describing this system, the number of the components of the order parameter and the dimensionality of the system. According to this hypothesis, different model systems, even real physical systems, are subject to the same "universal class" if they lead to the same Hamiltonian in the Ginzburg-Landau-Wilson (GLW) form on the same lattice structure. To study the GLW Hamiltonian, many sophisticated methods of statistical mechanics are at our disposal, including the renormalization group method, the most fruitful procedure in the area of critical phenomena up till now. For 2D molecular systems, it is desirable to develop a method to derive an effective Hamiltonian which is simple enough to be tractable but without losing the essential features of the system. In Chapter 2, assuming that the centers of mass of the molecules are confined to a fixed lattice, we show that under very general conditions, the orientational motion of a 2D diatomic molecular system can be described by an effective spin Hamiltonian in the anisotropic XY form. The parameters of this spin Hamiltonian can be found by the effective parameter procedure (EPP) proposed in this chapter. We performed Monte Carlo simulations using parameters obtained by EPP, the results are encouraging when compared with that obtained from molecular dynamics simulation using the exact Hamiltonian. The advantage of this effective parameter procedure over the conventional

small parameter expansion method is discussed in this chapter.

In Chapter 3, the phase diagram and the nature of the phase transition of the effective spin Hamiltonian are studied by using various methods, including Migdal-Kadanoff real space renormalization group (MKRG) and Monte Carlo renormalization group (MCRG). The results show that in this anisotropic XY model, long-range order is present at sufficiently low temperatures and the ferro-paramagnetic phase transition is Ising-like. Under MKRG procedure, the system iterates to an Ising-like system, and MCRG gives the correlation length critical exponent a value close to that of 2D Ising system. The special feature of this model is that it supports vortex excitations while possessing the simplest domain-wall pattern. A quench study gives the first simulation picture which clearly shows the interaction between these two types of excitations. We also give an energy-entropy argument to explain why the Kosterlitz-Thouless transition observed in isotropic XY model gives way to an Ising-like transition when the anisotropy is present in our model.

The coupling between the different degrees of freedom can drastically change the nature of phase tansitions. In Chapter 4, we release the mass centers of the molecules. By minimizing the potential energy and searching for the zero point of the internal stress tensor, we find that the ground state of this system is a centered rectangular lattice, and its spacings are very close to those of the δ-phase of oxygen monolayer on graphite if we use the parameters appropriate for oxygen molecules. We conduct constant-pressure (force/length) molecular dynamics (MD) simulations to explore the phase diagram along the zero

pressure line. A ferro-paraelastic phase transition is discovered at 20.6K, the long-range orientational order is lost, the centered rectangular lattice at low temperatures becomes triangular. The discontinuities found in the orientational order parameter, the lattice anisotropy order parameter, the energy, the density and the orientational diffusion coefficient indicate that the transition is first order. The physical mechanism of this first order transition is discussed in light of the role played by topological defects. At 38.0K, this plastic phase with triangular structure melts to a liquid. Again, the discontinuities of the energy and the density suggest that the transition is first order. In addition, the MD method used in our simulations is also documented in this chapter.

CHAPTER 2

LENNARD-JONES MOLECULES ON A TWO-DIMENSIONAL LATTICE: A MODEL ANISOTROPIC XY SYSTEM

I. INTRODUCTION

A clear understanding of the observed structural phase transitions in 2D molecular "solids" requires adequate knowledge of the anisotropic intermolecular potential. The commonly used intermolecular potential consists of two parts, one (V_{es}) associated with the interaction between electrostatic multipole moments of the individual molecules and the other (V_r+V_{dis}) is the sum of short-range steric repulsion and polarization interactions. The latter two are usually obtained from an atom-atom potential model (standard Lennard-Jones potential between atoms of one molecule and those of the other).

In contrast to V_r+V_{dis}, the contribution to V_{es} from the interaction between i-th and j-th molecules can be expressed directly in terms of spherical harmonics $Y_{lm}(\hat{n}_i)$ and $Y_{l'm'}(\hat{n}_j)$, $\hat{n}_i$ and $\hat{n}_j$ being the unit vectors representing the orientations of the two molecular axes. The maximum value of l appearing in the expansion of V_{es} depends upon the electric multipole moments of the molecular species under study. For

example, the largest contribution to the intermolecular interaction for N_2 molecules comes from the latter's electric quadrupole moment which corresponds to l=2. The repulsion and dispersion contributions to the intermolecular potential can in principle be expanded[2.1] as an infinite series in powers of the parameter α=d/R, where 2d is the interatomic separation of a given molecule and R is the intermolecular separation (see Fig. 2.1). Only when α<<1, the first few terms in the spherical harmonic expansion (l<2) make the dominant contribution and the resulting Hamiltonian has a simple form. But for realistic systems such as O_2 and N_2 on a graphite substrate[2.2] α≃0.15. For these systems one has to keep many terms in the spherical harmonic expansion and the resulting Hamiltonian takes a complicated form.

To study the adequacy of the above-mentioned expansion procedure, we start from a 2D molecular solid for which the intermolecular potential is of Lennard-Jones form (the corresponding Hamiltonian is denoted as H_{exact}=H_{ex}), construct an effective spin Hamiltonian H_{sp} and compare the exact thermodynamic properties of H_{sp} and H_{ex}. Properties of H_{ex} are available from recent molecular dynamics (MD) simulation studies.[2.3] Such a comparison will tell us about the correctness of the procedure for obtaining H_{sp} from H_{ex}. Our ultimate aim is to apply a similar procedure to realistic 2D molecular systems like O_2 and N_2 on graphite which show orientational phase transitions involving both orientational and translational degrees of freedom.[2.2] Although the discussion of Sec. II and III of this chapter are quite general, for numerical studies, we have chosen a simple system where the centers of mass of the molecules are constrained to be on a 2D square lattice and

the molecular orientations are confined to the plane of the lattice. This choice was dictated by the availability of MD simulation studies in this system.[2.3]

The outline of this chapter is as follows. In Sec. II we carry out a straightforward expansion of the atom-atom potential in powers of α and analyze the thermodynamic properties of the resulting H_{sp}. We then discuss the adequacy of H_{sp} to represent H_{ex} for α values of practical interest. In Sec. III, we introduce an alternate procedure which we refer as effective-parameter procedure (EPP) to obtain H_{sp} and compare its properties with those of H_{ex}. This procedure is physically equivalent to keeping only the leading terms in the spherical harmonic expansion, but calculating the coefficients up to all orders in α. Strictly speaking, one arbitrarily drops terms in the Hamiltonian involving higher l values even if their coefficients are not small. Results of calculations for H_{sp} obtained by using EPP are given in Sec. IV and compared with the exact results to see whether one is justified in dropping higher-order spherical harmonic contributions. A brief discussion of the applicability of this procedure to N_2 and O_2 on graphite substrates follows.

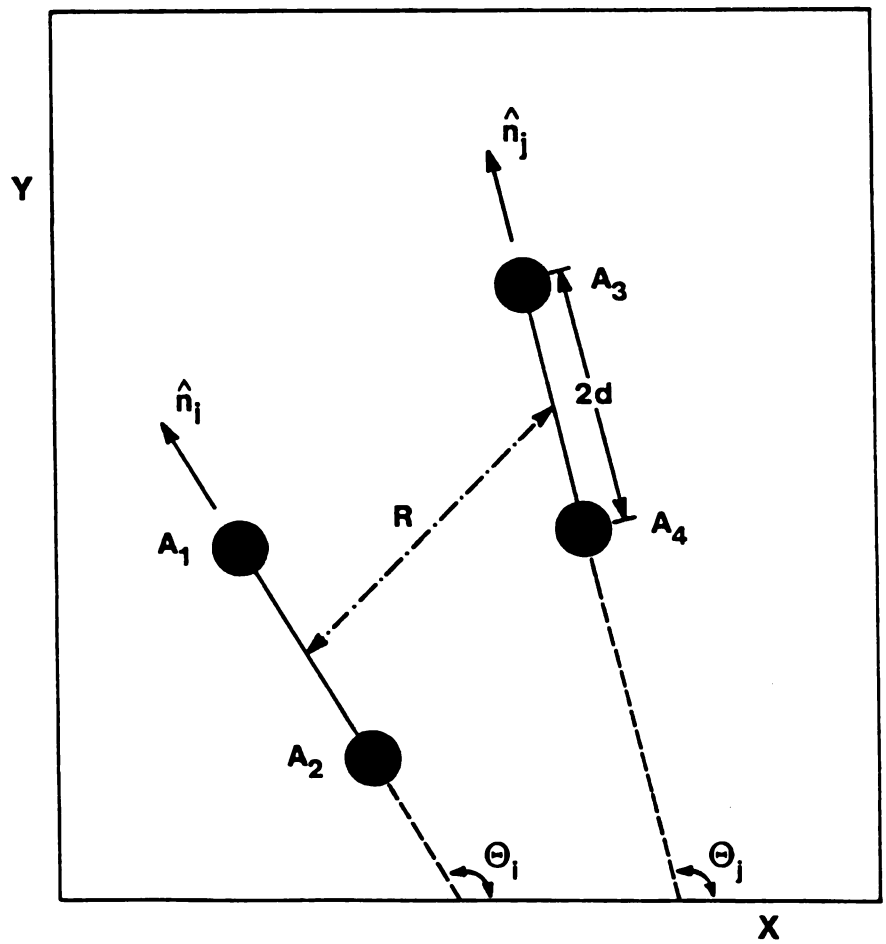

Fig. 2.1 Two diatomic molecules with intermolecular separation R and oriented along $\hat{n}_i$ and $\hat{n}_j$ directions. (A_1,A_2) and (A_3,A_4) are the atoms associated with the two molecules.

II. EFFECTIVE SPIN HAMILTONIAN (EXPANSION METHOD)

To obtain an effective Hamiltonian describing the intermolecular interaction, starting from an atom-atom potential, a straightforward method is to expand the latter in powers of the ratio a. The total Hamiltonian describing the interaction between molecules can be expressed in terms of the potential energy of interaction between i-th and j-th molecules, V_{ij}, i.e.,

$$H_{ex} = \sum_{\langle i,j \rangle} V_{ij} \qquad [2.1]$$

where

$$V_{ij} = V^{aa}_{A_1-A_3} + V^{aa}_{A_1-A_4} + V^{aa}_{A_2-A_3} + V^{aa}_{A_2-A_4}, \qquad [2.2]$$

and the atom-atom potentials $V^{aa}_{A_1-A_3}$ are given (for l =1 and m =3) by

$$V^{aa}_{A_1-A_3} = 4\epsilon[(\sigma/r_{13})^{12} - (\sigma/r_{13})^{6}]. \qquad [2.3]$$

In Eq. [2.3], $r_{13}=|(\vec{R}_i+d\hat{n}_i)-(\vec{R}_j+d\hat{n}_j)|$, is the distance between atom A_1 of the i-th molecule and the atom A_3 of the j-th molecule (see Fig. 2.1) ; $\vec{R}_i$ and $\vec{R}_j$ are the positions of the respective molecular centers of mass. Expanding V_{ij} in powers of a and keeping terms up to $O(a^4)$, we find that the pair interaction energy V_{ij} is given (in unit of 4ϵ) by

$$V_{ij} = v^0_{ij} + \sum_{k=i,j} h_k[s_{kx}\cos(2\psi_{ij}) + s_{ky}\sin(2\psi_{ij})] \qquad [2.4]$$
$$+ \sum_{k=i,j} D_{ij}[(s^2_{kx} - s^2_{ky})\cos(4\psi_{ij}) + 2s_{kx}s_{ky}\sin(4\psi_{ij})]$$
$$+ J_{ij}(s_{ix}s_{jx} + s_{iy}s_{jy})$$
$$+ K_{ij}[(s_{ix}s_{jx} - s_{iy}s_{jy})\cos(4\psi_{ij}) + (s_{ix}s_{jy} + s_{iy}s_{jx})\sin(4\psi_{ij})]$$

where ψ_{ij} is the angle that the vector connecting i and j sites makes with the x-axis (see Fig. 2.1) and

$$s_{kx} = \cos(2\theta_i), \quad s_{ky} = \sin(2\theta_j). \qquad [2.5]$$

The parameters appearing in [2.4] are given by

$$v_{ij} = (\sigma/R)^{12}(4 + 288a^2 + 10584a^4) - (\sigma/R)^6(4 + 72a^2 + 864a^4), \qquad [2.6a]$$

$$h_k = (\sigma/R)^{12}(168a^2 + 10752a^4) - (\sigma/R)^6(48a^2 + 960a^4), \qquad [2.6b]$$

$$D_{ij} = [1008(\sigma/R)^{12} - 120(\sigma/R)^6]a^4, \qquad [2.6c]$$

$$J_{ij} = [3528(\sigma/R)^{12} - 288(\sigma/R)^6]a^4, \qquad [2.6d]$$

$$K_{ij} = [6048(\sigma/R)^{12} - 720(\sigma/R)^6]a^4. \qquad [2.6e]$$

In the above, $R = R_{ij}$ and $a = d/R_{ij}$. If we consider only the nearest-neighbor interaction,[2.4] take the x-direction along a lattice bond and sum up all the pair potentials, the terms which are linear in $\cos(2\theta_i)$, $\sin(2\theta_i)$ drop out due to the symmetry of the square lattice, and the anisotropic part of the total Hamiltonian,

$$H_{sp} = \sum_{\langle i,j \rangle} (V_{ij} - v^0_{ij})$$

reduces to a simpler form given by

$$H_{sp} = \sum_i 4D(s_{ix}^2 - s_{iy}^2) + \sum_{\langle i,j\rangle} J(s_{ix}s_{jx}+s_{iy}s_{jy}) + \sum_{\langle i,j\rangle} K(s_{ix}s_{jx}-s_{iy}s_{jy}) \qquad [2.7]$$

where $\langle ij\rangle$ indicates all the nearest-neighbor pairs and D, J, K are those given by Eqs. (6c), (6d) and (6e) with R_{ij} equal to the nearest-neighbor distance. H_{sp} has the form of an XY model which has both single-site and interaction anisotropies.

Before discussing the finite-T properties of H_{sp} and comparing them with results of MD simulation, we would like to discuss briefly the nature of the ground state of H_{sp} for arbitrary values of anisotropy and interaction parameters D, J and K. Using the Luttinger-Tisza method,[2.5] we find the ground state of H_{sp} for different parameter values. The ground state is always a commensurate structure, and the Luttinger-Tisza method works.[2.6] We also find that, depending on the parameter values, there are six possible ground-state configurations: two antiferromagnetic (AF1, AF2), two ferromagnetic (F1, F2), and two herringbone type (HB1, HB2). These are shown in Fig. 2.2. In Fig. 2.3 we give the range of parameter values for which one of the above structures has the lowest energy.

To test the adequacy of the expansion up to $O(a^4)$ in obtaining the parameters of H_{sp}, we have calculated the orientational order-disorder transition temperature T_c of H_{sp} using mean-field approximation and compared it with the MD results for H_{ex}. The parameters used in the later calculations are:

ϵ =131.3x10^{-16} ergs, σ =3.708 Å,

D =0.6438 Å, and R =4.2488 Å.

Using these values for the parameters in Eqs. (6c), (6d) and (6e), we find D, J and K (expressed in unit of 10^{-16}ergs) equal to 39.78, 155.38, and 238.70, respectively.

The ground-state configuration for the above values of D, J and K is of the type AF2 which is in agreement with the low-temperature results of the MD simulation. For T>0, we assume that the molecules fluctuate about the orientations they have in the ground state, i.e., we assume that thermal averages of s_{jx} and s_{jy} are given by

$$\langle s_{jx} \rangle = (-1)^{l_{jx}+l_{jy}} \eta \qquad [2.8a]$$

and

$$\langle s_{jy} \rangle = 0 \qquad [2.8b]$$

where η is the order parameter and l_{jx}, l_{jy} are integers labelling the lattice sites. Approximating H_{sp} by its mean-field value H_{MF}, where

$$H_{MF} = \sum_i [4D(s_{ix}^2 - s_{iy}^2) + (J+K)s_{ix}\eta \Sigma (-1)^{l_{jx}+l_{jy}}] \qquad [2.9]$$

and defining $s_{ix}=\cos\theta$ and $s_{iy}=\sin\theta$ (note θ is not the orientation of molecule from now on), we find that

$$\eta = \frac{Tr(e^{-\beta H_{MF}} s_{ix})}{Tr(e^{-\beta H_{MF}})}$$

$$= \frac{\int_0^{2\pi} \cos\theta \exp[-4\beta D\cos(2\theta) + 4\beta(J+K)\eta\cos\theta]\, d\theta}{\int_0^{2\pi} \exp[-4\beta D\cos(2\theta) + 4\beta(J+D)\eta\cos\theta]\, d\theta} \qquad [2.10]$$

Assuming the transition to be continuous, we expand the right-hand side

in powers of η and calculate the mean-field transition temperature T_c^{MF} in the usual way.[2.7] The transition temperature is given by the transcendental equation

$$T_c^{MF} = \frac{2(J+K)}{k_B} \frac{2I_2(\beta_c)}{I_0(\beta_c)} \qquad [2.11]$$

where

$$I_{2n}(\beta) = \int_0^{2\pi} \cos^{2n}\theta \exp[-4D\beta\cos(2\theta)]d\theta \qquad [2.12]$$

Numerical calculation gives the reduced transition temperature $t_c^{MF}=k_BT_c^{MF}/\epsilon=5.3$. This is about a factor of 1.6 smaller than $t_c^{MD}=t_c^{ex}=8.4$ which was obtained from MD calculations for the full Hamiltonian H_{ex}.[2.3] Since the mean-field approximation neglects effects of fluctuations, one expects the exact transition temperature to be smaller than t_c^{MF}. Therefore, the exact transition temperature of H_{sp} is likely to be considerably smaller than the exact transition temperature of H_{ex}. This suggests that there is a serious deficiency in representing H_{ex} by H_{sp}.

To make further checks on the validity of the above expansion procedure used to obtain H_{sp} we have investigated the low-temperature behavior of a system described by H_{sp} using spin-wave approximation. At sufficiently low temperatures, we expect the deviation from the ground-state orientation to be small and therefore simplify H_{sp} by expanding θ_i about its ground-state value. Using $\theta_i=\theta_i'$, in one sublattice, and $\theta_j=\pi+\theta_j'$ in the other sublattice, where θ_i' and θ_j' are small, at low temperatures we have

$$H_{sp} = \sum_i 4D[1-(2\theta'_i)^2/2] - \sum_{\langle i,j\rangle} \{J[1-(\theta'_i-\theta'_j)^2/2] + K[1-(\theta'_i+\theta'_j)^2/2]\} \quad [2.13]$$

After dropping the constant term and the prime index, we find that

$$H_{sp} = H_{sw} + \text{const},$$

where the spin-wave Hamiltonian H_{sw} is given by (for J>0, K>0, and K>J)

$$H_{SW} = (2J + 2K - 8D) \sum_i \theta_i^2 + \sum_{\langle i,j\rangle} (K-J)\theta_i\theta_j \quad [2.14]$$

The spin-spin correlation function between one spin at the origin and the another at $\vec{r}$ lattice site is given by

$$g(\vec{r}) = \langle\cos(\theta_0-\theta_{\vec{r}})\rangle = \mathrm{Re}\langle\exp[i(\theta_0-\theta_{\vec{r}})]\rangle \quad [2.15]$$

We can calculate $g(r)$ following the procedure used by Wegner[2.8] for the isotropic limit (D=K=0) and obtain

$$g(\vec{r}) = \exp\left[-\frac{k_B T}{N} \sum_{\vec{k}} \frac{\sin^2(\vec{k}\cdot\vec{r}/2)}{\epsilon_{\vec{k}}}\right] \quad [2.16]$$

where, $\epsilon_{\vec{k}}$, the energy of spin-wave with wave-vector $\vec{k}$, is given by

$$\epsilon_{\vec{k}} = 2(K+J-4D)[1+\gamma(\cos k_x+\cos k_y)] \quad [2.17]$$

and

$$\gamma = (K-J)/2(K+J-4D) \quad [2.18]$$

In Eqs. [2.16] and [2.17] the distances are measured in units of the nearest-neighbor distance. In the thermodynamic limit, we can replace the summation over $\vec{k}$ by an integral over the square Brillouin zone. Following the notion of Wegner, we write

$$g(\vec{r}) = \exp\left[-\frac{k_B T}{2(K+J-4D)} f_2(\vec{r})\right] \quad [2.19]$$

where

$$f_2(\vec{r}) = \frac{1}{2\pi^2}\int_{-\pi}^{\pi} dk_x \int_{-\pi}^{\pi} dk_y \frac{\sin^2(\vec{k}\cdot\vec{r}/2)}{1+\gamma(\cos k_x+\cos k_y)} \qquad [2.20]$$

If $|\gamma|<1/2$, the integrand has no singularity in the first Brillouin zone. This condition is usually satisfied in the case of diatomic molecules physisorbed on a substrate, and is true for the parameters in this chapter. Thus, the anisotropy of the Hamiltonian eliminates the "infrared catastrophe" which is present in the isotropic XY model. In the limit $r\to\infty$, $g(\vec{r})$ is finite. For $T\to 0$ the order parameter is given by(2.9)

$$\eta = \lim_{r\to\infty}[g(\vec{r})]^{1/2} = 1 - aT, \qquad [2.21]$$

where

$$a = \frac{k_B T}{4(K+J-4D)} \frac{1}{(2\pi)^2}\int_{-\pi}^{\pi} dk_x \int_{-\pi}^{\pi} dk_y \frac{1}{1+\gamma(\cos k_x+\cos k_y)} \qquad [2.22]$$

We refer to a as the low-temperature order-parameter coefficient. Using the parameter of H_{sp} obtained by expansion to $O(a^4)$, we find that $a=0.074$. The value of a given by MD simulation of H_{ex} is 0.040. Thus comparing the values of transition temperatures t_c and a obtained from H_{sp} and H_{ex}, we conclude that the physical system represented by H_{sp} is quite soft.

As a plausible cause of this large discrepancy between mean-field and spin-wave results for H_{sp} and MD results for H_{ex}, we have explored the effect of further neighbors which were included in the MD simulations. For the parameters of interest this can be ruled out. For example, when we include 24 neighbors (in a 5x5 square lattice), the mean-field critical temperature changes by only about 0.4%.

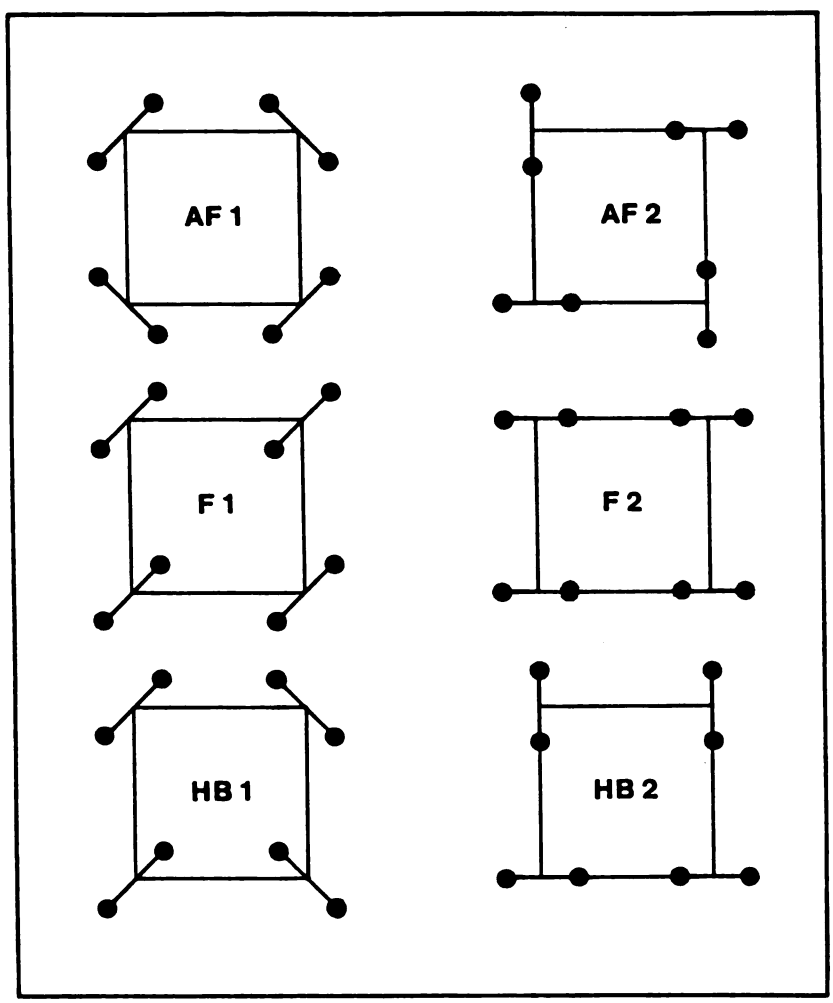

Fig. 2.2 Various ground-state configurations of the molecules whose centers of mass are confined to a square lattice. AF denotes antiferromagnetic; F denotes ferromagnetic; HB denotes herringbone.

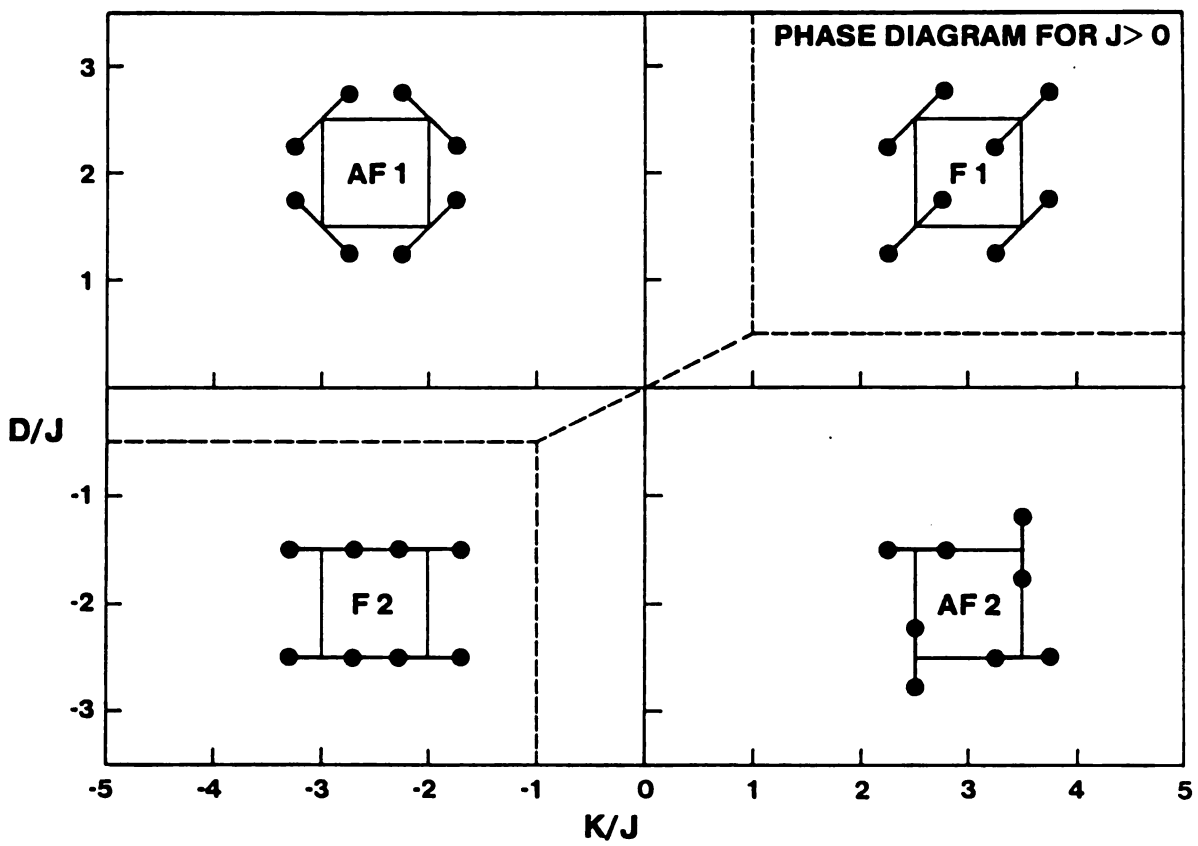

Fig. 2.3 Ground-state configurations for different values of D/J and K/J for J>0. For J<0, turn the figure upside down but keep K/J and D/J axes in coventional directions (i.e., positive to the right and up,respectively). HB structure can be ground state only when J=K=0, so it does not appear in this figure.

III. EFFECTIVE-PARAMETER PROCEDURE (EPP)

Because of the above-mentioned shortcomings associated with H_{sp} obtained from H_{ex} by expanding up to $O(a^4)$, we have to investigate the convergence of the expansion procedure. If we expand the pair interaction up to $O(a^6)$, we find that for the square lattice and AF1, AF2, F1, F2 configurations,[2.10] the total Hamiltonian still has the form of Eq. [2.7], but now (in units of 4ϵ)

$$D = [1008(\sigma/R)^{12}-120(\sigma/R)^6]a^4 + [72576(\sigma/R)^{12}-3024(\sigma/R)^6]a^6 \quad [2.23]$$

$$J = [3528(\sigma/R)^{12}-288(\sigma/R)^6]a^4 + [150528(\sigma/R)^{12}-4800(\sigma/R)^6]a^6 \quad [2.24]$$

$$K = [6048(\sigma/R)^{12}-720(\sigma/R)^6]a^4 + [241920(\sigma/R)^{12}-10080(\sigma/R)^6]a^6 \quad [2.25]$$

Except where a is very small ($a<<1$), the terms in the second brackets in D, J and K are quite comparable to those in the first brackets. Thus, a straightforward expansion procedure is not very encouraging. A simple estimate shows that for a configuration where the two molecules are oriented parallel to each other, the Taylor-series expansion of the interaction potential energy in a is given by $H=\sum_{n=0}^{\infty} a_n a^{2n}$. To obtain an accuracy of three digits of the potential energy for a=0.152, we have to keep terms with n=7, i.e., up to $O(a^{14})$ term. For parameters D, J and K, the convergence is even poorer. They increase rapidly for the first few terms and then decrease slowly. Furthermore, the Hamiltonian becomes more complicated as it contains terms which are of higher powers in s_{ix}, s_{iy} and a finite-T study of such complicated Hamiltonians is

practically impossible.

To avoid the difficulty associated with the expansion procedure, we use a different method to obtain an effective spin Hamiltonian. We assume that the interaction potential can be represented reasonably well by the form given in Eq. [2.7]. We have therefore four quantities, v_0, D, J and K, to be determined. We determine these parameters by fitting the four ground-state configurations AF1, AF2, F1, and F2, (two antiferromagnetic and two ferromagnetic). We call this the effective-parameter procedure (EPP). The values of D, J and K obtained by this procedure are found to be considerably different from those obtained by expanding up to either a^4 or a^6, and are discussed in the next section. We should point out that the above procedure is equivalent to writing

$$V_R + V_{dis} = \sum_{l,m} \sum_{l',m'} C_{lm,l'm'} Y_{lm}(\hat{n}_i)\, Y_{l'm'}(\hat{n}_j) \qquad [2.26]$$

and calculating the leading order coefficients $C_{lm,l'm'}$ by actual numerical integration. As we shall show in the next section, the coefficients obtained by the two procedures are very close (not exactly equal) to each other.

IV. RESULTS AND DISCUSSION

For the values of ϵ and σ given in Sec. II, the effective-parameter procedure gives values for D, J and K which are given in Table 2.1. The corresponding quantities obtained by direct integration (form Eq. [2.26]) are given inside brackets in the same table. These values are reasonably close to each other and differ drastically from those obtained by the expansion procedure carried out up to $O(\alpha^4)$. The model anisotropic XY system (described by H_{sp}) gives a reasonable value for the mean-field transition temperature (t_c^{MF}) and an excellent description of the low-temperature behavior of the order parameter obtained from the spin-wave approximation (see Table 2.2). It gives 0.042 for the coefficient a (see Eq. [2.21]) and the mean-field transition temperature t_c^{MF} is 15.3. To obtain the exact transition temperature for H_{sp}, we use a Monte Carlo (MC) procedure. Since MD calculations were performed for a 30x30 sample, we also use a same size sample for our MC simulation. We use periodic boundary condition and heat the system starting from the ground-state AF2 configuration (T=0). We find that after about 1000 MC steps per spin (MCS/S), the system reaches thermodynamic equilibrium for almost all the temperatures studied. We find that the transition temperature t_c^{MC} is between 8.2 to 8.7, the order parameter (see Fig. 2.4) drops sharply from 0.5 to 0.2 in this temperature range. In Fig. 2.4 we also give the results of the molecular dynamics calculations of Ref. (2.3). The agreement is very good if we note that MC calculations were performed with only 1000 MCS/S, whereas in the MD simulations the system was allowed to run uninterruptedly for several

thousand time steps (10000 to 20000) near the transition region.

In summary, the anisotropic XY Hamiltonian (Eq. [2.7]) with parameters obtained either by fitting to several ordered configurations or by numerical integration of the spherical harmonic expansion describes the thermodynamics of the actual system interacting via atom-atom Lennard-Jones potential reasonably well. For molecules like N_2, which possesses a relatively large electric quadrupole moment, the quadrupole-quadrupole interaction will also contribute to the parameters J and K of Eq. [2.7] and one should add these contributions, i.e.,

$$J = J_{LJ} + J_Q$$

$$K = K_{LJ} + K_Q$$

$$D = D_{LJ}$$

where J_{LJ}, K_{LJ} and D_{LJ} are obtained by using the effective-parameter procedure discussed in this chapter.

Table 2.1

The spin Hamiltonian parameters D, J and K of eqn. [2.7] obtained by expansion up to $O(a^4)$ and the effective parameter procedure (see text). All parameters are in units of 10^{-16}ergs.

parameters	Effective-parameter procedure	Expansin to $O(a^4)$
D	222 (221)	40
J	524 (483)	155
K	755 (741)	239

Table 2.2

The low-temperature order parameter coefficient a obtained by spin wave approximation and the reduced transition temperature t_c for different Hamiltonians. t_c has been obtained using mean-field approximation, Monte Carlo, and molecular dynamics calculations.

Model	a	t^{MF}	t^{ex}
Expansion $O(\alpha^4)$	0.074^a	5.3	X
Effective-parameter procedure	0.042^a	15.3	8.5 ± 0.2^c
Exact Hamiltonian	0.040^b	X	8.3 ± 0.1^b

a: Spin wave theory.

b: Molecular Dynamics.

c: Monte Carlo.

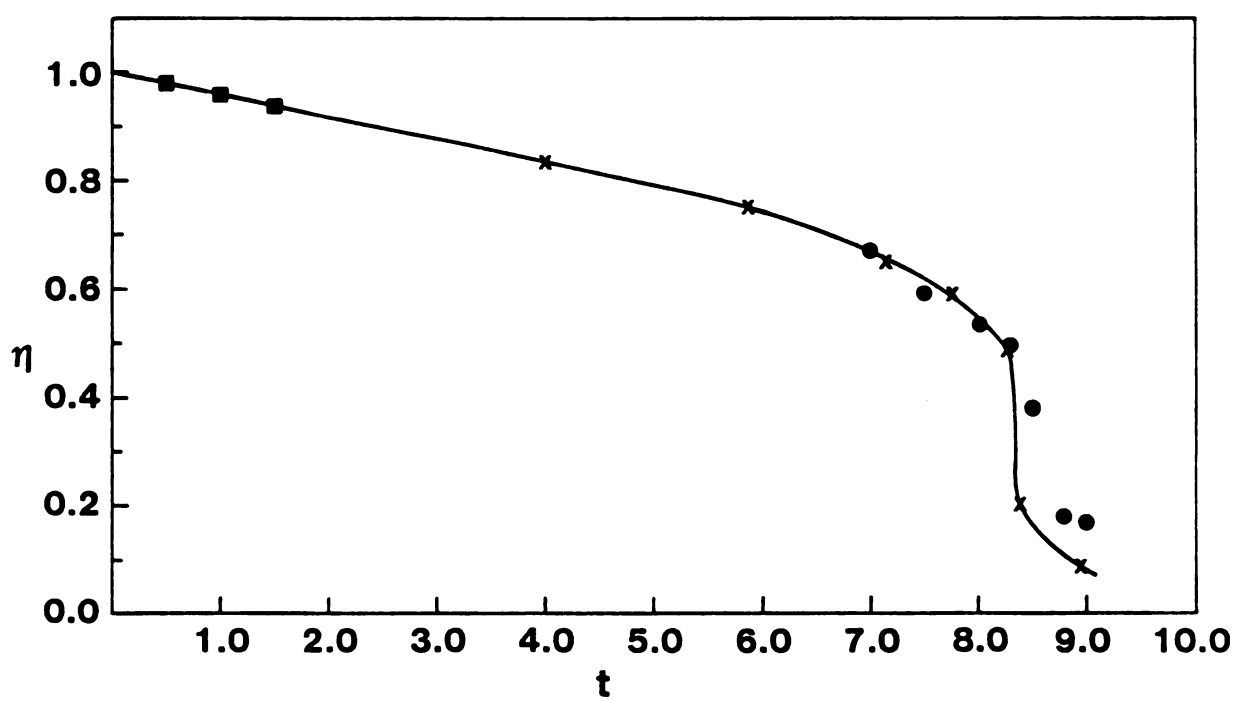

Fig. 2.4 Temperature dependence of the order parameter η. x denotes molecular dynamics results of H_{ex}, • denotes Monte Carlo results of H_{sp}, (obtained by using effective parameter procedure discussed in Sec. III of this chapter); ■ denotes spin wave results of H_{sp}.

CHAPTER 3

PHASE TRANSITION IN

ANISOTROPIC PLANAR ROTOR SYSTEM

I. INTRODUCTION

In recent years there has been considerable interest[3.1] in 2-dimensional (2D) or quasi-2D physical systems consisting of molecules adsorbed on a surface. Under certain physical conditions,[3.2] the molecular interaction V_{ij} can be represented reasonably well in the form[3.3]

$$V_{ij} = V_0 - J_{ij}\cos(\theta_i-\theta_j) - K_{ij}\cos(\theta_i+\theta_j+2\psi_{ij}) - A_{ij}[\cos(2\theta_i+2\psi_{ij})+\cos(2\theta_j+2\psi_{ij})] \qquad [3.1]$$

where θ_i is related to the orientation of the i-th molecular axis and ψ_{ij} is an angle describing the orientation of the intermolecular bond with respect to a preferred anisotropy axis. A useful method to derive such a spin representation for a realistic interaction was discussed in chapter 2. This mapping enables us to use various theoretical methods developed for attacking magnetism problems to the study of phase transition in 2D molecular systems.

The simplest Hamiltonian arising from V_{ij} is of the form

$$H = -J \sum_{\langle i,j \rangle} \cos(\theta_i - \theta_j) - K \sum_{\langle i,j \rangle} \cos(\theta_i + \theta_j + \phi_{ij}) \qquad [3.2]$$

The above Hamiltonian was used to study the properties of N_2 molecules on a graphite substrate for particular values of J and K.[3.4] However, a detailed study of the properties of H given in [3.2] in the entire parameter space is lacking and should be extremely interesting because of the growing attention to the molecular overlayer systems physisorbed on solid substrates. It is our purpose to present such a study in this chapter. Furthermore, this Hamiltonian by itself is well worth scrutinizing theoretically from the point of view of the role played by topological excitations in the phase transitions of 2D systems. Great effort was given to explore the driving mechanism of the phase transition in the present model.

For simplicity, we choose J>0, K>0, ϵ=K/J<1 and assume the rotors to be on a square lattice. On a square lattice, the angle ϕ_{ij} is a multiple of 2π, so it can be dropped and H is now written as

$$H = -J \sum_{\langle i,j \rangle} \cos(\theta_i - \theta_j) - K \sum_{\langle i,j \rangle} \cos(\theta_i + \theta_j) \qquad [3.3]$$

In this form, for K>J case, by replacing θ_i with $-\theta_i$ in one sublattice, we can interchange the roles of J and K in [3.3] and map it to J>K case.

The Hamiltonian given in [3.3] reduces to the well-known isotropic planar rotor (classical XY model) model for K=0. The 2D XY model has a very instructive history. For 2D isotropic Heisenberg model, which covers the 2D XY model, Mermin and Wagner[3.5] have rigorously proved that the long-range order can not exist at any finite temperature. But Stanley and Kaplan[3.6] pointed out the possibility of the existence of a low-temperature (low-T) in which, though LRO is lost, the spin-spin

correlation decays so slowly that the susceptibility becomes infinite (and remains so throughout this low-T phase), and gave evidence of a finite temperature phase transition for the 2D Heisenberg model, based on the analysis of high temperature series expansion for the susceptibility. Stanley gave similar evidence of such a transition for the XY model. Kosterlitz and Thouless[3.7] clarified the nature of the low-T phase by introducing the concept of "topological order". They contended that the low-T phase is characterized by the power-law decay of the spin-spin correlation, as proved by Wegner[3.8] with spin-wave approximation. However, the presence of the "topological defects", i.e., tightly bound vortex-antivortex pairs, modifies the harmonic picture. Now the local minimum, from which the small angle deviations excited by spin-wave are measured, not only has some kind of short-range order, but also contains vortices which interact with each other via a 2D coulomb potential logarithmic with respect to their separations. At the transition the pairs unbind and it leads to a new phase in which the spin-spin correlation decays exponentially. Bearing this new idea in mind, Jose et al.[3.9] have studied the effect of symmetry-breaking field terms of the form $h_p\cos(p\theta)$ on the isotropic XY model (JKKN model). They found for $p>4$, the system has two phase transitions; the one seen at lower temperature is conventional and the other at high temperature is KT-type. Between the low-T p-state ordered phase and high-T paramagnetic phase, there is an intermediate XY-like phase. If $p=4$, the system only has one phase transition but with non-universal critical exponents. For $p=2,3$, the system shows one phase transition but its nature is unclear when h_p is small. Similar picture is found in

the isotropic p-state clock model (Z_p model). For Z_p model, Einhorn et al.[3.10] have argued that in the low temperature ordered phase the vortex-antivortex (VA) pairs are bound to each other with strings which are domain boundaries constructed by the links in the dual lattice. In the original lattice, the orientation of spin changes by almost the same amount when one crosses any link of a particular string. The strings become floppy at certain temperature T_1, this results in the loss of LRO but the VA pairs are still bound to each other through a logarithmic potential. It leads to a KT-like phase which is then destroyed by the unbinding of VA pairs at a higher temperature T_2.

The theoretical advance in this area has been helped by the progress in computer simulations. Due to the lack of direct experimental verification, the computer simulation is an indispensable source of information. For example, the beautiful Monte Carlo results of Tobochnik and Chester[3.11] give a convincing proof of the KT theory.

Motivated by the above development, the immediate questions we would ask when faced with our model described by [3.3] are a) is there any phase transition in the system, if yes, then, how many; b) what is the nature of the phase transition, if the system could at least have one. Especially when the anisotropy is very small, does it have a significient effect on the KT transition? The quest for answers to the above questions concerns the rest of this chapter.

A special feature of our model described by [3.3] is that it allows for vortex excitation and yet has the simplest, namely 2, domain pattern due to the 2-fold degeneracy of the ground-state. In particular, we investigate a) the effect of the interaction anisotropy ($K \neq 0$) on the

Kosterlitz-Thouless (KT) transition;[3.7] b) the physical picture underlying the order-disorder transition for 2D anisotropic rotors; and c) the interplay of vortex and domain-wall excitation. The study of this interplay as a function of anisotropy is very important because of the role the domains show in the two phase transitions seen in the Z_p model for $p>p_c>4$. However, for the Z_p model, the 2-domain system (p=2) does not have vortex excitations, and when vortices do appear (p>4), the domain-wall structure is quite complicated for simulation studies.[3.12] Therefore the Z_p model is not ideally suited for studying the interaction between domains and vortices.

The remainder of this chapter is organized into 6 sections. In Sec. II we give the low-temperature spin-wave results to show the existence of the long-range order. Sec. III is devoted to the Migdal-Kadanoff real-space renormalization group (MKRG) procedure. In the low-temperature spin-wave approximation, our model is similar to the JKKN model with p=2. However, for the p=2 case,[3.9] when the single-site anisotropy is extremely small, i.e., the most interesting situation, Jose et al. did not give a conclusive result regarding the nature of the phase transition--whether it is KT type or something else, within the framework of Migdal-Kadanoff renormalization group. By using our real-space MKRG, we were able to show, even when K is as small as K/J=0.0001, our model iterated to an Ising-like system so the phase transition should be Ising-like. To substantiate our MKRG results, we performed Monte Carlo renormalization group (MCRG) simulations and the results are presented in Sec. IV. MCRG shows that the phase transition is Ising-like and the critical temperatures given by MKRG are in

excellent agreement with that obtained in MCRG. In Sec. V, applying a quench process, we are able to give the first computer simulation picture which shows the interaction between the vortices and domain-wall excitations. Unlike what one may intuitively imagine that all the strings from one vortex terminate at an opposite vortex thus completing a VA pair, we find that the strings from one vortex tend to bifurcate in our model and to meet more than one vortex with opposite sign. Then we provide an energy-entropy argument to explain this phenomenon and why, as long as the anisotropy is present, the phase transition shifts from KT type seen in an isotropic XY model to Ising-like in our model. Sec.VI contains an additional check for our results by employing high temperature series expansion approach. Finally, a short summary is presented in Sec. VII.

II. LOW-TEMPERATURE SPIN-WAVE APPROXIMATION

The ground state of our model is 2-fold degenerate, the spins orient either in the positive x-direction or in the negtive x-direction. At sufficiently low temperature, we can assume the spins only deviate a small angle from their zero-temperature positions. We start from one of the ground-state configurations in which the spins orient along the x-direction, and denote the angular deviations as θ'. We rewrite [3.3] as

$$H = -J \sum_{\langle i,j \rangle} [1-(\theta'_i-\theta'_j)^2/2] - K \sum_{\langle i,j \rangle} [1-(\theta'_i+\theta'_j)^2/2] \qquad [3.4]$$

Following Wegner,[3.8] after a Fourier transform, we find the spin-wave excitation spectum is given by

$$\epsilon_{\vec{k}} = 2(J+K) \left[1- \frac{J-K}{2(J+K)} (\cos k_x + \cos k_y) \right] \qquad [3.5]$$

If $K \neq 0$, then $(J-K)/2(J+K)$ will be always less than half, thus the excitation energy will never be zero if the anisotropy is present. It means that the ground-state structure where we start from is stable uder spin-wave purturbation. The system can possess LRO at sufficiently low temperatures. In contrast, there is no energy gap between the ground-state and excited states for the isotropic XY model and long wave-length spin-wave excitations destroy LRO at any finite temperature.

The order parameter $\eta = \langle \cos\theta_i \rangle$ can be calculated from the correlation function

$$g(\vec{r})=\exp\left[-\frac{k_B T}{N}\sum_{\vec{k}}\frac{1-\cos(\vec{k}\cdot\vec{r})}{\epsilon_{\vec{k}}}\right]$$

In the thermodynamic limit we can replace the sum by an integral over the first Brillouin zone,

$$g(\vec{r})=\exp\left[-\frac{k_B T}{4(J+K)}f(\vec{r})\right] \qquad [3.6]$$

where

$$f(\vec{r})=\frac{1}{(2\pi)^2}\int_{-\pi}^{\pi}\int\frac{1-\cos(\vec{k}\cdot\vec{r})}{1-\gamma(\cos k_x+\cos k_y)}\,dk_x dk_y \qquad [3.7]$$

and $\gamma=(J-K)/2(J+K)$. If $K\neq 0$, γ will be less than 1/2, so there is no singularity in the integrand of [3.7]; thus the anisotropy eliminates the "infrared catastrophe" seen in the isotropic XY model. In the thermodynamic limit, the relation between the order parameter and the correlation function is

$$\eta^2 = \lim_{r\to\infty} g(\vec{r}) \qquad [3.8]$$

For very large r, we can drop the fast oscillating term $\cos(\vec{k}\cdot\vec{r})$, then by transforming [3.7] into an elliptic integral, we were able to derive an expression for the order parameter

$$\eta = \exp\left\{-\frac{k_B T}{4J}\frac{1}{(1+\sqrt{\epsilon})^2}\sum_{n=1}^{\infty}\left[\frac{(2n-1)!!}{(2n)!!}\right]^2 a^{2n}\right\}$$

$$= \exp\left\{-\frac{k_B T}{4J}\frac{1}{(1+\sqrt{\epsilon})^2}\left[1+\frac{1}{4}a^2+\frac{9}{64}a^4+O(a^6)\right]\right\}, \qquad [3.9]$$

where

$$\epsilon=K/J,\ a=\left(\frac{1-\sqrt{\epsilon}}{1+\sqrt{\epsilon}}\right)^2 .$$

The convergence is satisfactory for K not too small, for example, if K is 0.1J, the expansion parameter a^2 has a value 0.0728. When $\epsilon=0$, i.e. $a=1$, the series in [3.9] will diverge. In fact, in the small K limit, the leading term in this series is $-\frac{1}{\pi}\ln\epsilon$.

[3.9] was used to check the Monte Carlo results at low temperature; the agreement is good below a third of the critical temperature.

III. MIGDAL-KADANOFF REAL-SPACE RENORMALIZATION GROUP PROCEDURE

To get a general idea about the phase diagram for H given in [3.3] we have used the Migdal-Kadanoff[3.13] real-space renormalization group procedure. We first move the vertical bonds and decimate the horizontal ones by integrating the partition function directly, and then move the bonds horizontally while decimating the vertical bonds. After these two operations, we take an average to restore the symmetry of the renormalized Hamiltonian. The above procedure defines an iteration in our calculation. We use a 60x60 matrix to store the interaction $V(\theta_i,\theta_j)$, after the initial values being input, all the numerical evolution can be done on it, the renormalized interaction can be obtained by

$$V'(\theta_1,\theta_2) = -\ln \int_{-\pi}^{\pi} d\theta_3 \exp[-V(\theta_1,\theta_3)-V(\theta_2,\theta_3)], \qquad [3.10]$$

where the absorption of the temperature into the potential is understood.

Even for a Hamiltonian initially without single-site field terms of the form $h_p\cos(p\theta)$, if $K\neq 0$, such terms will be generated in MKRG procedure. This is a reason why we can drop field term in [3.1] to get [3.2] without sacrificing the generality of our model. The treatment of this on-site field terms in MKRG procedure is non-trivial. We did not move them along with the bonds in view of the fact that when the Hamiltonian consists of on-site field terms only, it does not change after decimation. At high temperature our Hamiltonian does iterate to a

form where only the on-site field terms survive. So, after the iteration, we calculate the Fourier coefficients

$$C_m = \int\int_{-\pi}^{\pi} d\theta_1 d\theta_2 \cos(m\theta_1) V(\theta_1,\theta_2)$$

$$S_n = \int\int_{-\pi}^{\pi} d\theta_1 d\theta_2 \sin(n\theta_1) V(\theta_1,\theta_2)$$

up to m,n =6, which determine the strength of the on-site field terms, and keep them in the sites when we move the bonds which is now treated as only associated with the interaction. Explicitly, now eqn. [3.10] can be rewritten as

$$V'(\theta_1,\theta_2) + \sum_q h'_q [q(\theta_1)+q(\theta_j)] \qquad [3.11]$$

$$= -\ln \int_{-\pi}^{\pi} d\theta_3 \exp[-V(\theta_1,\theta_3)-V(\theta_2,\theta_3)- \sum_q h_q q(\theta_3)]$$

$$+ \sum_q h_q [q(\theta_1)+q(\theta_2)],$$

where $q(\theta)$ is of the forms $\cos(p\theta)$ or $\sin(p\theta)$. We look upon the on-site field terms generated in the MKRG procedure as some kind of average field produced by the decimated neighboring spins. We believe that this treatment of the on-site field terms improves the earlier calculations which effectively moved both the on-site field term and the interaction term.

As a check of the reliability of the above procedure, we have applied it to the JKKN model. When h_p=0, i.e., the isotropic XY case, there are two regions of J, in one the coupling J iterates to zero directly, but in the other J first increases to a certain value, then

decreases very slowly to zero. It indecates that during the iterations, certain other kinds of interactions with same global symmetry as J are produced though they are very small. We estimate that the turnout point is J=1.1, thus T_c=0.91, reasonable in comparison with the values obtained by other methods. For example, Tobochnik and Chester derived T_c=0.89.[3.11] For p=6, it appears there are three regions, one in which J goes to zero but h_6 has a fixed value, in the second both J and h_6 grow to infinity, and in the third (intermediate region), J first increases and then decreases slowly to zero. This is consistent with the findings of Jose et al.[3.9] discussed in Sec.I Introduction.

For our model, we find that as long as K≠0 (K/J≥0.0001), only after 10 to 20 iterations, the renormalization Hamiltonian H' can be represented by a simple form (see Fig. 3.1)

$$H' = -J_x \Sigma \cos\theta_i \cos\theta_j - A' \Sigma \cos(2\theta_i) \qquad [3.12]$$

with a small correction of the form $\Sigma A_p \cos(p\theta_i)$, p>2. There exists a temperature T_c such that for $T<T_c$, both J' and A' iterate to infinity (T=0 fixed point); for $T>T_c$, A' iterates to a fixed value while J' approaches zero implying that the system iterates to a non-interacting Ising spin system. The form [3.12] is Ising-like, it suggests that the nature of phase transition could be Ising-like. The transiton temperatures obtained from MKRG are very close to those given by Monte Carlo renormalization group simulations (see Table 3.1). The projection of the RG flow on J-K plane is given in Fig. 3.2.

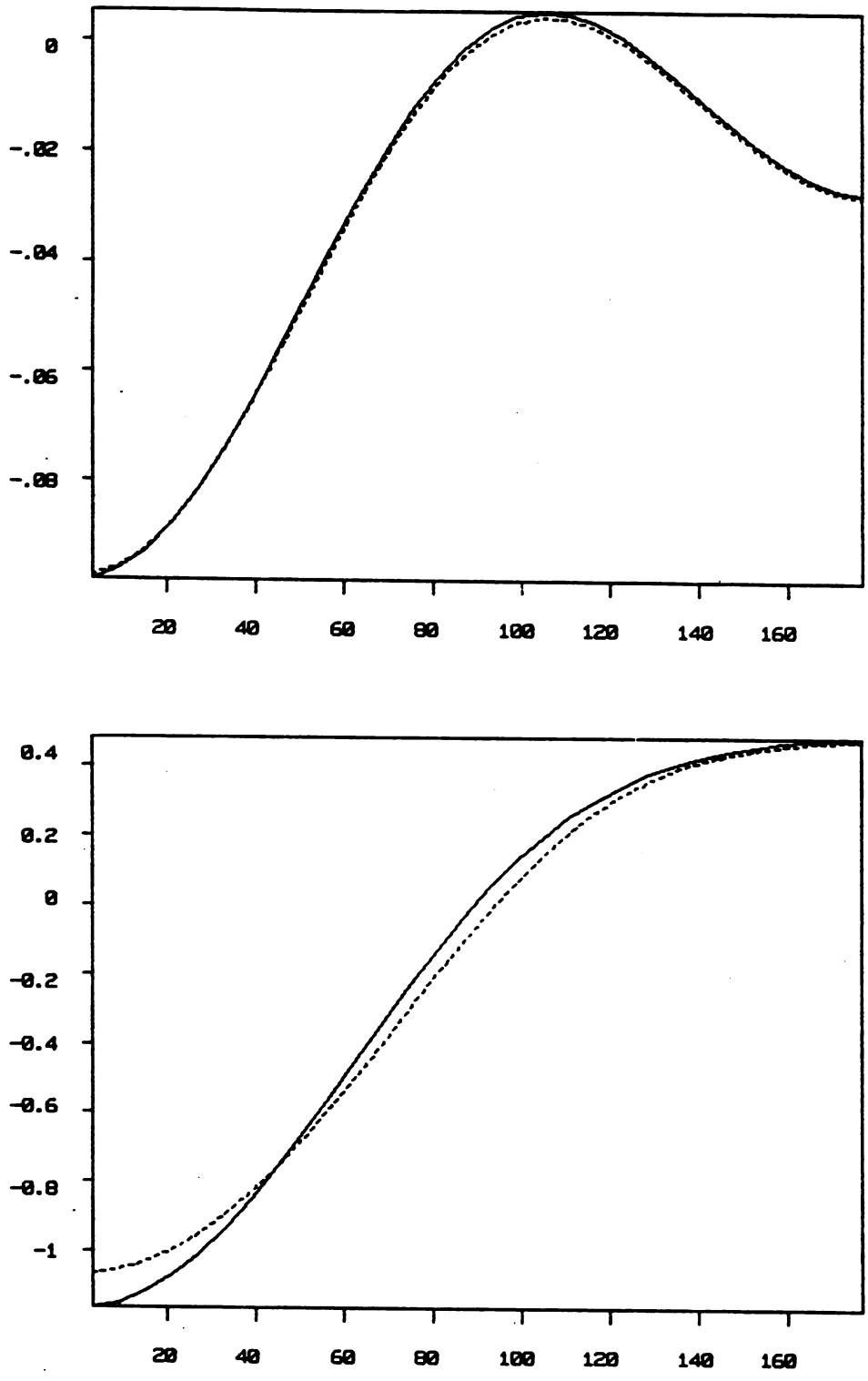

Fig. 3.1 Comparison of the approximate interaction (solid line) given in eqn. [3.12] with the renormalized interaction after 10 iterations. One spin is fixed at θ=0, the abscissa is the orientation of another spin. Top: the initial parameters are J=1.1, K=0.0001J (iterate to infinity). Bottom: the initial parameters are J=1.2, K=0.0001J (iterate to zero).

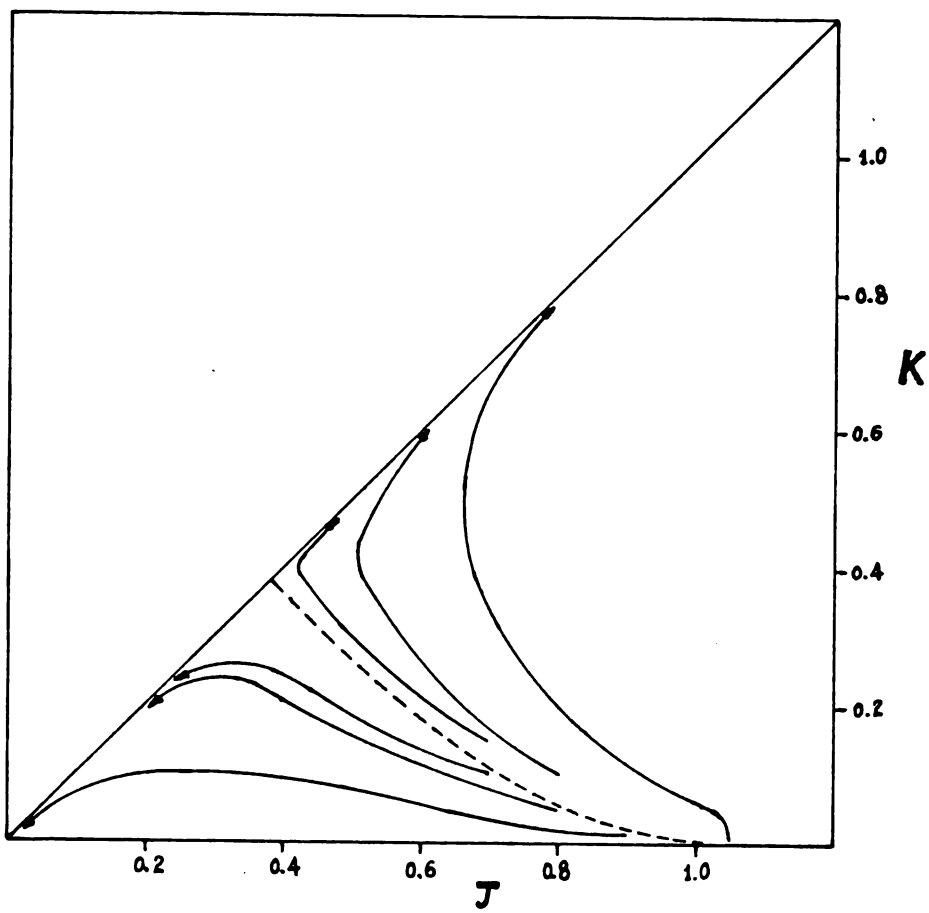

Fig. 3.2 The projection of RG flow generated in Migdal-Kadanoff real space renormalization group procedure on the J-K parameter plane. The dashed line indicates the boundary of two regions, in one region the flows go to the zero temperature fixed point, in the other they go to the infinite temperature fixed point.

IV. MONTE CARLO RENORMALIZATION GROUP SIMULATIONS

To study the thermodynamic properties of H given in [3.3] and support our MKRG results of the previous section, we have performed Monte Carlo simulation of NxN systems with N=16 and 32. To prepare our samples, we start from a random configuration at the reduced temperature $T^*=T/k_BJ=2.0$, which is supposed to be well above the transition temperature, where k_B is the Boltzmann constant. From now, we will always talk of the reduced temperature and drop the * mark except in Sec. VI. Using the standard Metropolis[3.14] procedure, we let the systems run at this temperature for a few thousand Monte Carlo steps per spin (MCS/S); we then reduced the temperature gradually with a temperature step less than 0.2, until T=0.2 was reached and the order was well developed. For the small K case, the systems were cooled to a temperature equal to K. After the cooling process, we heated the systems back. At every temperature stop, the number of MCS/S were usually 5000-8000; however, near the the critical temperature, $1.1\text{x}10^4$ MCS/S were discarded and $1.2\text{x}10^4$ MCS/S were used to compute the thermal averages.

Calculations of the thermodynamic quantities such as average magnetization (η), specific heat (C) and susceptibility (χ) indicate that the system shows only one phase transition for the three values of K/J chosen in our simulations (0.01, 0.1, 1.0). We have found that C and χ increase rapidly near the critical temperature, furthermore they tend to peak at the same temperature (see Fig. 3.3) suggesting that the transition is Ising-like. In contrast, for K=0, it is

believed[3.11] that C peaks at a temperature slightly higher than $T_c=T_{KT}$ where χ diverges.

Since it is difficult to locate the transition temperature from the T-dependence of thermodynamic quantities in simulation studies in finite size systems, we have used the MCRG procedure proposed by Schenker and Tobochnik[3.15] to find T_c. The essential feature of this procedure is the following: one starts from two systems of different sizes, say 1024 spins and 256 spins, the block spin is obtained by summing the spins around a plaquette vectorially, and then normalizing the sum. The plaquettes are selected in a way so that every spin is used and only used once to construct the block spin. One repeats this procedure until reached the limit imposed by the size of the system, such as 2x2. Our experience shows that the thermodynamic average on a 2x2 block spin lattice usually has bizarre behavior therefore we didn't use them. Next, thermodynamic quantities are calculated and matched for two block spin lattices of the same size but originating from different spin systems. Denoting T_1 as the temperature of the originally larger spin system and T_2 as that of the smaller one; if the thermodynamic quantities of the two block spin lattices match, we expected that the correlation lengthes are same in these two block spin lattices, then if $\Delta T(=T_2-T_1)=0$, the correlation lengthes are infinite in the original spin systems because after different numbers of iteration they are equal in the block spin lattices, thus in this case we have a critical point; and $\Delta T<0$ is an ordered phase, $\Delta T>0$ is a disordered phase. The correlation length critical exponent υ can be derived from the formula[3.15]

$$\upsilon = \ln 2/\ln(1+\frac{d\Delta T}{dT_t}|_{T_t=T_c}) \qquad [3.13]$$

In Fig. 3.4 we plot the nearest-neighbor correlation functions for the 8x8 block spin lattices obtained from the two systems, the larger one (32x32) denoted by o and the smaller (16x16) denoted by •. The crossing of the two curves gives the transition temperature T_c and it only shows one phase transition. The 4x4 block spin lattices give similiar results.

In Table 3.1, we give the value of T_c measured in units of $J(1+\epsilon)$ for three different ϵ values. The MKRG and MCRG give almost same critical temperatures thus these two procedures mutually corroborate their applicability for investigating this model. All three values of υ are much close to 1, the Ising value, rather than to ∞, the KT value. Therefore, the results are consistent with the conjecture that a non-zero anisotropy ($K\neq 0$) makes the transition Ising-like.

However, lacking a comparison with the results for the isotropic XY model, we are unable to say whether this MCRG procedure is sensitive enough to distinguish the difference between Ising-like and KT-like transitions when the sizes of the systems allow us only to perform a few iterations, especially if the anisotropy is very small. In present situation, the fact that $\upsilon \simeq 1$ is suggestive only when it is related to other evidences for an Ising-like transition in the model studied here. We will return to this concern about the finite size of the systems used in the above MCRG procedure after the calculation of the excitation energy for vortex in our model in Sec. V.

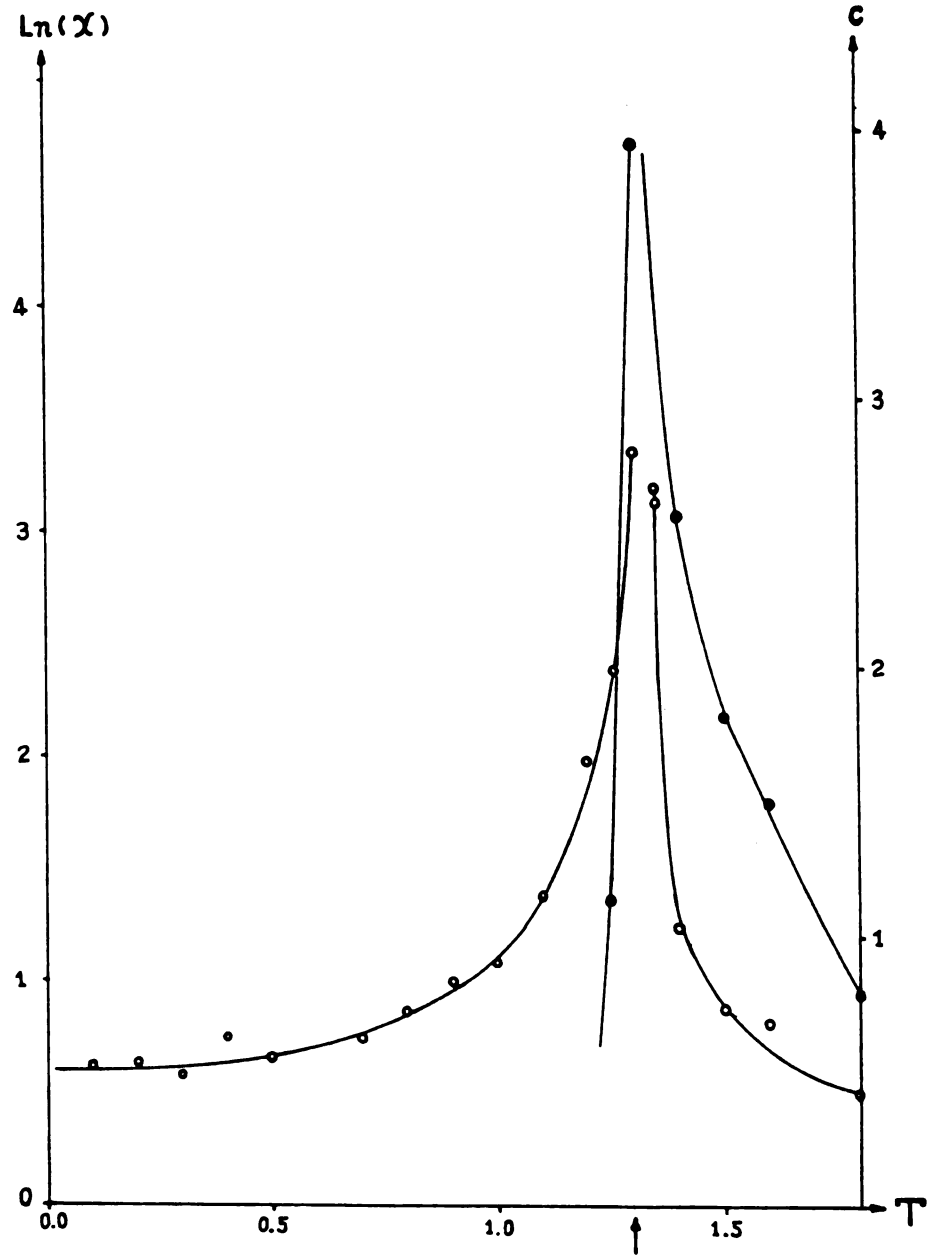

Fig. 3.3 Specific heat (denoted by •) and susceptibility (denoted by o) obtained in the Monte Carlo simulations for K=0.1J case. Note C and χ diverge at same temperature.

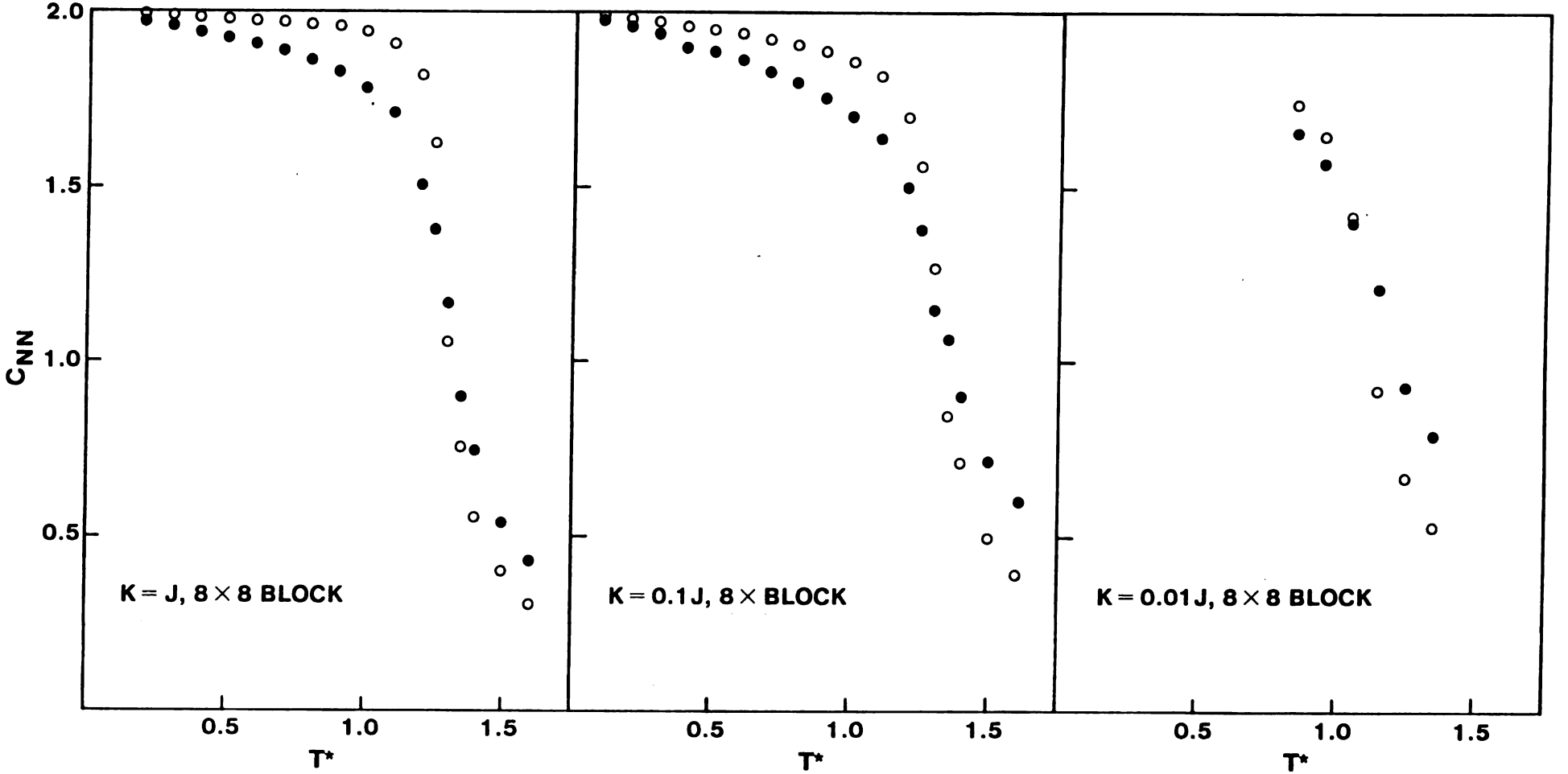

Fig. 3.4 Nearest-neighbor correlation as a function of T^* using MCRG analysis for K/J=1.0, 0.1 and 0.01. 8x8 block spin lattices are matched starting from (16x16) and (32x32) systems.

Table 3.1

The critical temperatures obtained by MKRG and MCRG for three K/J values 0.01, 0.10 and 1.00, where $T^*=k_BT/J(1+\epsilon)$. The correlation length critical exponents υ calculated by MCRG are also presented, these values are close to $\upsilon_{Ising}=1.0$. For XY model, $\upsilon_{XY}=\infty$.(3.9)

	MKRG	MCRG	
ϵ	T^*	T^*	υ
0.01	1.02	1.04	1.00±0.04
0.10	1.18	1.20	0.97±0.09
1.00	1.32	1.34	1.04±0.08

V. VORTICES AND STRINGS

If we examine the configuration generated in our MC simulations, we can see that after the phase transition takes place, there are domains in which the spin orientations are close to one of the two ground-state structures, and the VA pairs tend to reside inside the walls. (see Fig. 3.5). The vortex and antivortex are defined as following: we calculate the sum of differences of the spin orientation (in the range from $-\pi$ to π) traveling around a plaquette counterclockwise; if the sum is 2π, we define a vortex in the center of this plaqutte, if the sum is -2π, then we have an antivortex.

To understand clearly what types of excitations destroy the long-range order, we have made a series of MC quench studies. At a temperature above the critical point, the density of vortex-antivortex pairs is considerately high. However, most of them only have a few MCS/S "life-time". From a topological point of view,[3.16] a tightly bound VA pair is essentially different from an isolated vortex. The former can annihilate itself by rearranging spins locally, but the effect of the latter in the system extends to everywhere no matter how far it is away from the center of the vortex. Therefore, to eliminate an isolated vortex, or a well-developed defect, all the spins in the system have to be reoriented, consequently these defects would have a much longer MC "life-time" in a quench process. After suppressing the short "life-time" noise, an adequate quench picture is expected to reveal those well-developed defects.

In Fig. 3.5(a-d), we give our quench results starting from two

initial temperatures $T>T_c$ and $T<T_c$. In both cases, the system was quenched instantly to T=0.1 and then monitored up to 2000 MCS/S. For the system quenched from $T<T_c$, the VA pairs annihilated each other after 50 MCS/S, and after a few hundred MCS/S, the order parameter goes back to the value corresponding to T=0.1. In contrast, the quench from the high T ($T>T_c$) phase shows drastically different behavior. In a few MCS/S, again most of the closely spaced VA pair which are trapped inside wide domain walls annihilated each other but after a long "time" one finds that relatively long lived defects remain in the system. They consist of VA pairs connected by relatively sharp domain walls (strings on the dual lattice[3.10]). The total magnetization is near zero after 2000 MCS/S after quench. This picture indicates that the LRO is destroyed by the formation of domains like what heppens in the 2D Ising model.[3.17] Thus our MKRG and MCRG results that the phase transition is Ising-like are further supported by our quench study.

It can be easily shown that the energy of a single vortex in a system described by [3.3] is same as in the isotropic XY model, i.e., the anisotropic parameter K does not enter the total energy of this configuration. But the ground state energy now is -2N(J+K) instead of -2NJ, where N is the number of spins in the system, so the excition energy of a single vortex becomes

$$E \simeq \pi J \ln N + 2KN, \qquad [3.14]$$

whereas in the isotropic XY model the excitation energy only contains the first term in [3.14]. Thus in the thermodynamic limit the dominant term in vortex excitation energy is no longer logarithmic with respect to the size as for the isotropic XY model but linear to it as long as

the anisotropy is present, K≠0, no matter how small it is.

For finite systems, we anticipate that in order to find Ising-like behavior, the system size should be larger than a characteristic length for our model when the anisotropy is small. In the length scale less than this characteristic length, the first term in [3.14] is dominant and the system showes an XY-like behavior; however, beyond this characteristic length scale, the second one in [3.14] becomes leading term and the Ising-like behavior prevails. By making these two terms equal, we can give an estimate for this characteristic length L. If K=0.1J, L is about 8 lattice spacing; for the K=0.01J case, L increases to 33 lattice spacing. Remembering the largest system we used is 32x32, we stopped at this case K=0.01J in our MCRG simulations. Although the system may show XY-like behavior at intermediate length scale for small anisotropy case, the nature of the phase transition is determined by the large-scale behavior of the system. The results of our MCRG studies are probably correct on the ground that it seems possible to iterate the XY-like behavior (if it is present in our systems) out and to reach the Ising-like region in our finite systems for the three ratios of K/J we chose. The existence of a characteristic length also demonstrates itself in our MKRG procedure. If we start with J very close to 1.1 (the turnpoint in J axis) and very small ratio of K/J, such as 0.0001, the RG flow will linger in the neighborhood of this turnpoint during first several iterations, then go to K=J line in a faster pace. If K is not so small, the RG flow goes to K=J line in a few iterations. Note if K=J, the second term in [3.14] is larger than the first term for any integer N.

The particular type of long-lived defect structure that we see can be understood from a simple energy-entropy argument. The excitation energy can be reduced to be finite through managing a VA pair separated by finite distance *l*. Assuming the difference of the spin orientation between the two domains separated by a wall is equally divided among the strings of this wall because this arrangement reduces the excitation energy, we find that the energy cost per unit length (lattice spacing) ΔE for a wall of width w joining a VA pair to be roughly

$$\Delta E = wJ\left(1-\cos\frac{2\pi}{\omega}\right) + 2Kw \qquad [3.15]$$

If $K=0$, ΔE decreases continuously as $w\to\infty$, so there is no clear domain wall pattern in the isotropic XY model; but if $K\neq 0$, the minimum of ΔE shifts to a finite w; for such a wall, the energy cost is proportional linearly to the separation between vortex and antivortex instead of logarithmically as for the isotropic case. At finite temperatures, such an energy cost can be balanced only by an entropy term which is also proportional linearly to the size in order to minimize the free energy. This entropy could not come from free vortices, because in 2D vortex is a point defect whose entropy is proportional logarithmically to the size. So a mechanism different from the unbinding of VA pair ought to be introduced. The entropy associated with the domain wall of length *l* is linear in *l*, therefore to minimize the free energy, it becomes favorable to produce these domain-walls at a certain critical temperature and their floppiness, i.e., the tension of the string goes to zero, is the cause of the phase transition. It is also the reason why the phase transition becomes Ising-like in the presence of the

anisotropy K term.

An interesting feature of Fig. 3.5 is that the strings, contrary to what one may intuitively imagine, do not start from one vortex and then terminate at an opposite vortex so to complete a VA pair. Rather they like to connect as many different vortices of opposite sign as possible. Thus the opposite vortices can align alternately along the strings to build the walls. We show two possible domain-wall configurations connecting a VA pair in Figs. 3.6(a) and 3.6(b). The first 3.6(a) is discussed above, in the second 4.6(b), the walls become thinner but the total energy cost is same as in 3.6(a). Since the total wall length is now doubled and the second configuration has more entropy thus it is expected to have a higher probability to be formed at sufficiently high temperatures, but in this configuration the strings also have a higher probability to meet more vortices than one, and it is indeed the case seen in our simulation.

To comprehend why a KT-like phase transition is absent in our model after the Ising-like phase transition takes place, we plot the log of the vortex pair density vs. the reciprocal of temperature. (see Fig. 3.7) The slope which gives a measurement of the chemical potential needed to produce a VA pair reduces drastically at the critical temperature. This is similar to what happens at the KT transition temperature in the isotropic XY model,[3.11] in Fig. 3.7 we insert the result of the Monte Carlo simulation performed by Tobochnik and Chester for isotropic XY model. We believe that above the Ising-like phase transition the effective VA interaction is too weak to allow an intermediate XY-like phase as in $Z_p(p>4)$ case.

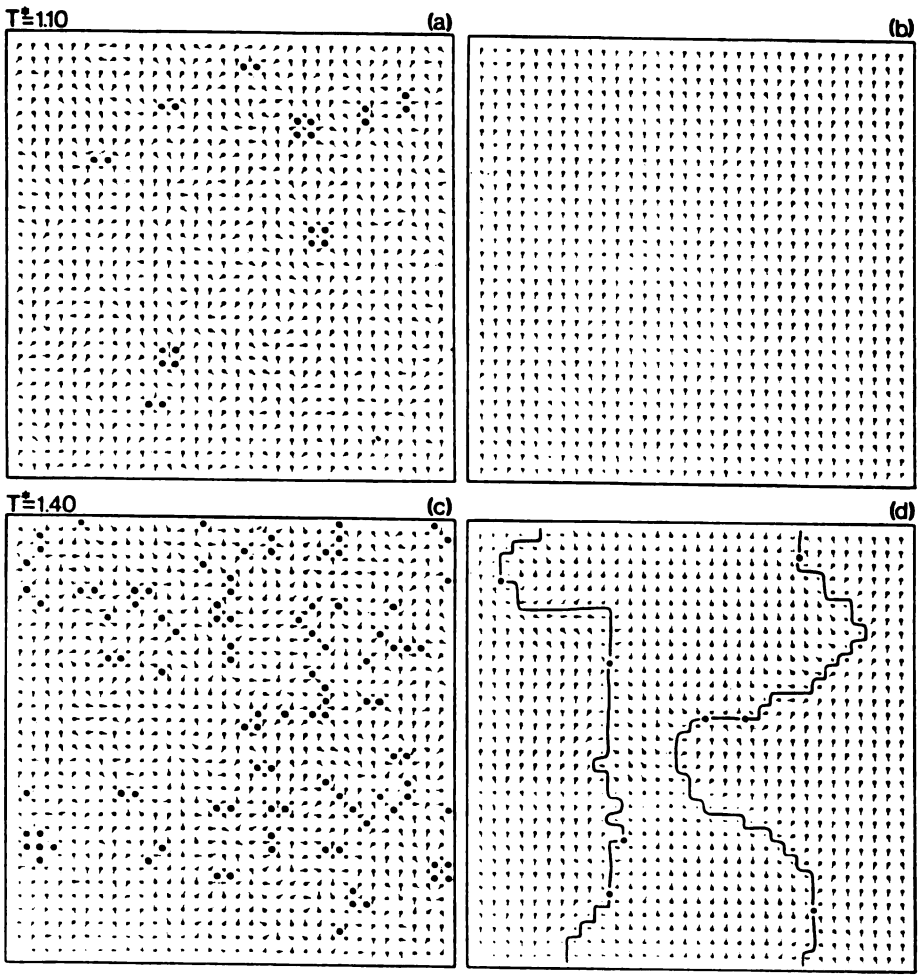

Fig. 3.5 Quenching studies starting form T* to 0.1 for K=0.1J case. •=vortex and o=antivortex. a: T=1.1<T_c (before quench). b: T=0.1 (50 MCS/S after quench, from T=1.1). c: T=1.4>T_c (before quench). d: T=0.1 (50 MCS/S after quench, from T=1.4).

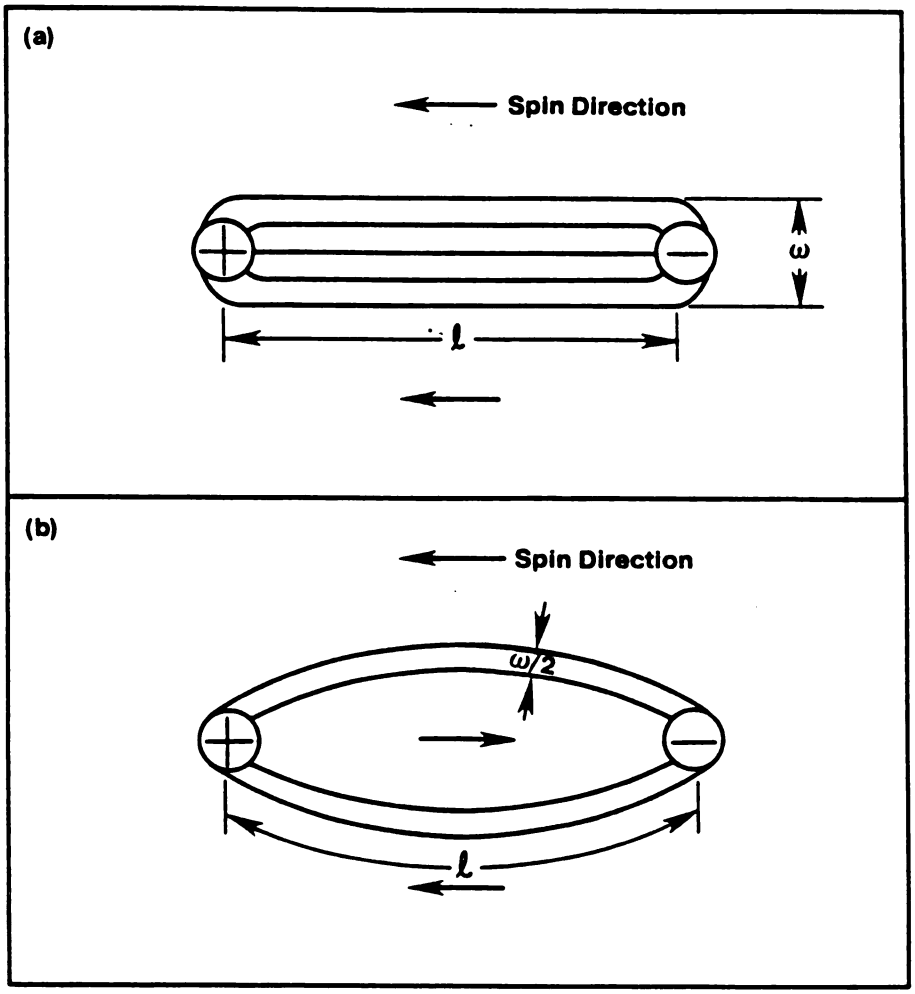

Fig. 3.6 Two possible vortex-antivortex configurations.

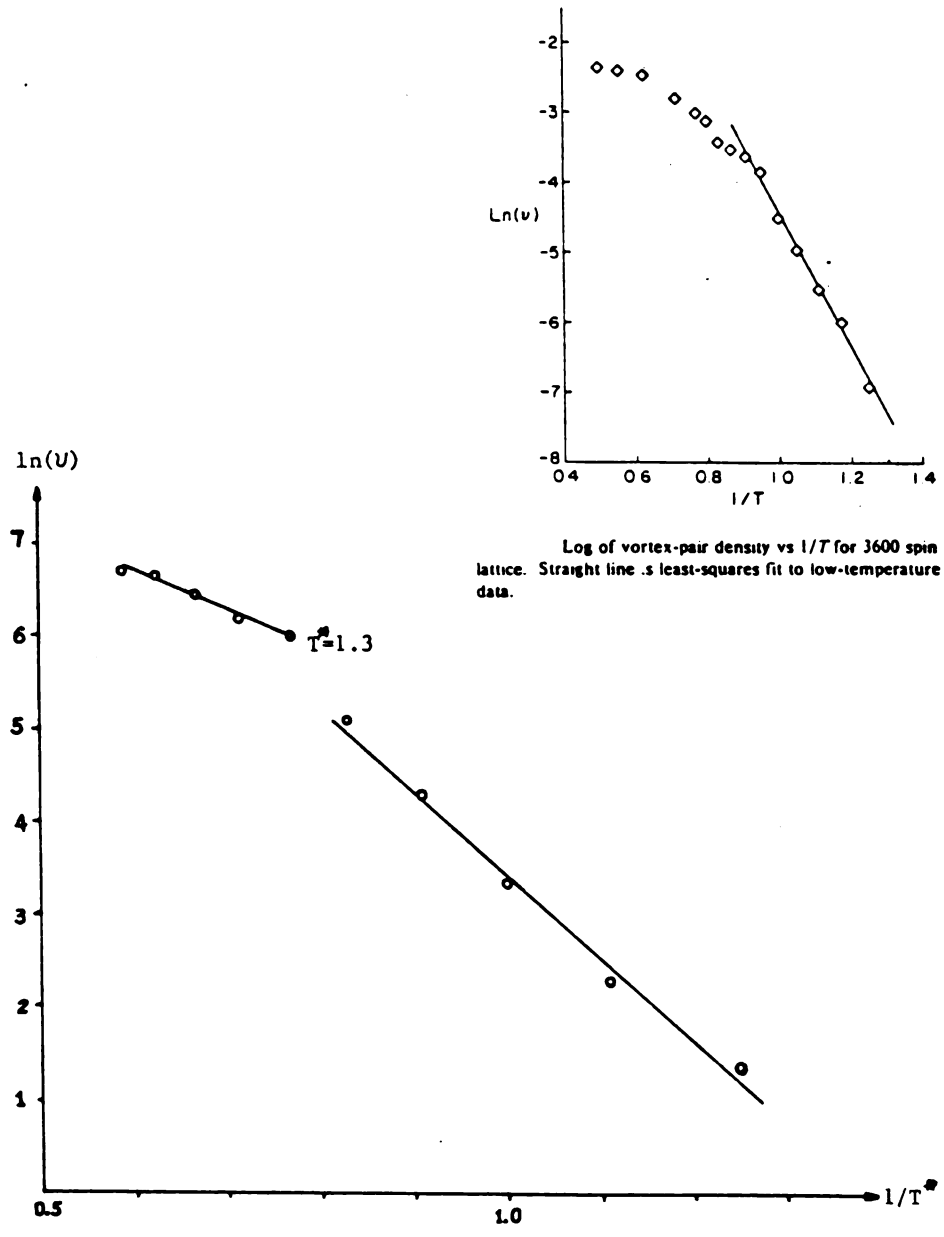

Log of vortex-pair density vs $1/T$ for 3600 spin lattice. Straight line .s least-squares fit to low-temperature data.

Fig. 3.7 Log of the number v of VA pair vs 1/T for the 32x32 spins system in K=0.1J case. The insertion is the results of Tobochnik and Chester for isotropic XY model.

VI. HIGH TEMPERATURE SERIES EXPANSION

As an additional check, we have used the high temperature series expansion (HTSE) to predict the critical temperature for our model in the K=J limit. In this case, the Hamiltonian given by [3.3] reduces to a simpler form

$$H = -(J+K)\sum_{\langle i,j\rangle}\cos\theta_i\cos\theta_j, \qquad [3.16]$$

and the calculations of HTSE becomes slightly easier.

For the partition function Z, according to the cumulant theorem, we have

$$\begin{aligned}\frac{1}{N}\ln Z &= \frac{1}{N}\ln\int_{-\pi}^{\pi} d\theta^N \exp[-\beta(J+K)\sum_{\langle i,j\rangle}\cos\theta_i\cos\theta_j] \\ &= \frac{1}{N}\ln\langle\exp[-\beta(J+K)\sum_{\langle i,j\rangle}\cos\theta_i\cos\theta_j]\rangle \\ &= 2\pi + \frac{1}{N}\sum_{m=1}^{\infty}\frac{1}{(2m)!}\langle V^{2m}\rangle\beta^{2m} \qquad [3.17]\end{aligned}$$

where

$$\langle V^2\rangle = \langle H^2\rangle - \langle H\rangle^2$$

$$\langle V^4\rangle = \langle H^4\rangle - 4\langle H^3\rangle\langle H\rangle - 3\langle H^2\rangle^2 + 12\langle H^2\rangle\langle H\rangle^2 - 6\langle H\rangle^4$$

.....

and $\beta=1/k_BT$. On a loose lattice such as square lattice, all the odd terms vanish due to the correspondence between the ferromagnetic and antiferromagnetic configurations. The values of $\langle H^{2n}\rangle$ are then calculated by counting all the graphs which contribute to the integral and the weights associated with these graphs.(3.18)

The internal energy per spin U and the specific heat C can be derived from [3.17] as

$$U = -\frac{1}{N}\frac{\partial}{\partial\beta}(\ln Z), \quad C = -\frac{k_B}{N}\beta^2\frac{\partial U}{\partial\beta} = \sum_{n=1}^{\infty} a_n x^{2n},$$

where $x=\beta(J+K)$.

Up to n=4, the specific heat is

$$C = 0.5x^2 + 0.8906x^4 + 1.0970x^6 + 1.2822x^8 \qquad [3.18]$$

If the phase transition is Ising-like, then we expect that the specific heat has a leading term of the form[3.17]

$$C = -A\ln(1 - x^2/x_c^2), \ (A>0), \qquad [3.19]$$

thus the coefficient a_n will have an asymptotic form

$$a_n \xrightarrow[n\to\infty]{} A/(nx_c^{2n})$$

or

$$\ln(na_n) \longrightarrow \ln A - 2n\ln x_c = \ln A + 2n\ln T_c^* \qquad [3.20]$$

Using a_2, a_3, a_4 given in [3.18], a linear regression gives

$$T_c^* = 1.303.$$

Note this value is in good agreement with those given by MKRG and MCRG.

VII. SUMMARY

We hve studied the nature of the phase transition in a system described by the Hamiltonian given in [3.3] with various theoretical methods. The results obtained depict a consistent physical picture. Our main results are as following.

The system possesses long-range order at low temperature. There is only one phase transition in this model. Between the low-temperature ferromagnetic phase and high-temperature paramagnetic phase, there is no intermediate XY-like phase.

Besides the spin-wave excitation, the system has vortex-antivortex pairs and domain-wall excitations. Near the critical point, the VA pairs tend to get trapped in the walls suggesting an attraction between these two types of excitations.

The phase transition is Ising-like. This conclusion is based on the facts a) the system iterates to an Ising-like system either in the low-temperature ferromagnetic phase or in the high temperature paramagnetic phase in the MKRG procedure; b)specific heat apparently diverges at the critical temperature where the susceptibility also apparently diverges; this behavior is not consistent with the prescription of KT phase transition but is expected for an Ising-like phase transition; c)the correlation length critical exponent υ calculated by MCRG adopts a value close to the Ising value 1; d)Monte Carlo quench study shows that the LRO is destroyed by the formation of domains with opposite spin orientations as seen in the 2D Ising model.

MKRG and the energy-entropy argument suggest that if a

symmetry-breaking anisotropy, no matter how small it is, is present then it dramatically changes the nature of the KT phase transition. In our model, the phase transition becomes Ising-like caused by the formation of domain-walls whereas without the anisotropy it is a KT phase transition caused by the unbinding of VA pairs. The ultimate reason for this change is that in the presence of the anisotropy, the dominant term in VA pair excitation energy is linearly proportional to the separation instead of logarithmic in the thermodynamic limit.

CHAPTER 4

PHASE TRANSITIONS IN DIATOMIC MOLECULAR MONOLAYER

I. INTRODUCTION

Phase transition from an orientationally disordered plastic phase to an orientationally ordered ferroelastic phase in 3-dimensional (3D) molecular solids occurs in many physical systems and is a well studied phenomena.[4.1] However, similar phenomena in 2D systems have only recently been investigated in adsorbed molecular monolayers on graphite substrate and the study of such transition is in infant stage. Typical systems are molecular oxygen[4.2] and nitrogen[4.3] on a graphite substrate. In fact the whole area of structural phase transition in molecular overlayers is of great current interest.

One of the interesting characteristics of molecular solids is the competition between direct and indirect (lattice mediated) intermolecular interactions which lead to different types of orientational ordering. Since the effect of this competition is pronouced in 2D systems due to the enhanced fluctuations[4.4] one expects to see multiple stage transitions[4.5] and fluctuation-driven

first order phase transitions[4.6] in 2D systems.

In this chapter we report the results of the molecular dynamics (MD) study of a 2D ferro-paraelastic phase transition by using constant-pressure (force/length) ensemble. The system consists of 400 diatomic molecules whose mass centers and orientations are confined to a 2D plane denoted as the XY plane. The molecules interact through atom-atom Lennard-Jones potentials,

$$V_{atom\text{-}atom} = 4\epsilon[(\sigma/R)^{12} - (\sigma/R)^{6}]. \qquad [4.1]$$

Adopting the parameters propriate to oxygen, this system closely resembles the δ-phase of oxygen molecular monolayer absorbed on graphite substrate. In the δ-phase the axes of oxygen molecules are primarily confined to the graphite substrate surface. The corrugation of the substrate potential is known to be small[4.7] and has been neglected in the present study.

In addition to the study of the nature (continuous or discontinuous; one or two transitions) of 2D ferro-paraelastic phase transition we also attempt to understand the nature of the topological excitations that drive such a transition. Since the orientational modes of this system can be represented approximately by a 2D anisotropic XY Hamiltonian,[4.8] one expects, besides the librons and phonons, vortex-antivortex (VA) pair, domain-walls and vacancy-like excitations to be present and drive the phase transition depending on their relative thermodynamic importance.

A promising candidate of 2D ferroelastic structure is the δ-phase of O_2 on graphite. At low temperature, the molecules orient parallel to

each other and their centers of mass form an almost centered rectangular lattice (see Fig. 4.1(a)) with b/a=2.46.[4.2] which can be also treated as a distorted triangular lattice. With increase in temperature it is possible that the system undergoes a ferro-paraelastic phase transition. In the paraelastic phase which can be denoted as an orientationally disordered 2D plastic phase (we will use this name from now), the centers of mass of molecules form an isotropic triangular lattice. There are three possible ferroelastic structures which are related to each other by rotating $2\pi/3$ and the ground state is three-fold degenerate.

If we describe the above transition by strain (the orientational degrees of freedom being integrated over) then the strains

$$\psi_1 = \frac{1}{2}(\epsilon_{xx}-\epsilon_{yy}), \qquad \psi_2 = \epsilon_{xy},$$

can be identified as the two components of the order parameter[4.9] and the Ginzburg-Landau-Wilson Hamiltonian has the form

$$H_{GLW} = -\frac{1}{2}\sum_{i=1,2}|\Delta\psi_i|^2 + r_2\sum_{i=1,2}\psi_i^2 + w(\psi_2^3-3\psi_1^2\psi_2) + u\sum_{i=1,2}(\psi_i^2)^2. \qquad [4.2]$$

This Hamiltonian is claimed to have a continuous transition belonging to the same univervality class as the 3-state Potts model.[4.9] Since for the actual system consisting of molecules the above Hamiltonian is only approximate and the configurations with antiferro ordering (herringbone structure, (see Fig. 4.1(b))) have relatively low potential energy, departures from the above predicted behavior are likely to happen, one of the aims of this chapter is to explore this possiblity.

Furthermore, on qualitative grounds, one has reasons to conjecture

that the present system may show two transitions in going from the ferroelastic phase to the plastic phase under suitable contiditions. First the long-range orientational and ferroelastic order is lost by the formation of domain walls between three possible ferroelastic domains, in this phase the system has triangular structure on large length scale. On a triangular lattice, the VA pair structure (in the effective XY Hamiltonian description) is close to the herringbone (HB) structure, (see Fig. 4.2) . Since the HB structure has an energy only 5.4% higher than the ground state, or because of the presence of the phonon excitations, the thermal average over all possible configurations of domain walls generates infinitesimal relative rotations of nearest neighbors in an average sense, it is possible that in this phase that the vortices are still not free and form bound VA pairs and the orientational correlation function only decays logarithmically. This intermediate phase, which is similar to the XY-like phase present in Z(p) models when p>4,[4.10] goes to the high temperature paraelastic phase with exponentially decaying orientational correlation through a Kosterlitz-Thouless-like[4.11] transition. Although the detection of such a subtle phase directly in a MD simulation is difficult, we make some effort to find if the ferro-paraelastic transition in this system takes place in two stages.

The long controversial problem about the nature of 2D melting, i.e., whether the transition is first-order or second-order, is also studied in this chapter.

In Sec. II we give the ground state structure and prove that the long-range orientational order is present in our system. The molecular

dynamics simulation method we used is documented in Sec. III in great detail. The existence of a plastic phase is suggested by the MD results which are presented in Sec. IV, the ferro-paraelastic transition is thought to be first-order. The driving mechanism for this transition is dicussed. In the final section Sec. V, along with the results of the simulations for the melting transition, which is believed to be first-order, we make a few comments about the phase diagram of this 2D diatomic molecular system.

In all the following calculations, the parameters we used are those reportedly appropriate for the oxygen molecule,[4.7] i.e.,

$$\epsilon = 54.34k_B, \qquad \sigma = 3.05\mathring{A},$$

$$d = 0.604\mathring{A}, \qquad m = 15.995m_a,$$

where m_a is the atomic mass unit. When we talk about the quadrupole-quadrupole interaction, for the computational convenience, the quadrupole moment is constructed by putting $2Ze$ charge on the molecular center and $-Ze$ on the two atomic positions. The value we used is Ze=0.111 esu, it corresponds to a quadrupole moment $Q=-0.39\times10^{-26}$ esu.cm^2.

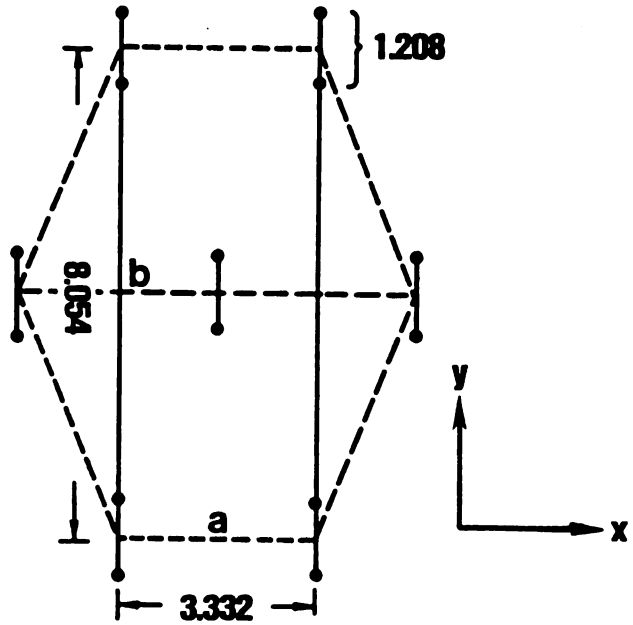

CENTERED RECTANGULAR

E=-8.28

ρ=0.693

Fig. 4.1 (a) The gound state configuration. The unit of energy U is ϵ, the unit of density ρ is σ^{-2}. In effective spin Hamiltonian, the spin orientation is the twice of that of the molecule.

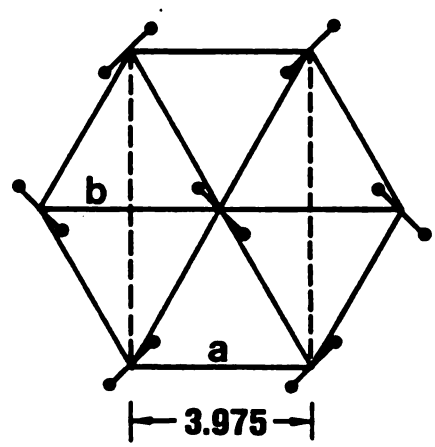

HERRING BONE

E=-7.83

ρ=0.680

Fig. 4.1 (b) The herringbone configuration which corresponds to antiferromagnetic ordering in spin language.

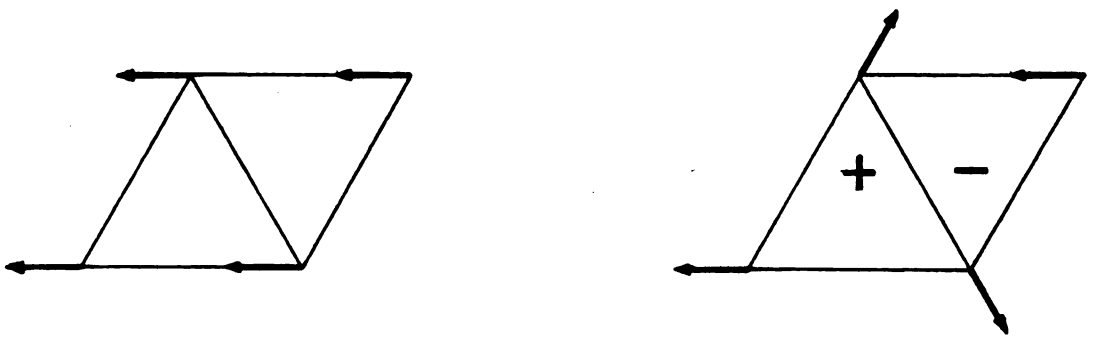

Fig. 4.2 (a) In spin representation, to form a VA pair in ferro-ordering state, at least one spin has to rotate $\pi/3$.

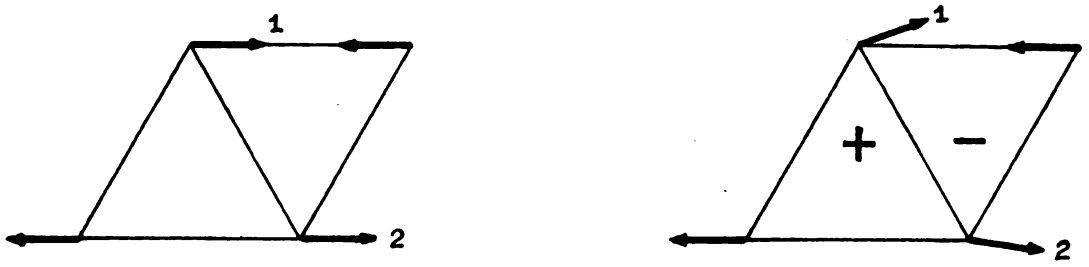

Fig. 4.2 (b) In antiferro-ordering state, to form a VA pair, spin 1 and spin 2 only need to deviate slightly from the local minimum. The vortex, as topological defect, is referred to ferromagnetic ordering.

II. THE GROUND STATE

By using a pattern search program, Etters et al.[4.7] found that the ground state of the low-density phase of oxygen monolayer on the graphite substrate is a centered rectangular lattice (see Fig. 4.1(a)) with a=3.32Å and b=8.07Å. The oxygen molecules lie flat on the substrate surface and are orientationally ordered along the b axis. Because we believe our system is closely related to this δ-phase, we start from this structure for searching the potential minimum. A nearly zero value of the internal stress tensor is an additional criterion we used for the location of the minimum. This procedure gives the same structure as found by Etters et al. with slightly different lattice lengths, a=3.332Å and b=8.054Å. Calculated for a 19x19 lattice, the potential energy is -8.28ϵ with a surface tension of $0.0064\epsilon/\sigma^2$. The internal stress tensor $P_{\mu\nu}$ and the surface tension p, (from now we will call it "pressure"), are calculated through virial formula in its 2D form,

$$P_{\mu\nu} = \frac{1}{\Omega}\left(\sum_i m\dot{x}_i^{\mu}\dot{x}_i^{\nu} + \sum_{\langle i,j\rangle} F_{ij}^{\mu}x_{ij}^{\nu}\right), \qquad [4.3]$$

and $p=\frac{1}{2}(P_{xx}+P_{yy})$, where Ω is the area of the system, $\vec{F}_{ij}$ is the force acting on molecule i by molecule j, $\vec{x}_{ij}=\vec{x}_i-\vec{x}_j$. If we add the quadrupole-quadrupole interaction, the change of the lattice lengths is less than 0.3%, and the change of the ground state energy is less than 2%. Taking the coverage of a $\sqrt{3}\times\sqrt{3}$ structure as the coverage unit, which corresponds 0.0636 molecules/Å^2 on graphite substrate, the ground

state of our system has a coverage of 1.172.

Using effective Hamiltonian, we found that the herring-bone structure (see Fig. 4.1(b)) is energetically favorable for a triangular lattice. We also searched whether there is a potential minimum for such a configuration. The finding is that the energy has a minimum when lattice spacing a is 4.006Å, with a value of -7.38ϵ, slightly higher than the ground state energy.

Although true translational long-range order is absent in such a 2D system, it is possible for the system to possess orientational long-range order. Using the harmonic expansion at sufficiently low temperatures, it is easy to show that there is a gap between the ground state energy and the libron excitation energy spectum. For example, if the lattice is rigid, an effective spin Hamiltonian[4.8] for the nearst-neighbor orientational interaction is

$$V(\theta_i,\theta_j)=-0.388+0.625(\cos2\theta_i+\cos2\theta_j)-0.303(\cos4\theta_i+\cos4\theta_j)$$
$$-0.584\cos(2\theta_i-2\theta_j)\ -0.409\cos(2\theta_i+2\theta_j), \qquad [4.4]$$

where θ_i and θ_j are the angles between the molecular axes and the line connecting the centers of these two molecules. In the previous two chapters, we have already seen that such an anisotropic interaction leads to orientational LRO. In the framework of the harmonic expansion, if we take into account both the libron and phonon excitations, the harmonic Hamiltonian can be written down as

$$H_{\text{harm}}=\sum_{\vec{k}}\epsilon_{\vec{k}}\psi_{\vec{k}}\psi_{-\vec{k}}+\sum c_{\vec{k},\vec{q}}\psi_{\vec{k}}\phi_{\vec{q}}+\sum_{\vec{q}}\epsilon_{\vec{q}}\phi_{\vec{q}}\phi_{-\vec{q}}\ , \qquad [4.5]$$

where $\vec{k}$ is the wave-vector of phonon modes and $\vec{q}$ is that of libron

modes. In the calculation of orientational correlation, the integration over ψ_k in $\langle H_{harm} \rangle$ will leave a term $\exp(\beta c_{\vec{k},\vec{q}}^2 \phi_{\vec{q}}^2 / 4\epsilon_{\vec{k}})$, so the effective libron excitation spectrum can be thought as

$$\epsilon'_{\vec{q}} = \epsilon_{\vec{q}} - \sum_{\vec{k}} a_{\vec{k}} c_{\vec{k},\vec{q}}^2, \qquad [4.6]$$

where $a_{\vec{k}}$ is a coefficient, and $c_{\vec{k},\vec{q}}$ is expected to be linear to k in the small k limit as in 3D case. The coupling with the translational degrees of freedom can only reduce the gap with an amount proportional to the square of coupling, except for some special case where the gap may accidentally become zero. Thus if the orientational LRO is present for a fixed lattice, generally speaking, it will persist after we release the mass centers of the molecules.

III. THE CONSTANT-PRESSURE MOLECULAR DYNAMICS

In comparison with Monte Carlo simulation, which is well documented, in some aspects even seems standardized, and a few excellent review books are already available,[4.12] molecular dynamics has more room for user's imagination and creativeness, some details scatter in the literature or even remain in the research notes of experts. On the another hand, I was witnessing a rapid growth of the applications of computer simulation in this department in recent years, and further growth in this tendancy could be foreseen, as in every major institution, when more and more computational facilities become accessible to physists. For these reasons, I would like to give a detailed description of the MD method we have used.

A: Constant-Pressure Ensembles and Stress Tensor for Multiatomic Molecular System

To allow our system to change its lattice structure as that occurs in a ferro-paraelastic phase transition, we have applied a constant-pressure molecular dynamics (MD) method first proposed by Anderson[4.13] and later elaborated by Parrinello and Rahman[4.14]. Take a monoatomic molecular system as an example, the main features of this method are as follows: first one defines a MD cell characterized by vectors a and b, positions of the molecule are expressed in the basis consisting of a and b instead of actual Cartesian coordinates. The vectors a and b are allowed to change in the simulation, but at any instant the positions of molecules are expressed as

$$\begin{pmatrix} x \\ y \end{pmatrix} = \begin{pmatrix} a_x & b_x \\ a_y & b_y \end{pmatrix} \begin{pmatrix} s^{(a)} \\ s^{(b)} \end{pmatrix}, \qquad [4.7]$$

where $\vec{a}=a_x\hat{x}+a_y\hat{y}$ and so on. Because of [4.7] if the MD cell changes during the simulation, the positions of the molecule will be still well defined. We will use the term "scaled coordinates" for s, the components of s are in the interval (0,1). One then attaches a mass W to the MD cell vectors. This is analogous to putting a piston on a gas system, the motion of the piston is determined by the external force and the pressure of the gas. To obtain the equations of motion, one then needs a Lagrangian, and a possible one is

$$L = \frac{1}{2}\sum_i m\dot{s}_i' G\dot{s}_i - V + \frac{1}{2}W\mathrm{Tr}\dot{h}'\dot{h} - p\Omega \qquad [4.8]$$

where h is the 2x2 matrix appearing in [4.7], G=h'h, Ω is area of the MD cell, Ω=|h|, and p is the external hydrostatic pressure.

The equations of motion generated from this Lagrangian are

$$m\ddot{s}_i = h^{-1}\sum_{\langle i,j\rangle}\begin{pmatrix} F_{ij}^{(x)} \\ F_{ij}^{(y)} \end{pmatrix} - mG^{-1}\dot{G}\dot{s}_i \qquad [4.9]$$

This equation describes the motion of the *i*-th molecule with a coordinate system whose basis vectors are *a*, *b*. For *a* and *b* themselves, the equation of motion is

$$W\ddot{h} = \Omega(P_{\mu\nu}-p)h'^{-1} \qquad [4.10]$$

where

$$P_{\mu\nu} = \frac{1}{\Omega} \left(\sum_i m\dot{x}_i^{\mu} \dot{x}_i^{\nu} + \sum_{\langle i,j \rangle} F_{ij}^{\mu} x_{ij}^{\nu} \right), \qquad [4.11]$$

In eqn. [4.11] we formally write $x_i = hs_i$, $\dot{x}_i = h\dot{s}_i$. $P_{\mu\nu}$ has the form of the internal stress tensor calculated by using virial theorem. Eqn. [4.10] shows that the change of volume and shape of the MD cell is driven by the imbalance between the external pressure and the internally generated stress. The constant of motion is readily identified as the enthalpy H given by

$$H = \frac{1}{2} \sum_i m\dot{x}_i\dot{x}_i + V + p\Omega \qquad [4.12]$$

with a small correction $2k_BT$ due to the 4 degrees of freedom of the MD cell vectors.

The choice of MD cell mass W is theoretically arbitrary if only the equilibrium properties of system are concerned because those properties of the system are independent of the masses of its contitutients in the classical statistical mechanics. As proved by Anderson,[4.13] the time average of a physical quantity along the trajectory produced by this Lagrangian is equal to the isoenthalpic-isobaric ensemble average of that quantity.

This novel simulation method has proved to be extremely powerful in studying the phase transitions involving structural rearrangement as beautifully shown by Rahman and coworkers.[4.14] Klein et al.[4.15] generalized it to the multiatomic molecular systems by adding a term $\sum_i \omega_i I \omega_i$ to the Lagrangian given in [4.8], where I is the moment of inertia of molecules, ω_i is the angular velocity of i-th molecule. In

this term, there is no coupling of the rotational dynamics with the MD cell vectors unlike the term corresponding to the motion of the centers of mass $\sum_i \dot{s}_i' G \dot{s}_i$, so [4.11] keeps the same form where only the motion of the centers of mass contributes to the stress tensor $P_{\mu\nu}$. It means that no matter what kind of orientational order the system has, the volume and the shape of the system will be decided directly by the motion of the centers of mass. This may be reasonable for either a fluid or for a solid which only undergoes an isotropic expansion or compression when orientational order changes. For our system, where the disorder of the molecular orientation is expected to play a crucial role in the ferro-paraelastic phase transition, we realized the need to develop a proper procedure to accommodate the contribution of the rotational motion to the structural change.

For a rigid rotor, the rotation does not contribute to the hydrostatic pressure, which therefore is determined totally by the motion of centers of mass. But the rotation does make its mark on the stress tensor. For our diatomic molecular system, if we write down the equations of motion for every atom with the constraint of the rigid rotor condition, then rewrite these equations in C.M. (R) and relative (r) coordinates, for the latter, we have

$$m\ddot{\vec{r}} = \frac{1}{2}(\vec{F}_1 - \vec{F}_2) + \vec{F}_{\text{constraint}} , \qquad [4.13]$$

where $\vec{F}_1$ is the force acting on atom 1 and $\vec{F}_2$ on atom 2 of a particular molecule. In polar coordinates, if we note that $\dot{r}=\dot{\vec{r}}=0$ for a rigid rotor and insert r=d, the above equation becomes

$$-md\dot{\theta}^2 = \frac{1}{2}\,(F_1^{(r)} - F_2^{(r)}) + F_{constraint}, \qquad [4.14]$$

$$md\ddot{\theta} = \frac{1}{2}\,(F_1^{(\theta)} - F_2^{(\theta)}) \ . \qquad [4.15]$$

Eqn. [4.15] is simply the equation of motion for the orientational variable θ, and eqn. [4.14] shows that in order to satisfy the rigid rotor condition, the center of mass must provide a force with magnitude

$$F_{constraint} = -md\dot{\theta}^2 - \frac{1}{2}(F_1^{(r)} - F_2^{(r)}), \qquad [4.16]$$

to atom 1 so the centrifugal force could be balanced. For atom 2 a force with same magnitude but opposite direction must be provided. Taking account of the contribution of this force in the virial expression for the internal stress tensor, we obtain

$$P_{xx} = P_{xx}^{c.m.} - \sum_i d\cos\theta_i \sin\theta_i (F_{i1}^{(\theta)} - F_{i2}^{(\theta)})$$

$$P_{yy} = P_{yy}^{c.m.} + \sum_i d\cos\theta_i \sin\theta_i (F_{i1}^{(\theta)} - F_{i2}^{(\theta)})$$

$$P_{xy} = P_{xy}^{c.m.} - \sum_i d\sin\theta_i \sin\theta_i (F_{i1}^{(\theta)} - F_{i2}^{(\theta)})$$

$$P_{yx} = P_{yx}^{c.m.} + \sum_i d\cos\theta_i \cos\theta_i (F_{i1}^{(\theta)} - F_{i2}^{(\theta)}) \qquad [4.17]$$

From eqn. [4.17] we can see that the hydrostatic pressure p which is $\frac{1}{2}(P_{xx}+P_{yy})$ only includes the contribution of the centers of mass, however $P_{\mu\nu}$ may have a significient part coming from the rotation. For

our system, at low temperatures, the molecular axes oscillate around their ground state orientations, (see Fig. 4.1(a)), the term $-d\cos\theta_i\sin\theta_i(F_{i1}^{(\theta)}-F_{i2}^{(\theta)})$ is always positive, so the contribution of the rotation increases the xx-component meanwhile decreases the yy-componenet of the stress tensor, this makes it easier for the system to transform to a trianglar structure. To exclude this contribution in simulations is equivalent to make the system artificially rigid, and worst of all, if the coupling of the librons and the phonons reduces the gap in the libron excitation spectum to a negative value making the structure shown in Fig. 4.1(a) unstable under the perturbation of librons, we might fail to detect this instability in the simulation because the stress tensor was not properly calculated.

Suppose we connect the two atoms of a molecule with a very stiff spring, so that the coupling of the orientational and translational (for centers of mass) degrees of freedom with the vibrational degrees of freedom is neglegible. In the limit the elastic constant of this spring approaches infinity, we have a rigid rotor system described by the Lagrangian

$$L = \frac{1}{2}\sum_i m\dot{s}_i'G\dot{s}_i + \frac{1}{2}\sum_i I\dot{\theta}_i^2 - V + \frac{1}{2}W\mathrm{Tr}\dot{h}'\dot{h} - p\Omega \qquad [4.18]$$

with the internal stress given by [4.17]. The intramolecular vibration contributes to the total energy a term $2Nk_BT$ which is omitted in our calculations. Eqn. [4.15] and the equations of motion generated by [4.18], i.e., [4.9], [4.10], [4.15], are used in our MD simulations

When the stress is calculated by using eqn. [4.17], the

antisymmetric component of the stress tensor $\omega=\frac{1}{2}(P_{xy}-P_{yx})$ is zero for a system initially with zero total angular momentum as it should be. On Cyber 750, through 10^4 time steps, the standard deviation of is of the order 10^{-14}. This is probably the reason why some researchers who did not include the rotatioal contribution to $P_{\mu\nu}$ found that the total angular momentum was not conserved in their MD simulation in which the Anderson-Parrinello-Rahman method was used to study the properties of multiatomic molecular systems. For a system initially without net translational momentum, the "generalized momentum" $\sum_i h\dot{s}_i$ should be zero in the simulation, too. ω and $\sum_i h\dot{s}_i$ are monitored in our simulation in order to check the accuracy of the algorithm used. It is important to make sure that there is no net total momentum in the system. A non-zero total momentum means that the center of mass of the system is moving, this gives every molecule an additional velocity; it will increase the pressure calculated by using virial formula and makes the system artificially soft in the simulation.

B: Numerical Solution of the Equations of Motion

To integrate the equations of motion, we have used a predictor-corrector algorithm[4.16] whose accuracy is up to $O(\Delta t^5)$ for our case. If we denote the position variable of a molecule by q^0, and let

$$q^n=\frac{(\Delta t)^n}{n!}\frac{d^n}{dt^n}q^0,$$

where Δt is the time step used in the integration, then the predictor values of the position variable and its derivatives up to order 5 are

given by

$$
\begin{aligned}
p^0 &= q^0+q^1+ q^2+ q^3+ q^5+ q^6 \\
p^1 &= q^1+2q^2+3q^3+4q^5+ 5q^6 \\
p^2 &= q^2+3q^3+6q^5+10q^6 \\
p^3 &= q^3+4q^5+10q^6 \\
p^4 &= q^5+ 5q^6 \\
p^4 &= q^6
\end{aligned}
\qquad [4.19]
$$

These predictor values are input into the equations of motion to calculate the accelarations, so we get the corrector value of the second derivative c^2. $\Delta=c^2-p^2$ is then used to correct those predictor values,

$$c^n= p^n+ f_n\Delta \qquad [4.20]$$

where f_n are 3/16, 251/360, 1, 11/18, 1/6, 1/60.

The advantage of this predictor-corrector method is that the differences c^0-p^0 and c^1-p^1 give estimates of the errors of the position and the velocity. The procedure can be repeated if necessary, by using the corrector as the next predictor. However, usually to predict and correct once are satisfactory. When the external pressure is zero, so that the enthalpy is equal to the internal energy, we found that in 10^4 time steps, the deviation of energy is less than 0.3%.

To initiate the integration, we need to know the initial positions and their derivatives. To save computer time, it is desired that the system is close to equilibrium even in the initial configuration. Starting from the ground state configuration, we assign a small positional deviation to every molecule. The deviation can be a product

of a fixed value and a random number with approximate Gaussian distribution. The fixed value is time interval Δt multipled by the mean square root velocity at required temperature T_0 according to the Maxwell-Boltzmann distribution. The time step used in this "initiation stage" is one tenth of that used in the simulations. The approximate Gaussian random number is generated by a simple procedure.[4.17] The central limit theorem says that the sums of n random numbers, no matter what kind distribution those random numbers have, when n approaches infinity, will reach a normal distribution. Using the available function subroutine RANF( ) on Cyber 750, which generates a random number in interval (0,1) with uniform distribution, we take a sum of 12 such random numbers. Since the expectation and variance of the uniform distribution on interval (0,1) are 1/2 and 1/12, the sums will have expectation and variance 6 and 1. By subtracting 6 from the sum, we have an approximate standard normal distribution, almost indistinguishable from a true Gaussian distribution by eye, with the desired feature: no number has a magnitude bigger than 3, no molecule will have a initial velocity larger than three times the mean square root velocity. The molecules now move to the new position q_1 form the ground-state position q_0, the velocity is given by

$$v = (q_1 - q_0)/\Delta t \qquad (q=x,y,\theta). \qquad [4.21]$$

To make the total momentum zero, we shift all the velocities, i.e.,

$$v_i' = v_i - \frac{1}{N} \sum_i v_i,$$

where N is the number of the molecules. Since the velocities have an

almost Gaussian distribution, $\sum_i v_i$ is close to zero, and therefore the shift is very small. Then, the velocity v_x is multiplied by a factor $\sum_i v_{iy}x_i / \sum_i v_{ix}y_i$ to make the total angular momentum zero, since $\sum_i md^2\dot{\theta}_i$ is already adjusted to zero. Finally, the adjusted velocities are used to calculate the temperature T of the system by the equipartition theorem

$$\frac{3}{2}Nk_BT = \frac{1}{2}\sum_i m(v_{ix}^2+v_{iy}^2+d^2\dot{\theta}_i^2), \qquad [4.22]$$

All the velocities then are multiplied by a factor $\sqrt{T_0/T}$ to force the system to have the required temperature T_0, which is not too far from zero.

A simple integration procedure, namely

$$q_{n+1} = 2q_n - q_{n-1} + q_n$$

can be used with the small time step Δt to obtain the first few configurations. Then these positions are transformed to position and derivatives at time step n by the equations

$$\begin{pmatrix} q^0 \\ q^1 \\ q^2 \\ q^3 \\ q^4 \\ q^5 \end{pmatrix} = \frac{1}{120} \begin{pmatrix} 0 & 0 & 120 & 0 & 0 & 0 \\ -6 & 60 & 40 & -120 & 30 & -4 \\ -5 & 80 & -150 & 80 & -5 & 0 \\ 5 & 5 & -50 & 70 & -35 & 5 \\ 5 & -20 & 30 & -20 & 5 & 0 \\ 1 & -5 & 10 & -10 & 5 & -1 \end{pmatrix} \begin{pmatrix} q_{n+2} \\ q_{n+1} \\ q_n \\ q_{n-1} \\ q_{n-2} \\ q_{n-3} \end{pmatrix} \qquad [4.23]$$

Note that the superscript indicates the order of the derivative, the subscript labels the time step. At this stage, the calculation is

performed with a fixed MD cell corresponding to the ground state structure. After obtaining the high-order derivatives, we change the value of Δt in q^n from the small initial value to that used in the simulations. This finishes the "initiation stage" and the equations of motion are now ready to be integrated.

C: Aging and Generation of the Equilibrium Ensembles

The next stage of simulation is the "aging" stage as called by Rahman. The volume and the shape of the MD cell are now allowed to change by introducing the mass W attached to the MD cell vectors. W will affect the relaxation time of fluctuations of the MD cell, and in our simulations we choose $W = m/N$. This choice is found to be reasonable for our system because in simulations, the vibration period of the MD cell is smaller than the length of a typical MD run (2000 time steps), but much larger than the correlation time of the dynamics of molecules.

In the aging stage, after every m time steps, where m is a predetermined number, the instantaneous temperature of the system is calculated by using [4.22], then all the derivatives are multipled by a factor of $\sqrt{T_0/T}$ to force the temperature to be T_0. Because the system is initially in a state not far from the ground state, the temperature may rise rapidly at the beginning while a considerable amount of potential energy transforms to kinetic energy. The procedure of adjusting all the derivatives instead of the velocities only, shortens the relaxation time of this tumultuous period, and helps the system to reach equilibrium much faster. After running the system for a few thousand time steps, we switch off the temperature adjustment, and run

the system for several segments (each segment consisting of 500-1000 time steps) to see whether the averages of energy, temperature, pressure are stable and the kinetic energy is equipartitioned. If the result is unsatisfactory, the aging process is repeated. At a temperature not too close to the transition temperature, aging the system once appears sufficient. However, near the transition temperature, for example, in the solid-liquid coexistence region, 10^4 time steps may be needed for the system to melt to liquid from a solid state. After the aging process, the system is used to calculate the equilibrium or dynamic properties under study.

When the system is heated or cooled to a new temperature, the aging process is carried out again at this new temperature. Usually, except for quick quench studies, we give 500-1000 steps for the purpose of raising the temperature. These steps are divided into 10-20 segments, the temperature difference is uniformly distributed among these segments, so the heating (cooling) process is smooth and gentle. The cost of a rapid heating (cooling) is always an aging process intolerably long, and even spurious results in some cases. Close to the transition,the temperature step we used is as small as 0.02.

The final stage which we call as the "equilibrium stage", where the fluctuation of temperature is small. After m time steps, we adjust the instantaneous temperature to the desired value T_0 and record the information needed on tape for later calculations of the isobaric-isothermal ensemble averages. Usually, the average is calculated over 2000-3000 time steps, however, close to the transition temperature, $1.0\text{-}1.5\times10^4$ time steps are used.

D: Simulations of the Lennard-Jones System

Following the convention in MD simulations of the Lennard-Jones systems,[4.14,4.18] we use the reduced dimensionless units for computational convenience. It also has the advantage that the simulation results are independent of certain parameters, for example, the energy parameter ϵ and mass m. The lengths are expressed in units σ, the energies in units ϵ, the temperature in units ϵ/k_B and pressure in units ϵ/σ^2, m is the mass unit, these choices lead to a time unit $\sigma\sqrt{m/\epsilon}$, which is 1.8148×10^{-12}sec.. The high accuracy of the algorithm we have used and the relatively large cut-off distance 5σ (a popular value is 3.2σ) for the interaction potential enable us to use a relatively large time step, $\Delta t=0.01102$, corresponding to 0.02 picosecond, even when the fast librational motion is present.

The Lennard-Jones potential V(r) is cut off at $r_0=5\sigma$ and then modified to be of the form

$$V'(r)=\begin{cases} V(r)-V(r_0)+f(r_0)r-f(r_0)r_0, & r<r_0 \\ 0, & r>r_0 \end{cases} \qquad [4.24]$$

so that the potential and the force are both continuous at the cut-off, where

$$f(r)=-\frac{\partial V(r)}{\partial r}\ .$$

Since $f(r_0)$ is as small as -0.00031, the term linear in r in [4.24] does not affect the calculation significiently. In fact, this effect is

expected to be smaller than the statistic error, but the continuities of potential and its derivative are helpful to the accuracy of the integration. The large cut-off also gives more information about the radial distribution function of the mass centers (RDF_{cm}), because the RDF_{cm} is calculated along with the potential and force for the reason of computational convenience when pair-wise potential is used.

The major amount of computer time is spent on calculating the forces. To reduce the computation time, we divided the system into 16 blocks, the length of the block in one of the two directions (a and b) is five lattice spacing, which is much larger than the cut-off distance. The molecules in one block can only interact with the molecules in the same block or the neighboring blocks. The molecules are labelled from 1 to 400 and are distributed in the blocks according to their positions. In the central memory of the computer, every block has 40 addresses, this is sufficient to accommodate the labels of the molecules in a block, because the average number of molecules in one block is 25, with a possible variance of 5. In the central memory, these labels are the contents of the addresses symbolized by the block name. In calculations, the particular pair of molecules which interact with each other can be easily identified without searching all the molecules and comparing the separation with cut-off distance 5 for every pair of them. Thus the number of loops in calculation of the potential and force is proportional to N rather than to N^2.

When a molecule moves out of the MD cell, it should be replaced by its image according to the periodic boundary condition. However, to calculate the correlation functions of position, we have to know the

positions of every molecule even some of them may walk out of the MD cell. Rather than to add an array to count the number of transgressions, we exploit a hardware feature of the Cyber 750. A word in Cyber 750 has 60 bits, for a floating point real number, the first is a sign bit, the subsequent eleven are used to store the exponent and the remaining 48 store the coefficient. If we shift the the position variables (in the scaled coordinate) to be in the interval (24, 25), and the angular variables can be scaled in the units 2π, then shifted to the interval (24, 25), too, thus the first 5 bits of the 48 bits storing the coefficient will contain the integer part of the position variable. Even for a very long simulation run, it seems unlikely that the integer part can become less than 16 or larger than 32 resulting in a change of the number of the bits storing it, because a length of 8 in our scaled coordinate system corresponds to 160 lattice spacing! In fact, we have never found it happen in our simulations. Knowing exactly where the decimal parts are stored, it is trivial to fetch them only into the calculation of potential and force. Now the decimal part takes care of the periodic boundary condition, the integer part keeps the information whether the molecule flees out, altogether, they give the true position of the molecule. These data can be then used directly to calculate position correlation function without further manipulations. The only compromise we have to make is that the 14 significient digits Cyber 750 provides are now reduced to a number a little worse, but still better than enough, 12.

IV. THE FERRO-PARAELASTIC TRANSITION

Under zero external pressure, beginning at T=0.12, the temperature of the system is gradually raised with a temperature step 0.06. We found two phase transitions, the first one at T_1=0.38 (20.6K) where the system undergoes a ferro-paraelastic transition, the orientational LRO is lost and the lattice becomes triangular; the second transition occured at T_2=0.70 (38.0K) where the plastic phase melts to a 2d liquid.

Various physical quantities such as internal energy, density, radial distribution function, order parameters are calculated in the MD simulations. For the ferro-paraelastic transition, the results are consistent with a first-order behaviour, and do not show any clue of a two-stage transition. When the system is heated from T=0.36 to 0.38, all these quantities changes drastically in 8000 time steps, this simulation length corresponds to a real time 160 picoseconds. After that the system has a triangular lattice and the orientational order disappears. The system then run 1.2×10^4 time steps over which thermal averages are calculated.

A: Lattice Anisotropy Parameter and Orientational Order Parameter

We use $\gamma=(b/\sqrt{3}a-1)$ as a measure of the distortion of the lattice from a perfect triangular structure. In the ground state, a=3.332Å and b=8.054Å, γ has the value 0.396. Just before the transition, the MD cell gives a=3.462, b=8.055 and γ is as high as 0.343. The slow reduction of γ as T increases (see Fig. 4.3) proves that the ground state structure is stable under perturbations of librons and phonons.

After the transition, a increases suddenly to 4.006 and b is 7.066, these values correspond to a triangular lattice. An interesting thing is that the lattice spacing 4.006 is very close to that of the HB structure in Fig. 4.1(b). The curve of γ vs. T is plotted in Fig. 4.3.

For the orientational order, we take

$$\eta_2 = \frac{1}{N} \sum_i \cos(2\theta_i - 2\bar{\theta}) \qquad [4.25]$$

as the primary order parameter, where $\bar{\theta} = \frac{1}{N} \sum_i \theta_i$, and

$$\eta_6 = \frac{1}{N} \sum_i \cos(6\theta_i - 6\bar{\theta}) \qquad [4.26]$$

as an auxilary order parameter. If the orientational LRO is destroyed by the formation of the three equivalent domains and the ferro-paraelastic transition takes place in two stages, our test simulation studies show that η_6 has a sharp but relatively smaller drop at a critical temperature as η_2 does when the domain walls appears, it will decrease quite slowly until a higher critical temperature where it drops sharply again as the structure of the system becomes triangular. In this intermediate phase, η_2 keeps a value close to zero.

For the present system, both η_2 and η_6 have large drops at T=0.38, it contradicts the hypothesis of a two-stage transition. In Fig. 4.3 the orientational order parameters appear discontinuous at the transition temperature 0.38, and η_2 does not show a slow decaying tail. It is a well-known phenomenon that such a tail is always present after the transition as a finite size effect in computer simulation if the transition is second order.[4.12] These facts suggest that the transition is first order. The tail of η_6 is due to the local short

range ferro-ordering along three equivalent directions. After transition, in the system there are small patches where this ordering persists.

B: Radial Distribution Fuction

Because the ground state structure can be treated as distorted triangular lattice, the radial distribution function of the mass centers of molecules (RDF_{cm}) can be viewed as that every peak in a set characterizing the triangular lattice is split to a doublet. In particular, the peak coming from the 6 nearest-neighbors in a triangular lattice will split into two separate peaks, one coming from two neighbors with separation a, the other from the four neighbors with a distance $(a^2+b^2/4)^{1/2}$. In the case where the formation of domain walls destroys the orientational LRO, the radial distribution function of the mass centers of molecules (RDF_{cm}) will have two sets of coexisting peaks: one reflecting the distorted triangular lattice structure (coming from the domains) and the other characterizing the triangular structure (coming from the wall region). Especially, between the two peaks characterizing the 6 closest neighbors in the distorted triangular lattice, emerges a new peak signaling the appearce of the triangular structure in the wall region. This is what happens in some of our test runs.

In the first 8000 time steps when the system is heated to T=0.38 from 0.36, the splittings between the two close peaks which correspond to a single peak of triangular lattice becomes narrower as time increases, finally the splittings disappear and the RDF_{cm} shows a set of

peaks appropriate to a triangular lattice. Fig. 4.4(a) and (b) give the RDF_{cm} at T=0.36 and T=0.38, respectively

The explicit form of the radial distribution function $g(r)$ in Fig. 4.4 is

$$\langle n_{r^2, r^2+\Delta r^2} \rangle = \pi \Delta r^2 g(r) \qquad [4.27]$$

where $n_{r, r+\Delta r}$ is the average number of molecules in the ring whose area is $\pi\Delta r^2$. Because the horizonal axis is plotted in r^2, $g(r)$ will approach the value of the density as r^2 goes to infinity.

C: Energy and Density

In Fig. 4.5 and Fig. 4.6, the curves of energy E and density ρ vs. T are given. Both show a jump at T=0.38. The change of the entropy can be calculated by using the formula $\Delta S=\Delta E/T_c$ and it is 0.88 (in unit k_B). Since for a free rotor the total entropy is $\ln(2\pi)=1.83$, the considerable change of the entropy suggests that the rotors are nearly free. This fact, along with the discontinuities in the energy and the density, prefers the conclution that the transition is first order.

D: Orientational Diffusion Coefficient

In the ferroelastic phase, due to the symmetry of the diatomic molecule, there are two degenerate orientational states separated by π for every molecule. As the temperature increases, so does the probability for the molecules to overcome the energy barrier and shuttle between these two states. Before the rotors become free, one expects them to behave like hindered rotors and show a small orientational

self-diffusion coefficient at large time scale at certain temperatures. If the rotors are free, then even at a relatively shorter time scale the system will have a considerable orientational self-diffusion coefficient.

The orientational self-diffusion coefficient D_θ is expressed in the well-know Einstein's relation (in its 1D form)

$$D_\theta=\lim_{t\to\infty}\frac{1}{t}\langle[\theta(t)-\theta(0)]^2\rangle. \qquad [4.28]$$

In MD simulation, the average of orientational autocorrelation function is calculated as

$$f(t)=\langle[\theta(t)-\theta(0)]^2\rangle=\sum_{k=0}^{m_k-1}\frac{1}{m_k}\sum_i\frac{1}{N}[\theta_i(t+k\tau)-\theta_i(k\tau)]^2, \qquad [4.29]$$

where τ is a constant decided by the correlation time of the molecule dynamics, m_k is limited by the number of configurations available. Then we use linear regression to derive D_θ from $f(t)$ with different time scales.

When T is 0.30, at a time scale as large as 1600 time steps (32 ps), there is no evidence of the occurrence of orientational diffusion. Heated to T=0.36, we found $D_\theta=4.9\pm0.4\times10^{9}\text{rad}^2/\text{sec}$ for t>1000 time steps, at T=0.38, D_θ jumps to $1.49\pm0.08\times10^{11}\text{rad}^2/\text{sec}$ after the same number of time steps (see Fig. 4.7). Fig. 4.8 gives $\ln D_\theta$ vs. 1/T, note the slope changes at the solid-liquid transition region about T=0.70.

E: Strain Fluctuation and Elastic Constant

The gauge metrix G appearing in eqn. [4.8] reflects the change of the volume and shape of the MD cell, it keeps the information about the

strain. As Parrinello and Rahman have identified, the relation between G and the strain tensor can be expressed as

$$\epsilon(t)=\frac{1}{2}[h_0'^{-1}G(t)h_0^{-1} -1] \qquad [4.30]$$

where h_0 characterizes a reference MD cell, Rahman has recommended to use the average of h(t) over the simulation as h_0.(4.14)

The compliances are related to the fluctuations of the strain by the fluctuation-dissipation relation as(4.19)

$$\Gamma_{ijkl}=\frac{\Omega}{k_B T}\langle \epsilon_{ij}\epsilon_{kl}\rangle \qquad [4.31]$$

and the elastic constant C_{ijkl} can be obtained from the inverse of Γ_{ijkl}. However, the 4x4 matrix of Γ_{ijkl} is singular due to the permutation symmetry for the Cartesian index, by using the Voigt convention(4.20)

$$\Gamma_{\rho\sigma} = \begin{cases} \Gamma_{ijkl}, & k=l \ (\sigma\leq 2) \\ 2\Gamma_{ijkl}, & k=l \ (\sigma>2) \end{cases} \qquad [4.32]$$

one can get a 3x3 regular matrix and its inverse can be calculated. To obtain symmetric C_{ijkl} one then inverts the transformation of [4.32].

To derive accurate values of C_{ijkl} is difficult due to the large fluctuations of strain near the transition. However, the general features can be seen by comparing the values at T=0.36 and 0.38. We found that (in unit ϵ/σ^2, in terms of Lennard-Jones potential parameters)

for T=0.36, C_{11}=1.45, C_{22}=0.97, C_{12}=2.10, C_{44}=1.33;

for T=0.38, C_{11}=1.05, C_{22}=1.07, C_{12}=1.02, C_{44}=0.11.

Clearly, before the transition the system is highly anisotropic but after the transition it is isotropic, $C_{11}\simeq C_{22}$, but the ratio C_{44}/C_{11} and $(C_{11}-C_{12})/C_{11}$ drop sharply at the critical point. This fact can be visibly recognized from Fig. 4.9(b) where we have plotted the bonds connecting neighboring molecules, the amplitudes of phonons are much larger than that in Fig. 4.9(a).

F: Discussions

The prediction of the existence of a plastic phase from our MD simulations is consistent with the Monte Carlo (MC) simulation results of Etters et al.[4.7] for small clusters. In the simulation studies of clusters with different numbers of molecules, they found that there was an orientationally disordered phase when the number of molecules in the cluster ranged from 3 to 12 (the largest number in their simulations). Our MD results and their MC results are complementary to each other: they mimicked the behavior of the cluster using a more complicated O_2-O_2 potential which included both a Lennard-Jones part as ours and a small quadrupole-quadrupole part, the absorbate-substrate potential was also added in their simulations; we simulated the monolayer including only the dominant part of the O_2-O_2 potential. For the clusters, the the orientationally disordered behavior begins at about 5-7K for the molecules having 2 neighbors, and this temperature rises to 11-17K for molecules connecting 3 or 4 neghbors. For the monolayer, our simulation

shows that the transition takes place between 19.6 and 20.6K. The question whether this plastic phase exists in real oxygen monolayer remains yet to be observed experimentally. An interesting feature of bulk γ-O_2 worth mentioning here is that an orientational transition is believed to be present in this material prior to the melting temperature 54.8K.[4.21]

The discontinuities found in energy, density, orientational order and lattice distortion parameter, orientational diffusion coefficient suggest that the transition is first order. Considering the evidence that in 2D systems fluctuations may drive the orientational transition first order for a fixed lattice (a system believed to represent this situation is the N_2 monolayer physisorbed on graphite substrate[4.6]), coupling to phonon excitations is more likely to make the transition first order due to enhanced fluctuations.

To investigate the physical reasons for the observed first order transition we have counted the vortex density on triangular plaquetes as a function of T. Before the transition i.e. at T=0.36, there is only one VA pair but after the transition i.e. at T=0.38 the number suddenly jumps to 83. (see Fig. 4.9) This phenomenon can be understood as follows.

In the low T ferroelastic configuration on a triangle, if one molecule is fixed, then to form a vortex, one of the other two have to rotate at least $\pi/6$; but in a herringbone structure, if the molecule which has an orientation different from that of the other two is fixed, then the other two only need to rotate a small angle but in opposite directions in order to form a vortex (see Fig. 4.2). We have calculated

the potential wells in above two situations, assuming the neighboring molecules are fixed (see Fig. 4.10). The potential well for the ferro-ordering on the centered rectangular lattice is much narrower and deeper when the lattice spacings are close to the values appropriate for the ground state, but at T=0.36, it has nearly the same width as that for the herringbone ordering on the triangular lattice, even a rotation of $\pi/6$ does not cost too much energy. Therefore at low T the VA pairs are strongly suppressed, without enough sources of strings, it is difficult for the formation of domain walls.[4.22] As T rises, the orientational potential well broadens and becomes shallower and this change is not only due to the orientational fluctuation, but also drastically depends on the increase in lattice spacing caused by anharmonic phonons. At a critical temperature T_c, the core energy of the VA pair is sufficiently small so that the VA pairs appear in a large number and cause a first order transition. The coupling between orientational and translational degrees of freedom effectively reduces the core-energy of VA pair and drives the orientational order-disorder transition first order.

The low core-energy vortices tend to form clusters as can be seen from Fig. 4.9(b) and as observed by Saito in his dislocation vector system.[4.23] Thus in many areas in the system the local density of VA pair is very high. For ferro-ordering, the vortex, as topological defects, has a configuration which resembles closely the herringbone structure, and on a triangular lattice, this structure is the ground state for antiferromagnetic interaction. By coupling to the translational degrees of freedom, the nature of the orientational

interaction can be changed as the lattice spacing varies. The intermolecular interaction prefer the ferro-ordering at relatively small separations but favors antiferro-ordering at large separations, the crossover is at about 4.0Å. We have already given an effective spin Hamiltonian for a separation 3.332A in eqn. [4.3] and it is ferromagnetic in the spin language. When the separation is 4.0Å, the effective Hamiltonian becomes

$$V(\theta_i,\theta_j)= -1.826+0.722(\cos2\theta_i+\cos2\theta_j)+0.071(\cos4\theta_i+\cos4\theta_j)$$
$$+0.353\cos(2\theta_i-2\theta_j)+0.569\cos(2\theta_i+2\theta_j) \qquad [4.33]$$

and it is antiferromagnetic. Thus in the region where the local density of VA pair is high, to reduce the excitation energy it is favorable to change the local structure to be triangular with a lattice spacing of about 4Å. The net result of this lattice-mediated competition between ferro- and antiferro-ordering is that before a possible 3-state continuous Potts transition can take place, the ferroelastic phase undergoes an orientational order-disorder transition and becomes paraelastic simultaneously. The ferro-paraelastic transition becomes a synonym of the orientational order-disorder transition in this particular case in the sense that they are completed at the same critical temperature.

A configuration of a quench study is given in Fig. 4.11. The system is quenched from T=0.38 to 0.01 in 20 time steps by taking the kinatic energy out. There are only tiny domains with three equivalent distortion directions; but a great number of vortices is persistent in the system, and we find a hexagon with local herringbone structure. The picture is quite different from that appearing in Fig. 3.5.

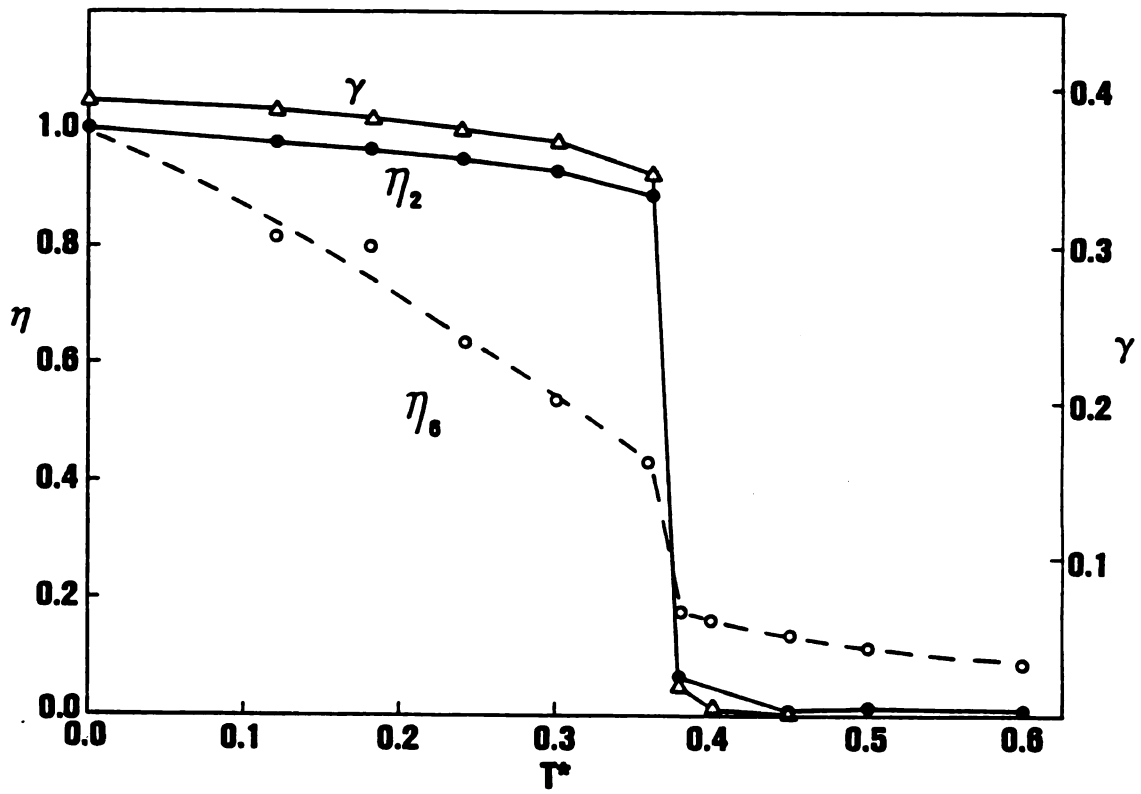

Fig. 4.3 Lattice anisotropy parameter γ and orientational parameters η_2 and η_6 vs. temperature. All parameters sharply drop at T=0.36.

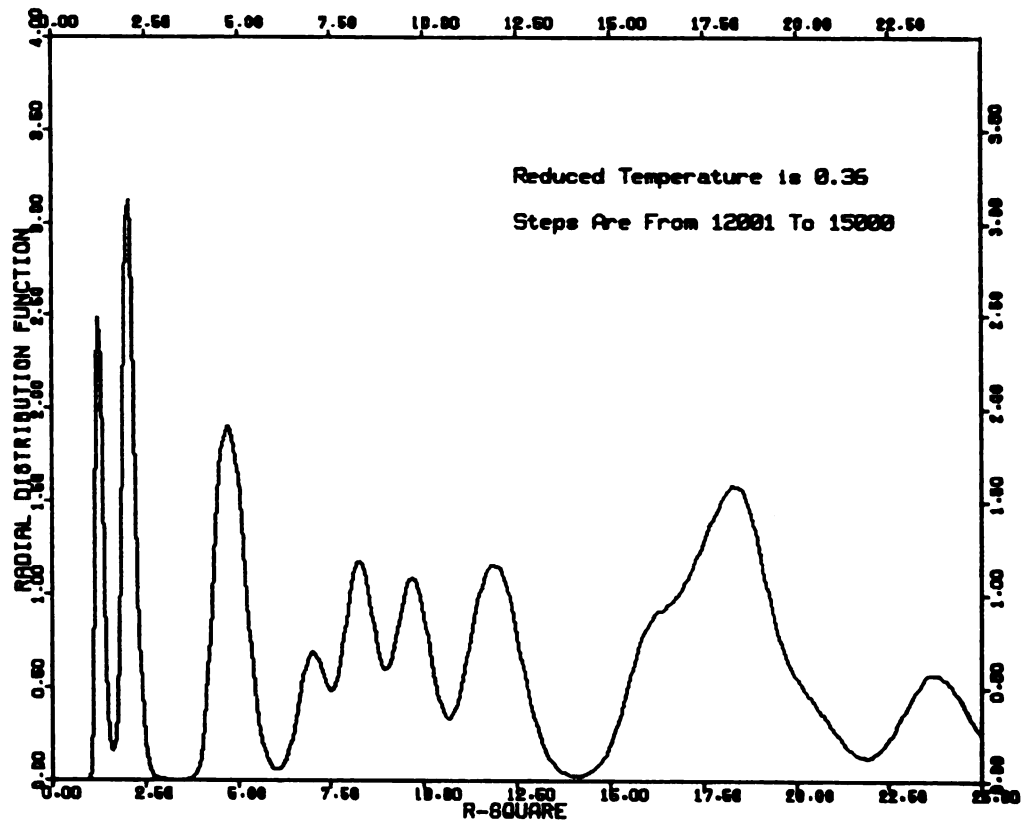

Fig. 4.4 (a) The radial distribution function of the mass centers of molecules at T=0.36, averaged over 3000 time steps (60 ps). The positions of the peaks indicate a centered rectangular lattice.

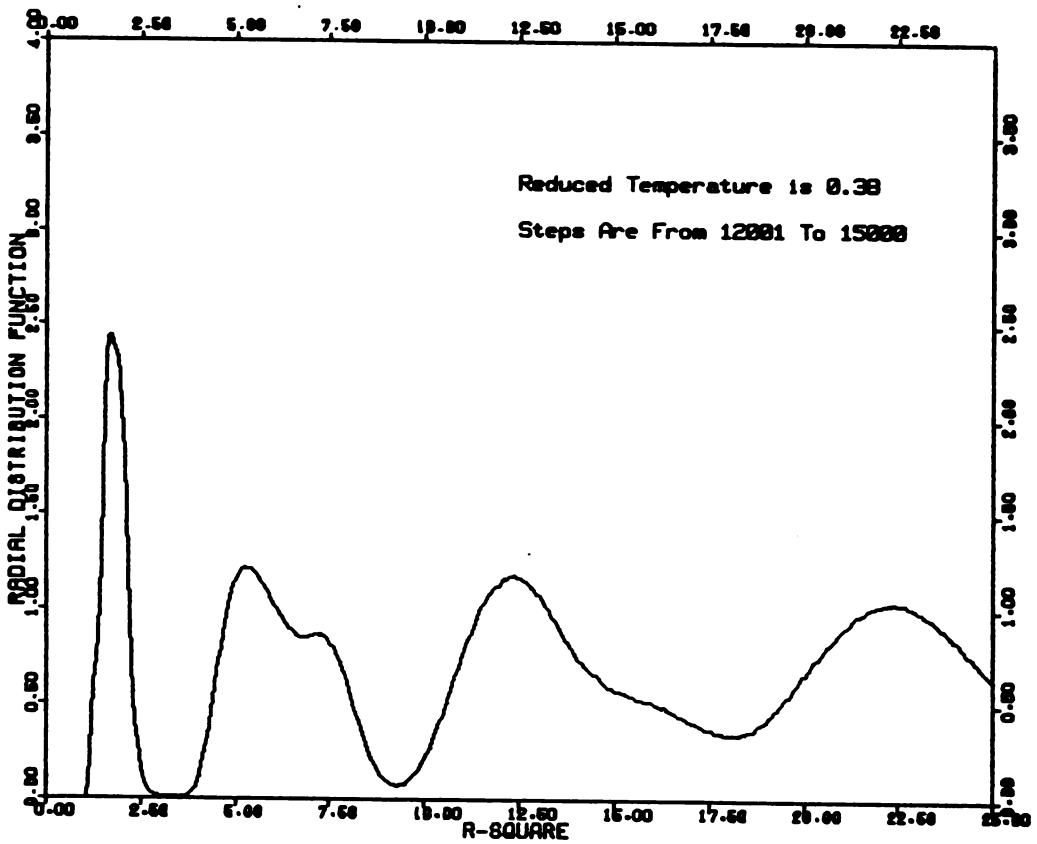

Fig. 4.4 (b) The radial distribution function of the mass centers of molecules at T=0.38, averaged over 3000 time steps (60 ps). The positions of the peaks indicate a triangular lattice.

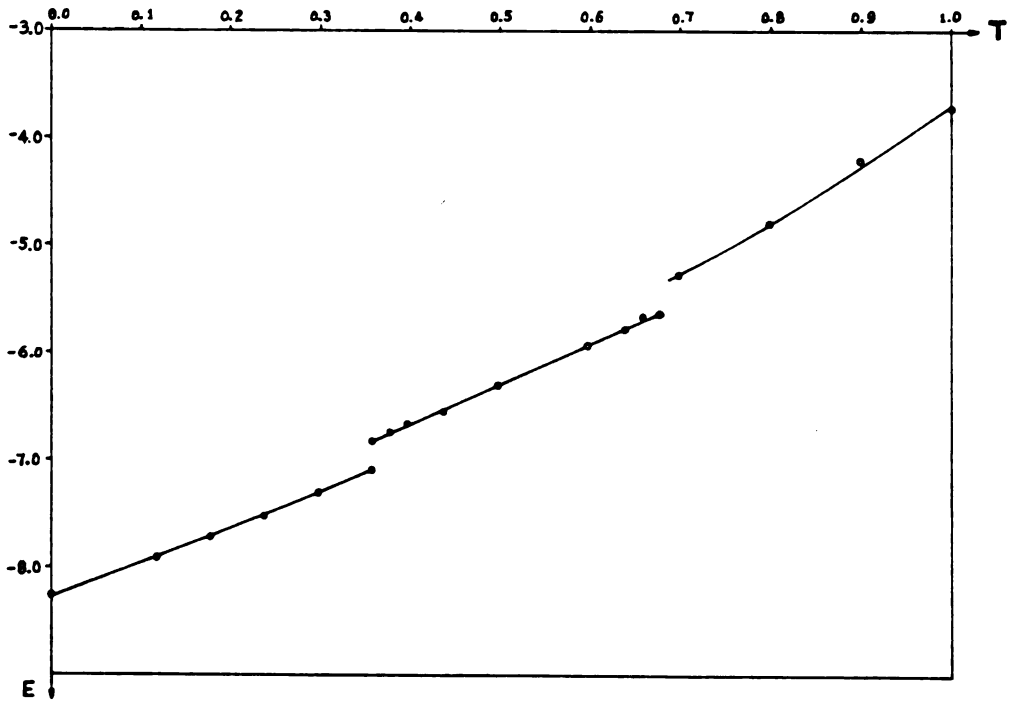

Fig. 4.5 Total energy E vs. temperature. Energy and temperature are in unit ϵ and ϵ/k_B respectively. At T=0.36 there are two data points, one is the data of heating run, the other is the data of a cooling run (cooled from T=0.38). The line are guides to the eye.

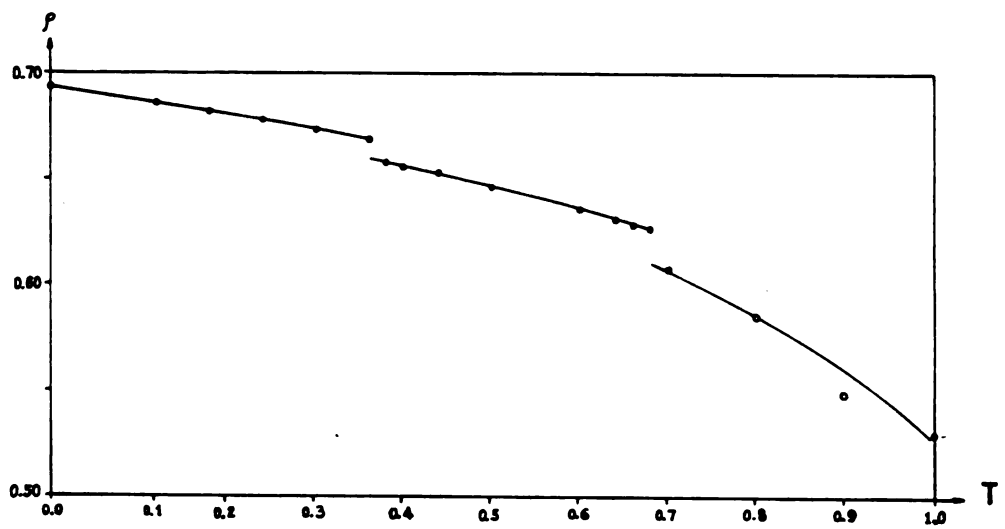

Fig. 4.6 Density ρ vs. σ^{-2} temperature. Density and temperature are in unit σ^{-2} and ϵ/k_B respectively. At T=0.36 there are two data points, one is the data of heating run, the other is the data of a cooling run (cooled from T=0.38). The line are guides to the eye.

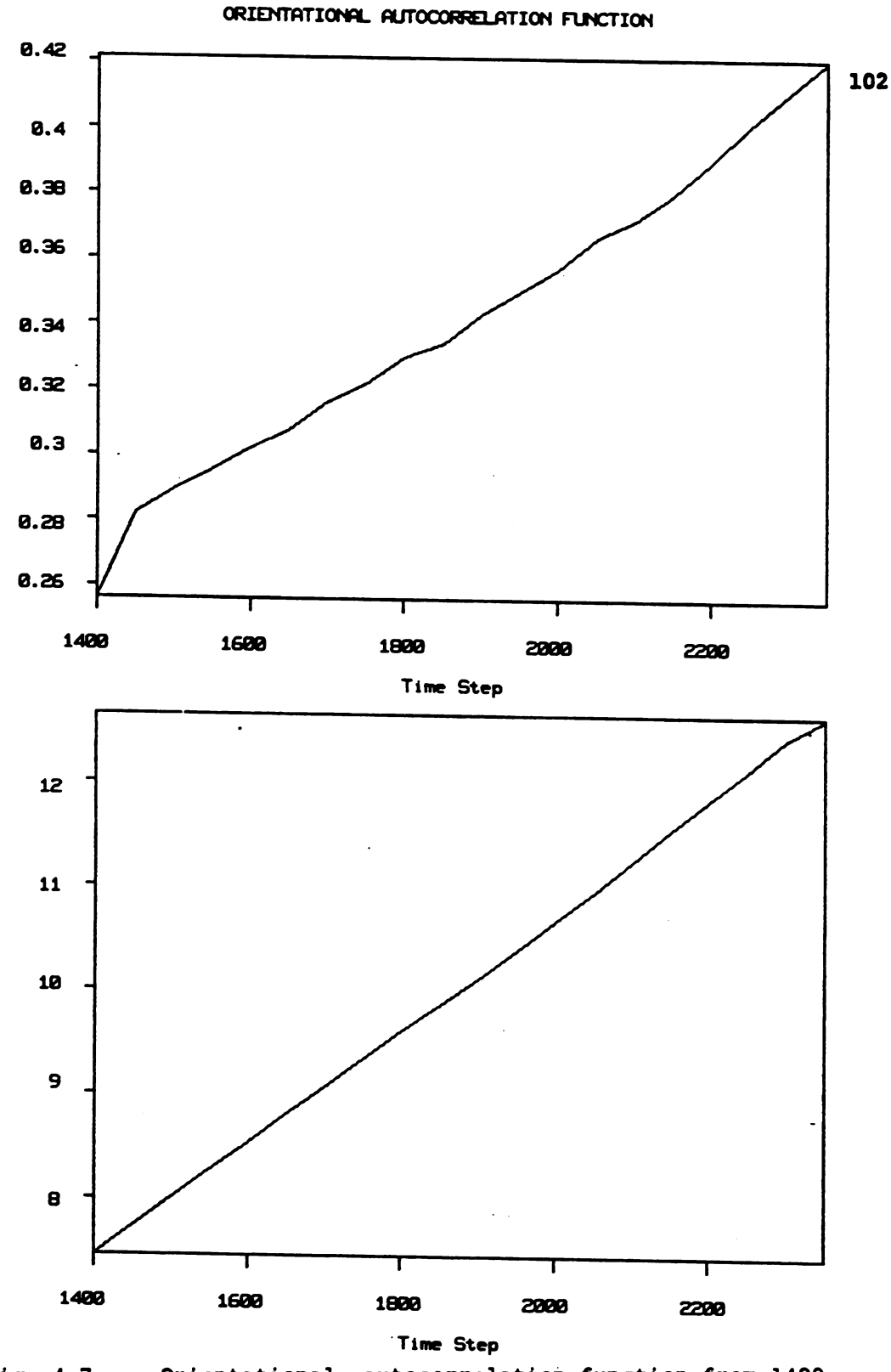

Fig. 4.7 Orientational autocorrelation function from 1400 to 2300 time steps. The vertical axes are in unit of rad^2. The temperature for the graph at top is 0.36 and it is 0.38 for the graph at bottom.

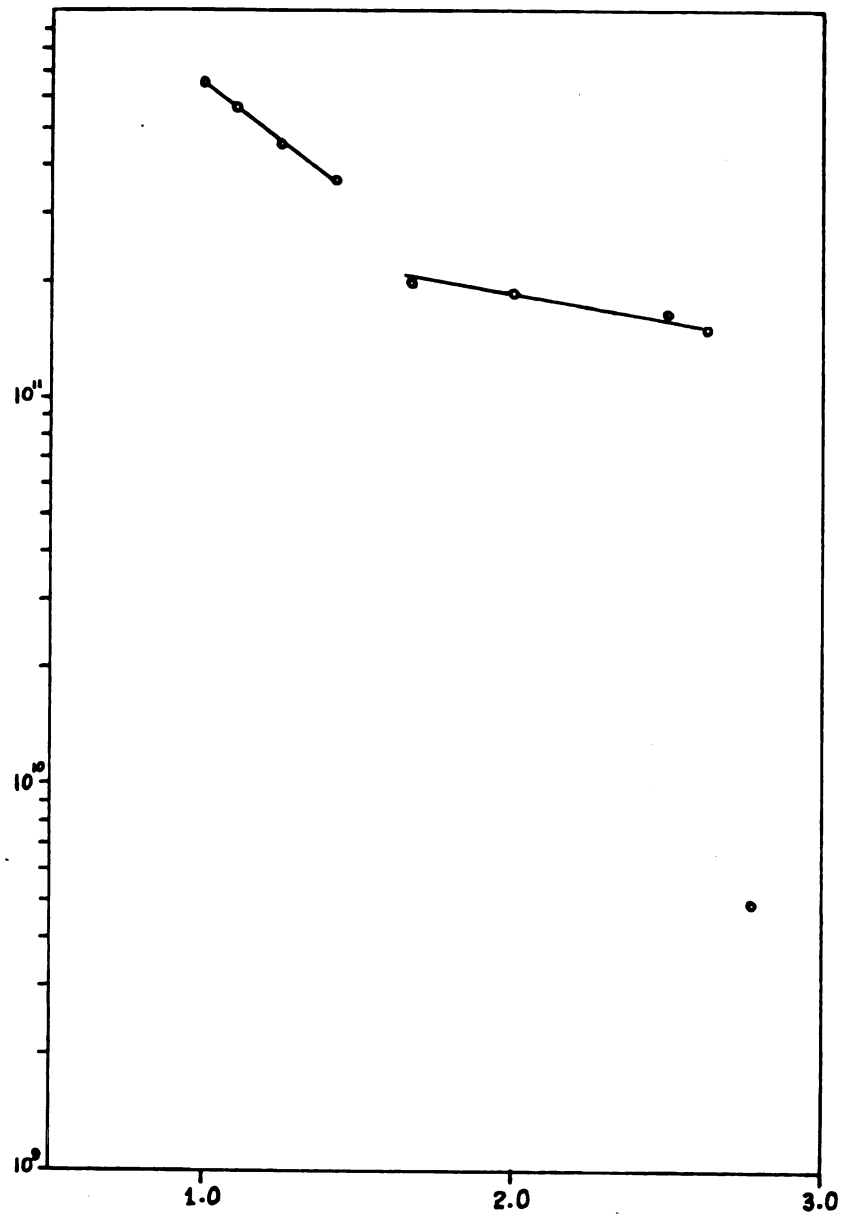

Fig. 4.8 Orientational diffusion coefficient D_θ vs. the reciprocal of temperature. Note D_θ is discontinuous at solid-liquid transition temperature 0.7.

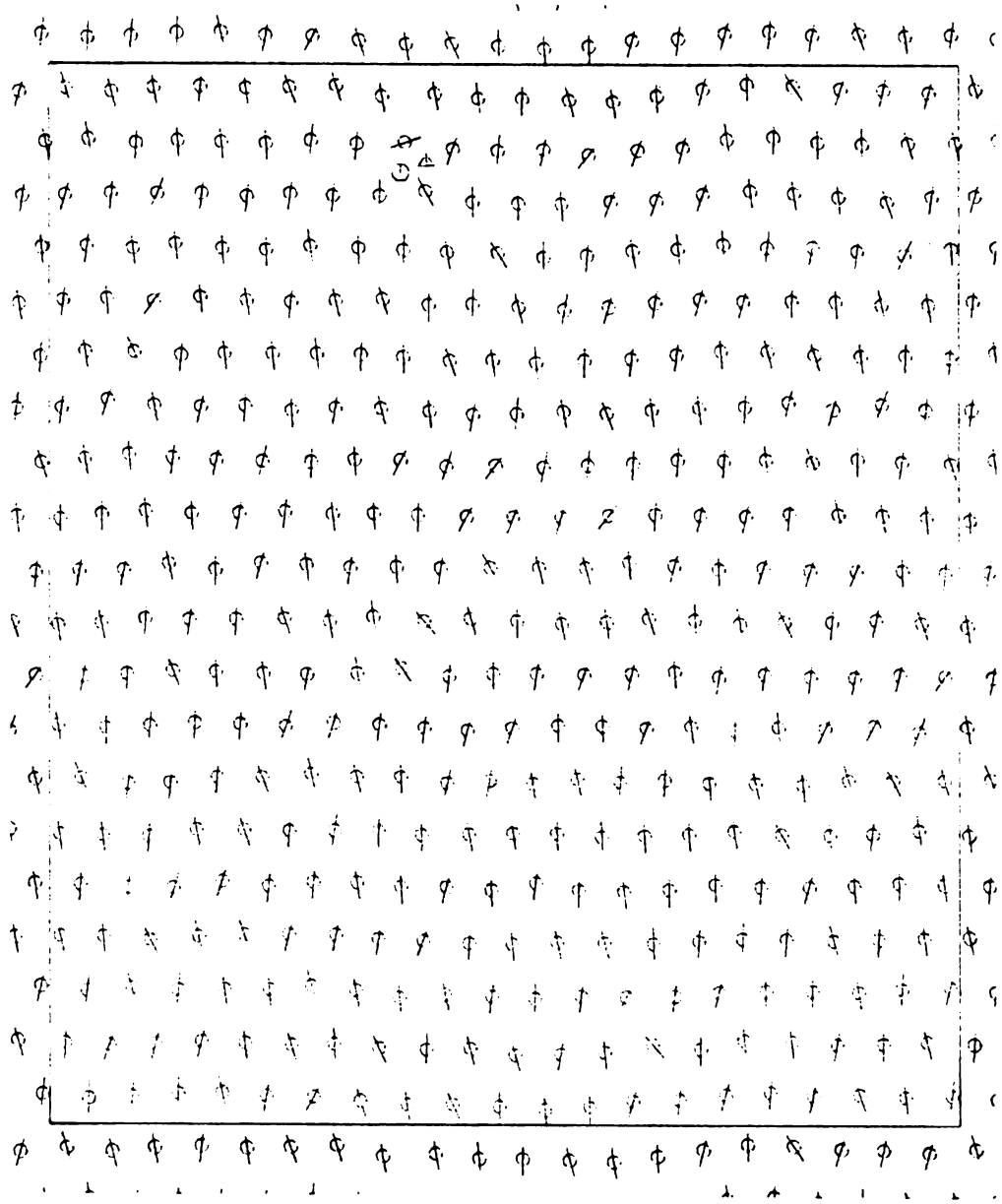

Fig. 4.9 (a) A snapshot of the configuration of molecules at T=0.36. The time step is 15000. In the picture, circle denotes positive vortex and triangle denotes negtive vortex, there is only one bound VA pair. The frame indicates the MD cell, the molecules outside of the frame are plotted according to the periodic boundary condition.

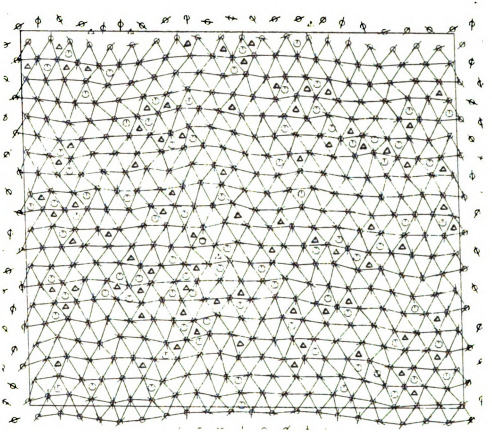

Fig. 4.9 (b) A snapshot of the configuration of molecules at T=0.38. The time step is 12000. After ferro-paraelastic transition, the number of VA pair suddenly jumps. In this picture, there are 83 such pairs.

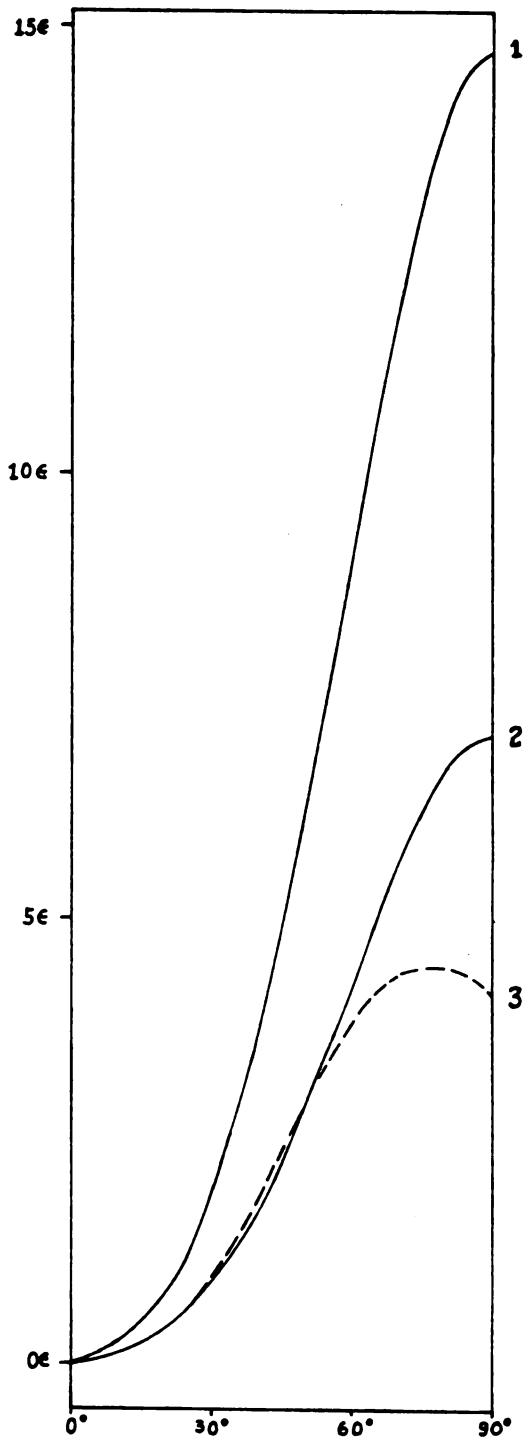

Fig. 4.10 Orientational potential well for molecule. Line 1 corresponds to the ground state, line 2 to the centered rectagular lattice at T=0.36, dashed line 3 to the triagular lattice (lattice spacing is 4.006) with antiferro-ordering.

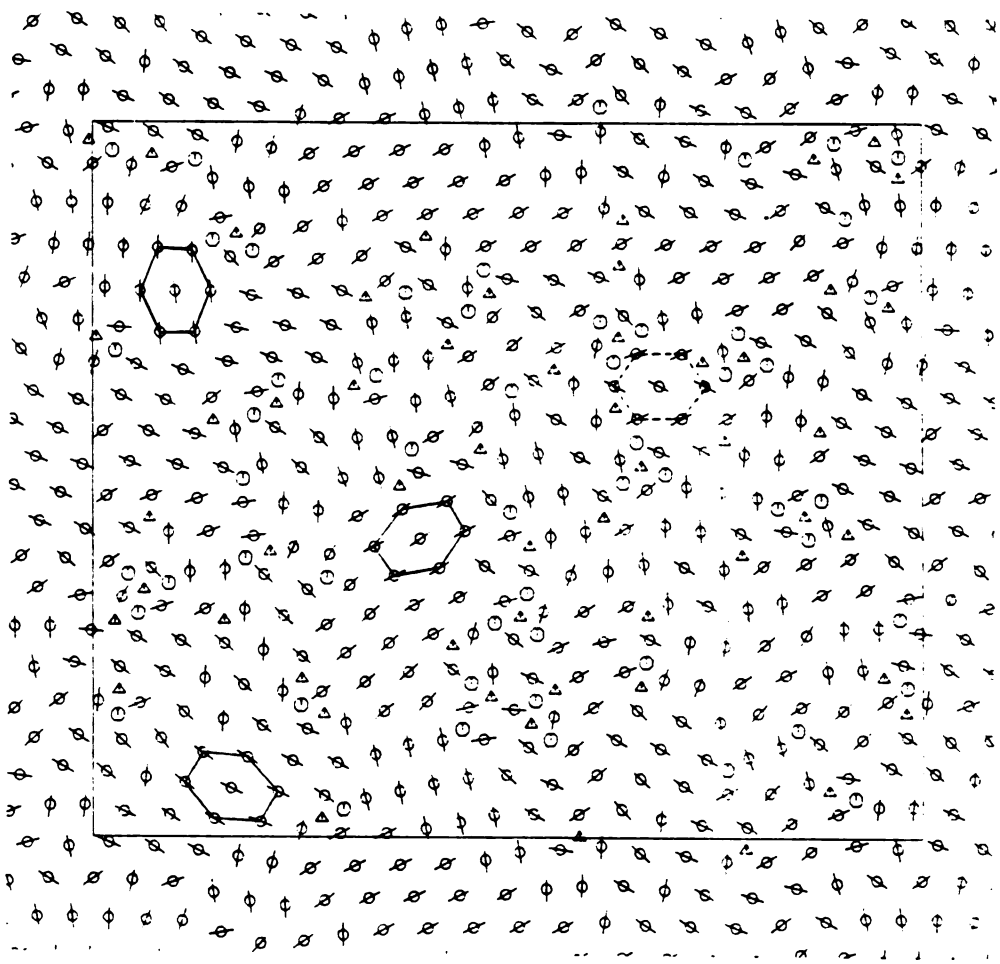

Fig. 4.11 A configuration after the system was quenced form T=0.38 to 0.01. Although 1000 time steps are passed, the density of VA pair is high, and the domains are small. A hexagon with local herringbone structure is marked by dashed lines.

VI. SUMMARY AND COMMENTS

We have also used the constant-pressure molecular dynamics method to explore the melting transition. We have reached the liquid phase at T=0.70, where the RDF_{cm} has less features, (see Fig. 4.12). In Fig. 4.13, we can find many dislocation pairs in the configuration of molecules. Fig. 4.6 and 4.7 show that the energy E and the density ρ both have a discontinuity at the melting temperature, these results indicate that the melting transition is first order as is seen in the computer simulations for 2D monoatomic molecular systems with Lennard-Jones potential.[4.24] The time scale in our simulation, however, is not sufficiently long to give the dislocation-mediated melting theory an exclusive test.

According to the results of our constant-pressure molecular simulations, the 2D diatomic molecular system studied first udergoes a ferro-paraelastic transition from an orientationally ordered ferroelastic phase to an orientationally disordered plastic phase at temperature T_1, then at a higher temperature T_2 the plastic phase melts to liquid. Both transitions are first order.

The driving mechanism for the ferro-paraelastic phase can be understood in the light of the role played by vortices. The sudden emergence of great number of vortices destroys the orientational long-range order. The physical reason why the transition is first order and why it does not take place in two stages can be found in the strong coupling between the orientational and translational degrees of freedom. This coupling reduces the chemical potential needed to generate VA pair,

so the orientational order-disorder transition occurs at a temperature much lower than that for a fixed lattice but with the same kind of molecular interaction[4.25] and the transition becomes first order. This coupling also rules out the possiblity of a two-stage transition by introducting the lattice-mediated competition between different orderings.

The reason for this transition to be first order is somewhat similar to that proposed by Van Himbergen[4.26] for an isotropic XY model with an interaction of the form

$$V(\theta_i-\theta_j)=V(\theta)=2J[1-(\cos^2\theta/2)^{q^2}],\ J>0 \qquad [4.34]$$

for $q^2>10$ in which case the transition from KT phase to the high T phase is first order. For $q^2<10$, the potential is rather soft and the KT transition is continuous. It will be very interesting to investigate the effect of the symmetry-breaking field terms of the form $h_p\cos(p\theta_i)$ on this Hamiltonian.[4.27] Whether a large q value will change the continuous Ising-like transition to become first-order when p=2, or whether at certain q the intermediate XY-like phase will disappear when p>4? These crossover behaviors between different types of phase transitions are of current theoretical interest.[4.28]

For diatomic molecules interacting with each other via atom-atom potentials, the interaction is highly anisotropic when the average separation between the molecules is small, but the anisotropic part of the interaction reduces rapidly as the separation increases. The relative strength of the anisotropic interaction can be measured by the ratio between the magnitude of of anisotropic terms and that of the

constant term in the effective spin Hamiltonian. This ratio for eqn. [4.33] is much smaller than that for eqn. [4.3]. Under zero external pressure, the system can expand freely as the temperature rises, and a tiny increase in the lattice spacing is sufficient to bring the interaction to become close to isotropic, but the translational potential well is still quite deep in comparison to the kinetic energy, so the topological defects mainly appear in the orientational space, and it leads to a stable isotropic plastic phase between anisotropic solid and isotropic liquid phase. However, if the external pressure (or an uniaxial stress along *a* direction) is sufficiently high, the system is considerably compressed from its zero-pressure state, the interaction will keep its highly anisotropic feature even at a temperature where the molecules have enough kinetic energy to become mobile. It is then possible that the translational topological defects, dislocations, have lower excitation energy than the orientational topological defects, and dislocations develop along with the orientational order. In this high-pressure region, the dislocation-mediated melting theory for anisotropic layers proposed by Ostlund and Halperin[4.28] will probably be applicable. The system may melt to an anisotropic liquid through a continuous transition as predicted by this theory, then at a higher temperature the system undergoes another transition to become an isotropic liquid. Even if the orientational topological defects play an important role in above transitions, due to the higher vortex core-energy caused by smaller separation between molecules, the transitions are possibly still continuous. If it is the true situation, then we have a model liquid crystal system with the well-known

Lennard-Jones potential and an external parameter, namely pressure which can be easily adjusted in computer simulation to obtain this phase. Such a model should be ideal in the theoretical study of the properties of 2D liquid crystal phase. From the view point of phase transition, another interesting problem is then what happens between these zero pressure and high pressure extreme cases? Multicritical points are possibly present where phase boundary associated with the first order transition meets critical line.

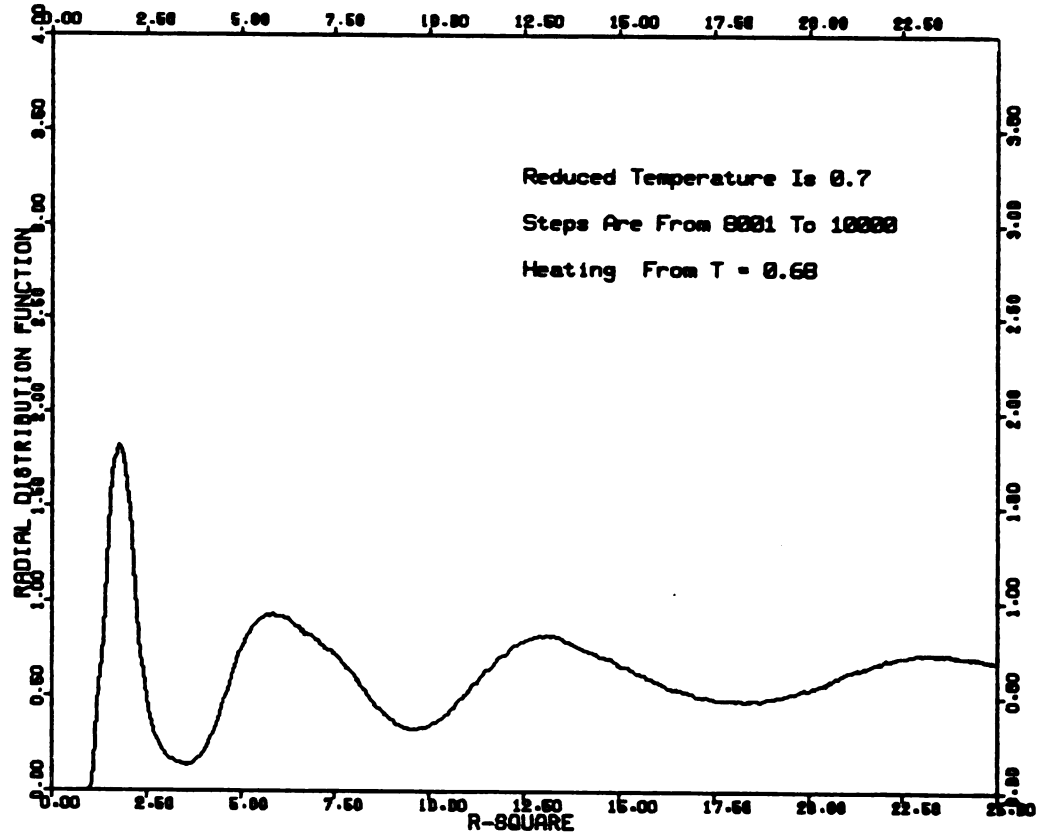

Fig. 4.12 The radial distribution function of the mass centers of molecules at T=0.70, averaged over 3000 time steps (60 ps). It shows liquid-like feature.

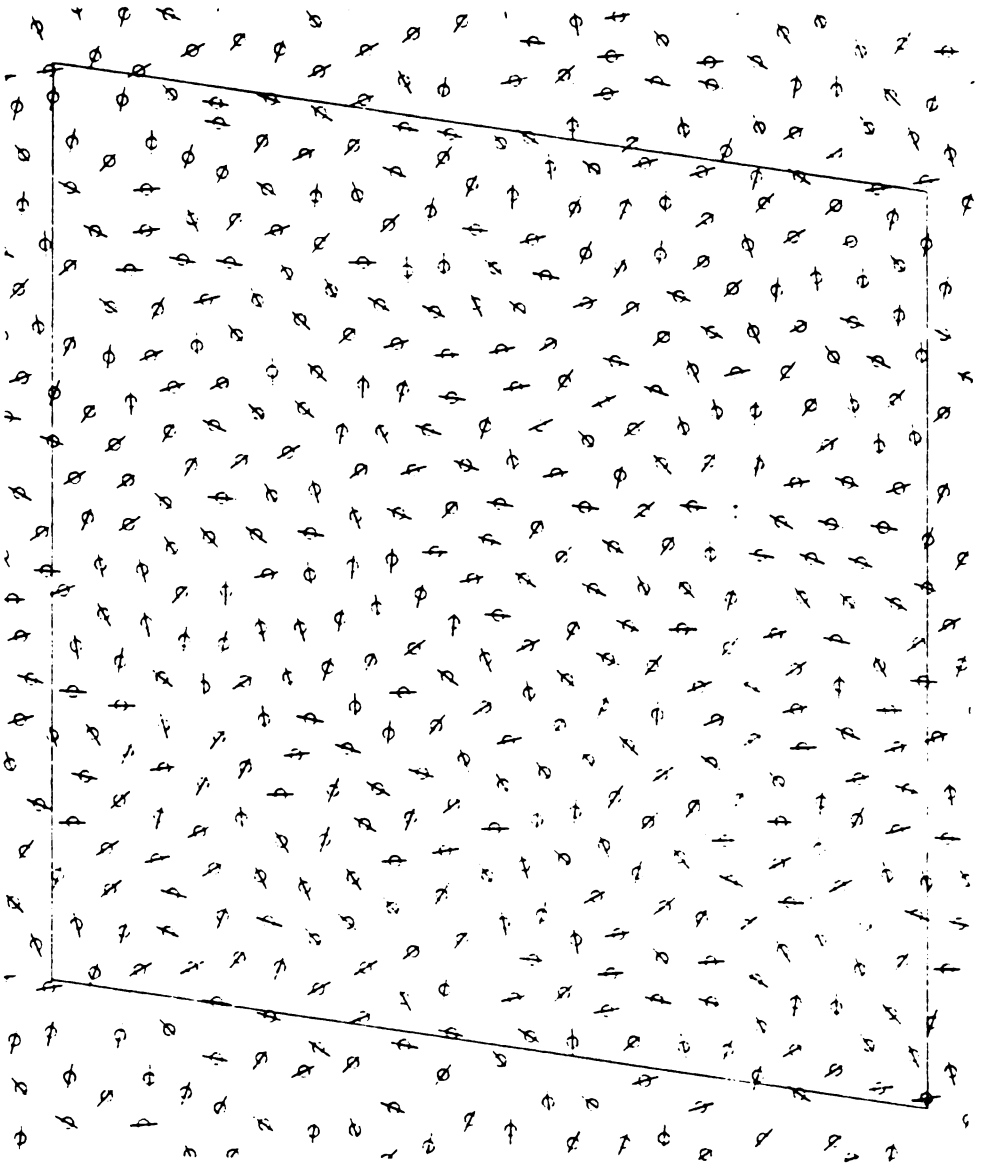

Fig. 4.13 A snapshot of the configuration of molecules at T=0.70. The time step is 12000. There are many dislocations.

REFERENCES FOR CHAPTER 1

(1.1) One may gain an appreciation for the multitude of novel 2D phenomena and the excitements in this field by referring to *Procedings of the International Conference on Ordering in Two Dimensions, Lake Geneva, may 1980,* Edited by S. K. Sinha (North-Holland, Amsterdam, 1980)

(1.2) J. Needham, *Science and Civilization in China*, Vol. 3, (Cambridge University Press, 1959).

(1.3) *Phase Transitions in Surface Film,* edited by J. G. Dash and J. P. Ruvalds, (Plenum Press, NY 1979).

(1.4) Recent experiments found that N_2 monolayer was possiblly incommensurate at high coverage. See S. C. Fain, Jr., and H. You, Bull.Am.Phys.Soc. 30, 333 (1985).

(1.5) For methane, R. Marx, and E. F. Wassermann, Surf.Sci. 117, 267 (1982); for ethane, F. Y. Hansen, R. Wang, H. Taub, H. Schechter, D. G. Reichel, H. R. Danner, and G. P. Alldredge, Phys.Rev.Lett. 53, 572 (1984).

(1.6) B. H. Grier, L. Passell, J. Eckert, H. Patterson, D. Richter, and R. J. Rollefson, Phys.Rev.Lett. 53, 814 (1984); S. Nose, and M. L. Klein, Phys.Rev.Lett. 53, 818 (1984).

(1.7) J. P. MacTague, and M. Nielson, Phys.Rev.Lett. 37, 596, (1976); M. Nielson, and J. P.MacTague, Phys.Rev. B19, 3096, (1979).

(1.8) See, for example, R. Marx, and B. Christoffer, Phys.Rev.Lett. 51,790 (1983).

(1.9) P. W. Stephens, P. A. Heiney, R. I. Birgeneau, P. M. Horn, J. Stoltenbe and O. E. Vilches, Phys.Rev.Lett. 45,1959 (1980).

(1.10) R. D. Etters, P. Pan, and V. Chandrasekharan, Phys.Rev.Lett. 45,645 (1980).

(1.11) M. F. Toney, R. D. Diehl, and S. C. Fain, Phys.Rev. B27,6413 (1983).

(1.12) J. M. Kosterlitz, and D. J. Thouless, J.Phys. C5, L124, (1972); J.Phys. C6, 1181, (1973).

(1.13) B. I. Halperin, and D. R. Nelson, Phys.Rev.Lett. 41, 121 (1978); D. R. Nelson, and B. I. Halperin, Phys.Rev. B19, 2457 (1979).

(1.14) A. P. Young, Phys.Rev. B19, 1855 (1979).

(1.15) Abraham showed that his computer simulation results suggested first-order transition, S. W. Koch, and F. F. Abraham, Phys.Rev. B27, 2964 (1983). A experimental example is, P. A. Heiney, R. I. Birgeneau, C. .G.Brown, P. M. Horn, D. E. Moncton, and P. W. Stephens, Phys.Rev.Lett. 48,104 (1982).

(1.16) S. Ostlund, and B. I. Halperin, Phys.Rev. B23, 335 (1981).

(1.17) Y. Saito, Phys.Rev. B26, 6239 (1982).

(1.18) H. Margenau, and N. R. Kestner, *Theory of Intermolecular Forces*, (Pergamon Press, NY 1971).

(1.19) A. I. Kitaigorodsky, *Molecular Crystal and molecules*, (Academic Press, New YorK, 1973).

(1.20) C. A. English, J. A. Venables, and D. R. Salahub, Proc.Roy.Soc.London, A340, 81 (1974).

REFERENCES FOR CHAPTER 2

(2.1) D. A. Goodings and M. Henkelman, Can.J.Phys. 49, 2898 (1971).

(2.2) M. F. Toney, R. D. Diehl, and S. C. Fain, Phys.Rev. B27, 6413 (1983); P. A. Heiney, P. W. Stephens, S. G. J. Mochrie, J. Akimatsu, and R. J. Birgeneau, Surf.Sci. 125, 539 (1983); and the chapter 4 of this thesis.

(2.3) R. K. Kalia, P. Vashishta, and S. D. Mahanti, Phys.Rev.Lett. 49, 676 (1982).

(2.4) For parameters of interest in this chapter, we find that the next-nearest neighbors contribute less than 10% of the nearest-neighbor contribution.

(2.5) J. M. Luttinger and L. Tisza, Phys.Rev. 70, 954 (1946); J. M. Luttinger, *ibid.* 81, 1015 (1951).

(2.6) The solution to the weak constraint problem satisfies the strong constraint, thereby the exact ground state of the Hamiltonian.

(2.7) See H. E. Stanley, *Phase Transitions and Critical Phenomena*, (Oxford University Press, London, 1971).

(2.8) F. Wegner, Z.Phys. 206, 465 (1967).

(2.9) For a system with D=0 and K<0, J<0, and K/J→0, we find that $\eta \sim \exp[-\text{const}(T/J)|\ln(K/J)|]$.

(2.10) The actual Hamiltonian, when terms of order a^6 are kept, has a form much more complicated than Eq. [7]. However, the additional terms drop out in H_{sp} beyond those given in Eq. [7] for ordered configurations shown in Fig. 2.2. Therefore dropping these additional terms in H_{sp} and studying changes in parameters D, J and K is meaningful only when one wants to test the stability of the ordered ground-state configurations when $O(a^6)$ terms are included.

REFERENCES FOR CHAPTER 3

(3.1) *Procedings of the International Conference on Ordering in Two Dimensions, Lake Geneva, may 1980,* Edited by S. K. Sinha (North-Holland, Amsterdam, 1980)

(3.2) When the substrate potential is strong and the density of adsorbed molecules is not too large, the principle axes of the molecules orient parallel to the surface; θ_i is the orientation of the i-th molecule.

(3.3) The previous chapter of this thesis.

(3.4) O. G. Mouritsen, and A. J. Berlinsky, Phys.Rev.Lett. 48, 181 (1982). K. Kaski, S. Knmar, J. D. Gunton, and P. A. Rikvold, Phys.Rev. B29, 4420 (1984).

(3.5) N. D. Mermin, and H. Wagner, Phys.Rev.Lett. 17, 1133 (1966).

(3.6) H. E. Stanley, and T. Kaplan, Phys.Rev.Lett. 17, 913 (1966); H. E. Stanley, Phys.Rev.Lett. 20, 150 (1968).

(3.7) J. M. Kosterlitz, and D. J. Thouless, J.Phys. C6, 1181 (1973); J. M. Kosterlitz, J.Phys. C7, 1046 (1974).

(3.8) F. Wagner, Z.Phys. 206, 465 (1967).

(3.9) V. Jose, L. P. Kadanoff, S. Kirkpatrick, and D. R. Nelson, Phys.Rev. B16, 1217 (1977).

(3.10) M. B. Einhorn, R. Savit, and E. Ravinovici, Nucl.Phys. 170, 16 (1980); R. Savit, Rev.Mod.Phys. 52, 453 (1980).

(3.11) J.Tobochnik, and G. V. Chester, Phys.Rev. B20, 3761 (1979).

(3.12) G. C. Grest, and D. J. Srolovitz, Phys.Rev. B28, 2693 (1983); In addition T. Schneider and E. Stoll have found that for 2D XY model with quartic anisotropy vortices were adsent near T_c, see *Solitons and Condensed Matter Physics,* (Springer-Verlag, 1978, p. 154).

(3.13) A. A. Migdal, Sov.Phys. JETP 42, 743 (1976); L. P. Kadanoff, Ann.Pyhs. (N.Y.) 100, 359 (1976).

(3.14) N. Metropolis, A. W. Rosenbluth, M. N. Rosenbluth, A. H. Zelle, and E. Zeller, J.Chem.Phys. 21, 1089 (1953).

(3.15) S. H. Schenker, and J. Tobochnik, Phys.Rev. B22, 4462 (1980).

(3.16) N. D. Mermin, Rev.Mod.Phys. 51, 591 (1971).

(3.17) B. M. McCoy, and T. T. Wu, *The Two-Dimensional Ising Model*, (Harvard University Press, Cambridge, Massachusetts 1973).

(3.18) C. Domb, in *Phase Transitions and Critical Phenomena*, Vol. 3,(Academic Press, 1975).

REFERENCES FOR CHAPTER 4

(4.1) F. Schwabl, Ferroelectrics, 24, 171 (1980); S. D.Mahanti, D. Sahu, Phys.Rev.Lett. 48, 936 (1982).

(4.2) M. F.Toney, R. D. Diehl, and S. C. Fain, Phys.Rev. B27, 6413 (1983); P. A. Heiney, P. W. Stephens, S. G. J. Mochrie, J. Akikatsu, and R. J. Birgeneau, Surf.Sci. 125, 539 (1983).

(4.3) R. D. Diehl, and S. C. Fain, Surf.Sci. 125, 116 (1983).

(4.4) *Ordering in Strongly Fluctuating Condensed Matter Systems*, edited by T. Riste, (Plenum Press, NY 1979).

(4.5) For example, R. Max, and B. Christoffer, Phys.Rev.Lett. 51, 790 (1983).

(4.6) O. G. Mouritsen, and A. J. Berlinsky, Phys.Rev.Lett. 48, 181 (1982).

(4.7) R. D. Etters, R. Pan, and V. Chandrasekharan, Phys.Rev.Lett. 45, 645 (1980); R.Pan, R. D. Etters, K. Kobashi, and V. Chandrasekharan, J.Chem.Phys. 77, 1035 (1982).

(4.8) See Chapter 2.

(4.9) E. Domany, and E. K. Riedel, Phys.Rev.Lett. 40, 561 (1978); Phys.Rev. B19, 5817 (1979).

(4.10) R. Savit, Rev.Mod.Phys. 52, 453 (1980).

(4.11) J. M. Kosterlitz, and D. J. Thouless, J.Phys. C6, 1181 (1973); J. M. Kosterlitz, J.Phys. C7, 1046 (1974).

(4.12) *Monte Carlo Methods in Statistical Physics* , Edited by K. Binder (Springer-Verlag, Berlin, 1978); *Applications of the Monte Carlo Method in Statistical Physics* , Edited by K. Binder (Springer-Verlag, Berlin, 1980).

(4.13) H. C. Anderson, J.Chem.Phys. 72, 2384 (1980).

(4.14) M. Perrinello, and A. Rahman, Phys.Rev.Lett. 45, 1196 (1980); J.Appl.Phys. 52, 7182, (1980); J.Chem.Phys. 76, 2662 (1980).

(4.15) S. Nose, and M. L. Klein, J.Chem.Phys. 78, 6928 (1983); Mol.Phys. 50, 1055 (1983).

(4.16) C. W. Gear, *Numerical Initial Value Problems in Ordinary Differential Equations*, (Pretice Hall, Englewood Cliffs, N.J. 1971).

(4.17) F. James, Rep.Prog.Phys. 43, 73 (1980).

(4.18) See, for example, L. Verlet, Phys.Rev. 159, 98 (1967).

(4.19) M. Sprik, R. W. Impey, and M. L. Klein, Phys.Rev. B29, 4368 (1984);

(4.20) M. Born, and K. Huang, *Dynamical Theory of Crystal Lattice*, (Oxford University Press, London, 1968)

(4.21) G. C. DeFotic, Phys.Rev. B23, 4714 (1981).

(4.22) M. B. Einhorn, R. Savit, and E. Ravinovici, Nucl.Phys. 170, 16 (1980).

(4.23) Y. Saito, Phys.Rev. 26, 6239 (1982).

(4.24) S. W. Koch, and F. F. Abraham, Phys.Rev. B27, 2964 (1983).

(4.25) R. K. Kalia, P. Vashishta, and S. D. Mahanti, Phys.Rev.Lett. 49, 676 (1982).

(4.26) J. E. Van Himbergen, Phys.Rev.Lett. 53, 5 (1984). However, there is other opinion about the nature of the transition in this model, see H. J. F. Knops, Phys.Rev. B30, 470 (1984).

(4.27) V. Jose, L. P. Kadanoff, S. Kirkpatrick, and D. R. Nelson, Phys.Rev. B16, 1217 (1977).

(4.28) See, for example, R. Swendsen, Phys.Rev.Lett. 49, 1302 (1982); E. Domany, M. Schick, and R. H. Swenden, Phys.Rev.Lett. 52, 1535 (1984).

(4.29) S. Ostlund, and B. I. Halperin, Phys.Rev. B23, 335 (1981).